Interventions for Ischemia-Reperfusion Injury in Skeletal Muscle

Rebecca June Wilson

Arlington, Virginia

Master of Science in Biochemistry and Molecular Genetics, University of Virginia,

Charlottesville, VA

Bachelor of Science in Biochemistry, Virginia Polytechnic and State Institute,

Blacksburg, VA

A Dissertation Presented to the Graduate Faculty of the University of Virginia in Candidacy for the Degree of Doctor of Philosophy

Department of Biochemistry and Molecular Genetics

University of Virginia

December 2017

Zhen Yan, Ph.D.

David F. Kashatus, Ph.D.

Marty W. Mayo, Ph.D.

Bryce M. Paschal, Ph.D.

Jeffrey S. Smith, Ph.D.

ABSTRACT

Tissues in our body rely on continuous supply of blood to receive O_2, nutrients and remove waste products. When blood flow is arrested it causes ischemia and homeostatic imbalance that jeopardizes tissue function and leads to tissue death if prolonged. Reperfusion, the restoration of blood flow, is required to resuscitate the ischemic tissue, however, it ignites a cascade of deleterious events that augment the initial ischemic insult exacerbating tissue dysfunction and/or death. Peripheral tissues, such as motor nerve fibers and skeletal muscle fibers (myofibers), are vulnerable to IR injury as a corollary of tourniquet application, a commonly used approach to prevent hemorrhage and provide bloodless field in trauma and surgical situations. A consequence of IR injury to motor nerve fiber and myofibers is reduced neuromuscular function, which compromises voluntary movement and reduces quality of life. Despite the prevalence of tourniquet use, there are currently no efficacious interventions that attenuate IR injury.

A vast body of interdisciplinary studies has revealed that mitochondria play a causal role in initiation and progression of IR pathology. The studies presented herein investigate the contribution that mitochondrial perturbations have on motor nerve fibers and myofibers in the context of tourniquet-induced IR injury to the hindlimb. We found that IR causes reduction in neuromuscular function, myofiber denervation, as well as mitochondrial oxidative stress. These studies uncovered that directly targeting mitochondria and enhancing covalent linkage of nitric oxide to protein thiols (protein *S*-nitrosation) in mitochondria as well as endurance exercise training preserved neuromuscular function following IR injury by two distinct mechanisms. These findings unveil practical and effective interventions that attenuate IR injury, which will likely improve outcome of tourniquet use.

ACKNOWLEDGEMENTS

Thank you first and foremost to my parents Maureen and Steve and sister Lauren for providing unwavering love and support through the years and encouraging me to relax and just "breathe in and breathe out". Thank you to Bill for the inspiration, adventures and laughs, and for putting up with all the travel the past 3 years. I also have to thank my pet rabbits Puffin and IgG-y, who are usually a pain to clean up after but are great companions and a joy to watch.

I would like to thank my mentor, Zhen Yan, for the guidance and support he provided on projects that took us into new areas of investigation that we weren't expecting. Thank you for pushing me to ask the tough questions and to be cautiously optimistic. I especially want to thank all the amazing people I've worked with in the Yan Lab, who made every day fun and worthwhile. Specifically, the perpetual "new" postdoc Josh Drake, who has served as a sounding board for my harebrained ideas and kept me relatively sane the past couple years. Rhianna Laker, my first friend in Charlottesville who took me under her wing and helped me grow as a scientist and goof off in Charlottesville. Mei Zhang has been the absolute best in more ways than I can possibly count.

A special thank you to all of my high school, college, and Charlottesville friends who have stuck around through and through. I would not have made it this far without knowing they had my back.

TABLE OF CONTENTS

LIST OF FIGURES

LIST OF ABBREVIATIONS

H^+	Proton
NMJ	Neuromuscular Junction
SNO	*S*-nitrosation
ROS	Reactive oxygen species
mtROS	Mitochondria reactive oxygen species
IR	Ischemia- reperfusion
ETS	Electron transport system
CK	Serum creatine kinase
SD	Standard deviation of the mean
Ncam	Neural cell adhesion marker
Tuj1	Neuron-specific class III β-tubulin
AchR	Acetylcholine receptor
α-BTX	α-bungarotoxin
ATP	Adenosine triphosphate
ADP	Adenosine diphosphoate
Pi	Inorganic phosphate
Na^+	Sodium
Ca^{2+}	Calcium
O_2	Molecular Oxygen
NADH	Nicotinamide adenine dinucleotide
$FADH_2$	Flavin adenine dinucleotide
OXPHOS	Oxidation phosphorylation

CHAPTER 1: INTRODUCTION

1.1.1. Ischemia-reperfusion injury

Ischemia-reperfusion (IR) injury, caused by temporary interruption of blood flow, is a significant factor in the pathology of a number of disorders and chronic diseases. In particular, peripheral tissues, such as motor nerve fibers and myofibers, are vulnerable to IR injury induced by abdominal aortic aneurism (1,2), vascular narrowing due to peripheral arterial disease (PAD) (3,4) or tourniquet application (5,6). The overall consequence of IR injury is tissue damage supplemented with loss of tissue function and/or vitality, ultimately jeopardizing neuromuscular function. For example, tourniquets are commonly used to prevent hemorrhage as a first response to traumatic injury or provide a bloodless operating field and preclude exsanguination during certain types of surgeries. Despite the utility, tourniquet use carries an inherent risk of IR injury, which is particularly damaging to motor nerves and myofibers principally due to their high energetic demands (7,8). Indeed, 26% of patients recovering from total knee arthroplasty, in which a tourniquet was used, report to experience complications, including profound limb swelling, nerve injury and muscle weakness (9,10). Severe IR injury may also require amputation. As recently as 2008, it was reported that among ~140 million patients with PAD who suffer an acute ischemic event ~10-30% required amputation within 30 days after the bout of IR injury (11). Thus, limb IR injury poses a significant clinical problem. Despite the prevalence of IR injury, there is no reliable invention (12–15).

The basis of IR induced tissue injury is insufficient energy supply due to O_2 starvation during ischemia. As a consequence, metabolic intermediates accumulate, intracellular ion levels become imbalanced and, if not remedied, eventually results in cell death (16,17). Reperfusion,

while required to resuscitate tissue, ignites pathogenic processes primed during ischemia, effectively compounding the original insult. Decades of reductionist science have uncovered that IR injury involves a complex, interconnected cascade of events activated by mitochondrial energetic dysfunction in the aftermath of metabolic stress (16–21).

1.1.1. Mitochondrial respiration

Maintenance of energy homeostasis to support basal and active functions of motor nerve fibers and myofibers relies on a sufficient supply of adenosine triphosphate (ATP), the majority of which is produced in an O_2-dependent manner by mitochondrial respiration (22). Mitochondrial respiration is an energy-conversion process that couples successive reduction-oxidation reactions within the electron transport system (ETS) with ATP synthesis (23) **(Figure 1).** This coupling is termed oxidative phosphorylation (OXPHOS). The ETS consists of four multimeric protein complexes imbedded in the inner mitochondrial membrane that transfer electrons from reducing equivalents to O_2 to form H_2O (24). Electrons enter the ETS by one of two routes: oxidation of NADH by NADH-dehydrogenase (complex I) (25) or oxidation of succinate by succinate dehydrogenase (complex II) (26). The electrons are used by complexes I and II to reduce the lipid soluble ubiquinol to ubiquinone with two electrons (26). Ubiquinone is oxidized by cytochrome bc_1 oxidase (complex III), and the electrons are channeled to cytochrome c reductase (complex IV) via cytochrome c (27). Finally, two electrons reduce molecular oxygen (O_2) and form two molecules of water. Energy obtained through the transfer of electrons down the ETC is used at complexes I, III, and IV to pump protons (H^+) from the matrix to the inter membrane space to generate an electrochemical gradient. This electrochemical gradient is largely responsible for mitochondrial membrane potential ($\Delta\psi_M$) (28) and drives the

synthesis of ATP by ATP synthase (complex V) (29). Consistent with this theory, early studies using O_2 electrodes revealed that in coupled mitochondria the amount of ATP produced is proportional to O_2 consumed (30).

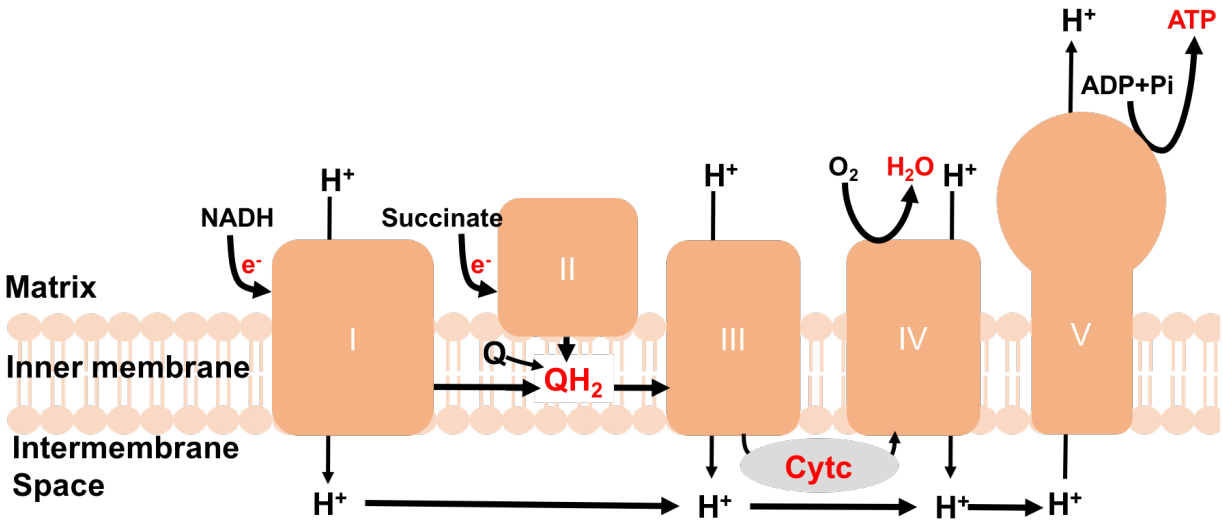

Figure 1: Simplified cartoon of mitochondrial OXPHOS. Electrons from NADH and succinate are transferred to complexes I and II of the ETS, respectively. These two electrons then reduce ubiquinol (Q) to ubiquinone (QH_2), which is then oxidized by complex III. The electrons are channeled from complex III by cytochrome c (Cytc) to IV where they reduce molecular O_2 to H_2O. Complexes I, III, and IV use free energy from electron transport to pump H^+ from the matrix to the intermembrane space, which generates an electrochemical gradient across the inner membrane that drives the production of ATP.

1.1.2. Mitochondrial and cellular events during ischemia

Disruption of the transport of electrons through the ETS due to lack of O_2 supply, such as during an ischemic event, halts OXPHOS. Reduction in OXPHOS compromises cellular ATP production/availability and results in accumulation of NADH and succinate as electron carriers in the ETS become maximally reduced (20). Mitochondria isolated from canine myofibers after 5 hours of tourniquet-induced ischemia display a 77.4% reduction in respiration, and an 80% reduction in cellular ATP availability (31,32). Furthermore, in an effort to maintain mitochondrial membrane potential ATP synthase reverses, hydrolyzing ATP to pump H^+ into the intermembrane space (33) **(Figure 2).** The consequence of OXPHOS inactivation and ATP consumption by ATP synthase is a rapid decline in cellular ATP, which sends the cells into a state of energetic stress and precipitates subsequent pathological events (34). If not remedied, ATP will be depleted beyond a 'critical value' leading to cell death (35,36). Evidence of motor nerve fiber and myofiber damage appears after 1 hour of ischemia and gradually worsens until the damage becomes irreversible after 6 hours (13,37,38). Thus, clinical guidelines recommend limiting duration of ischemia to the greatest degree possible (37–39).

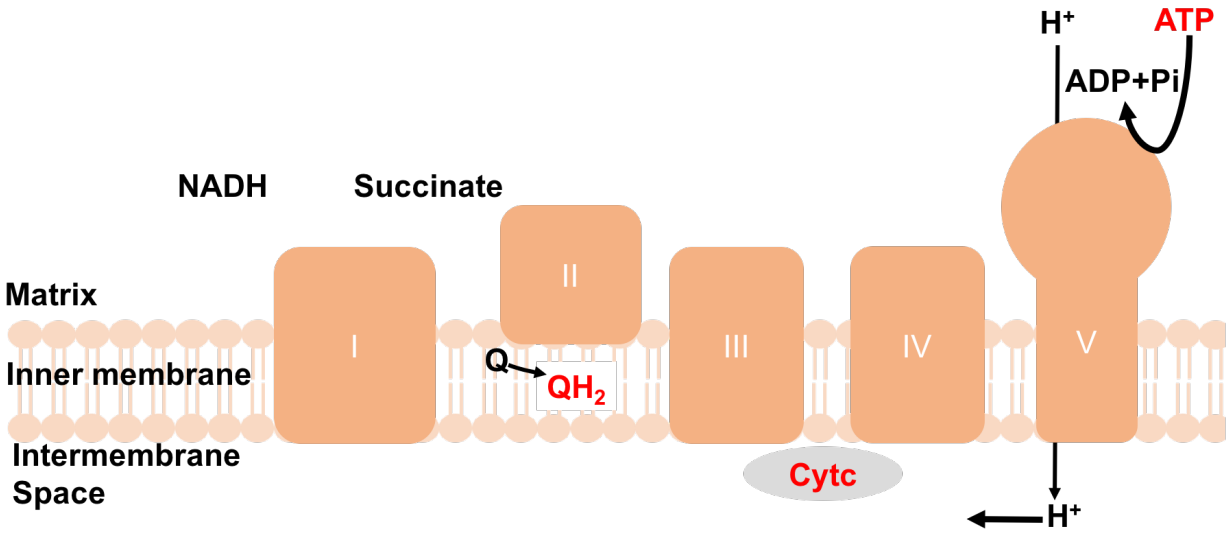

Figure 2: ETS during ischemia. In the absence of oxygen, electron transport through ETS is halted. Once electron carriers within the ETS become fully reduced, NADH and succinate accumulate in the matrix. In an effort to preserve mitochondrial membrane potential ATP is hydrolyzed by ATP synthase, and the energy obtained is used to pump protons into the intermembrane space.

Compared to other tissues, such as myocardium in the heart and neuronal network in the brain, motor nerve fibers and skeletal myofibers can tolerate longer durations of ischemia in part due to compensatory activation of anaerobic metabolism (13,16,17,40). Indeed, during ischemia motor nerve fibers have increased sensitivity to glucose (41,42), and myofibers upregulate glycolytic pathways and enhance glycogen breakdown to supply glucose for substrate-level phosphorylation (32,43). Additionally, energy consuming processes in motor nerve fibers and myofibers, including synaptic vesicle release and contraction, are inactivated, respectfully (44–46). During ischemia, compound muscle action potential, the most sensitive index of motor nerve fiber function, is absent (7,45,46). Importantly, alteration in nerve action potential conduction is due to ATP depletion during ischemia rather than denervation of NMJ (44,47). Similarly, force generation is completely absent in ischemic tibialis anterior muscles of rats when muscles were stimulated directly (48). Despite upregulation of glycolysis and inactivation of energy consuming processes, substrates for glycolysis are eventually exhausted, and ATP levels drop to critical levels (32,49). In the absence OXPHOS, metabolic intermediates accumulate (50,51), and ATPase-dependent processes, including ion transport mechanisms, become dysfunctional, causing intracellular ion imbalance (16,17,52)

In addition to inability to fully support motor nerve fiber function and cellular processes in myofiber, reliance on glycolytic pathways causes intracellular acidification and subsequent perversion in ion homeostasis (53). The last step of glycolysis is conversion of phosphoenolpyruvate to pyruvate with the release of 2 ATP per molecule of glucose consumed (54). During ischemia, pyruvate is oxidized by lactate dehydrogenase to replenish the coenzyme NAD^+ required for continuance of glycolysis (55,56). As a consequence, lactic acid accumulates within the cell , lowering the pH, which in turn inhibits glycolysis (43,53,55,57). To combat

intracellular acidification, plasma membrane Na^+/H^+ exchangers are activated while Na^+/K^+ (52,58) and Ca^{2+} ATPases are inhibited by the low ATP availability, causing an increase in intracellular Na^+ (59). In an attempt to attenuate intracellular Na^+ overload, Na^+/ Ca^{2+} antiporters on the plasma and inner mitochondrial membranes are reversed, wherein Na^+ is extruded and Ca^{2+} accumulates (32,60). In combination with antiporter reversal, Ca^{2+} ATPases on the endoplasmic and sarcoplasmic reticulum of motor nerve fibers and myofibers, respectively, are deactivated while Ca^{2+} release continues, ultimately resulting in intracellular Ca^{2+} overload (17,60,61). Excessive Ca^{2+} activates degenerative enzymes including proteases (62,63) and phospholipases (1,64,65), which degrade cellular components and contribute to irreversible damage. Furthermore, during ischemia, the mitochondrial permeability transition pore (mPTP), a non-selective pore in the inner membrane permissive to any solute <1.5kDa, forms but remains closed due to the low pH (66,67) **(Figure 3)**. These deleterious alterations during ischemia will lead to cell death if not remedied.

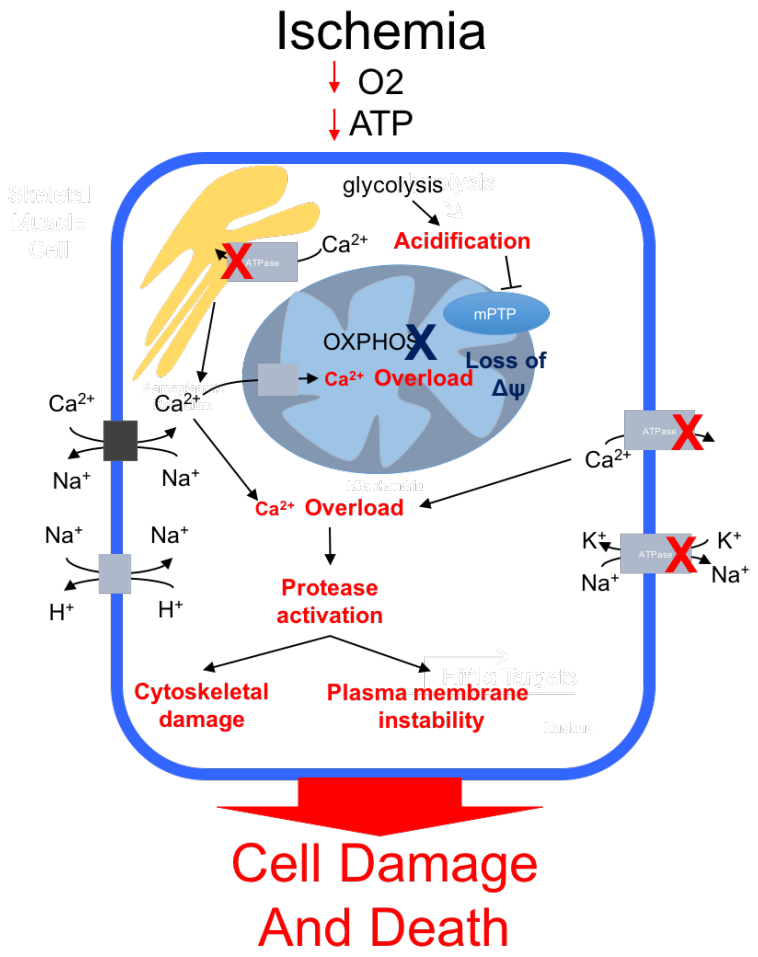

Figure 3: Major cellular abnormalities during ischemia. Loss of O_2 during ischemia inactivates OXPHOS leading to decrease in ATP content. Blue "X" denotes processes inactivated due to oxygen starvation, red "X" denote processes inactivated due to reduction of ATP. Intracellular acidification and inactivation of ATPases, which culminates in dysregulation of intracellular ion homeostasis. Accumulation of intracellular Ca^{2+} leads to Ca^{2+} overload in the cytosol and mitochondria, activating proteases, which damage cytoskeletal and plasma membrane components. Mitochondrial permeability transition pore (mPTP) forms during ischemia, but remains closed due to the low intracellular pH.

1.1.3. Mitochondrial and cellular events during reperfusion

Reperfusion is required to resuscitate ischemic tissue; however, it ignites pathogenic processes primed during ischemia and effectively compounds the original insult. Mitochondrial dysfunction underlies the initiation and progression of IR pathology. In particular, mitochondrial-derived reactive oxygen species (mtROS) and opening of mPTP compromise OXPHOS, trigger apoptotic and necrotic pathways and activate inflammatory cascades (19,20,68). Excessive ROS production in combination with insufficient ATP availability further perturbs ATP-dependent and independent ion exchangers, prolonging Ca^{2+} overload in the cytosol and mitochondria (69–71). Sustained elevation of Ca^{2+} activates proteases and phospholipases, leading to membrane degradation, decreasing cell function and increasing the probability of cell death (19,35,72–82) **(Figure 4).**

The first damaging event of reperfusion is a burst of ROS production from mitochondria. Accumulation of electron donors, as well as progressive impairment of mitochondrial function during ischemia determines mitochondrial ROS (mtROS) production upon reperfusion (16,17,20,83,84). The burst of ROS overwhelms endogenous antioxidant defense systems (72,73) and directly causes oxidative damage to mitochondria, leading to more ROS generation as well as disruption of ATP production (83,85–87) **(Figure 5)**. In conjunction with dysregulation of mitochondrial Ca^{2+} homeostasis, the burst in ROS can also cause opening of mPTP, leading to apoptotic and necrotic cell death. Moreover, mtROS-mediated mitochondrial damage causes the release of damage-associated molecular pattern molecules, such as mitochondrial DNA, instigating an inflammatory response, which contributes to IR injury and can continue for days after injury (88,89). The end result of excessive mtROS production in motor nerve fibers and myofibers is often structural alterations and reduced function, which may

manifest as muscle weakness and atrophy and/or paralysis (47,90,91). Reducing mtROS, preventing macromolecule oxidation, and/or rapidly detoxifying ROS represents attractive therapeutic strategies to attenuate IR injury (92–97).

Manipulation of antioxidant defenses has helped to uncover the involvement of mtROS in IR pathology. Mice lacking superoxide dismutase-1, an enzyme that catalyzes the dismutation of superoxide to hydrogen peroxide, are more susceptible to tourniquet-induced IR oxidative stress and experience rapid degeneration of neuromuscular junctions (NMJ), the chemical synapse form bed between motor nerve fibers and myofibers (44). Conversely, treatment with antioxidant molecules prior to IR can attenuate cell degeneration and dysfunction (79,98–100). Zhou et al., found that administration of the antioxidant osthole following spinal cord ischemia reduced mtROS, increased ATP generation and improved motor nerve fiber function (101). Similarly, using a model of tourniquet-induced IR injury, Tran et al., demonstrated that myofiber death could be attenuated with the superoxide dismutase mimetic Tempol or antioxidant molecule coenzyme Q (19,75). Antioxidants treatment is most effective when administered prior to injury, which may not be clinically feasible because IR is not always anticipated.

Although there are at least ten distinct sites in the mitochondrial matrix that can generate ROS (102–104), complexes I and III of the ETS are considered to be the main sources of mtROS during IR injury (20). Chouchani et al., have demonstrated that accumulation of succinate during ischemia drives reverse electron transport from complex II to complex I where electrons react with O_2 to form ROS in the matrix (50). Preventing reverse electron transport by covalently linking a nitric oxide moiety to a protein thiol, a process termed *S*-nitrosylation, of complex I significantly reduced mtROS production, mitochondrial dysfunction and cell death in the myocardium (50). Electrons delivered by ubiquinone can leak from complex III into the matrix

or intermembrane space and form mtROS (105,106). ROS production at Complex III is a consequence of functional alterations in the ubiquinone oxidation site caused by ischemic damage and can only be mitigated if the site is protected or if electron flow upstream of complex III is reduced (105).

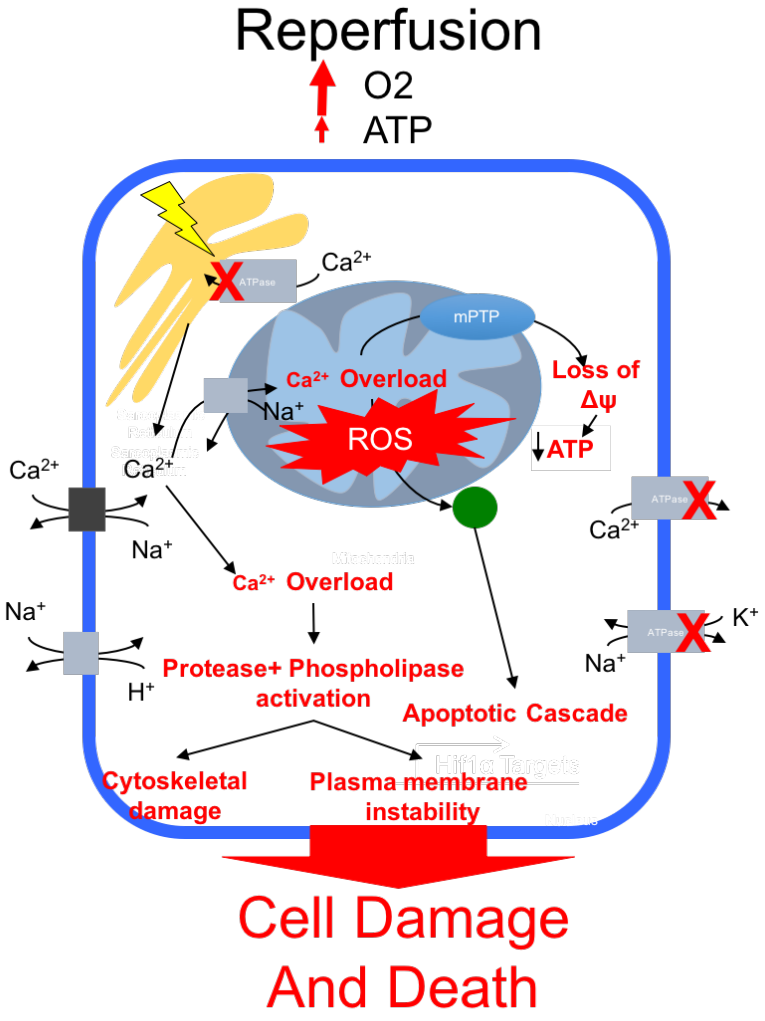

Figure 4: Major cellular abnormalities during reperfusion. Upon reintroduction of oxygen, ETS is reactivated; however, this leads to a burst of ROS production. Reperfusion restores pH leading to disinhibiting and opening of mPTP, which in turns causes loss of mitochondrial membrane potential and ATP production as well as release of pro-apoptotic factors. Ion imbalance develops as ATP levels are insufficient to support ATP-dependent ion pumps on the plasma membrane and endoplasmic reticulum. Red "X" denotes processes inactivated due to reduction of ATP. Together, these perturbations lead to cell damage and death.

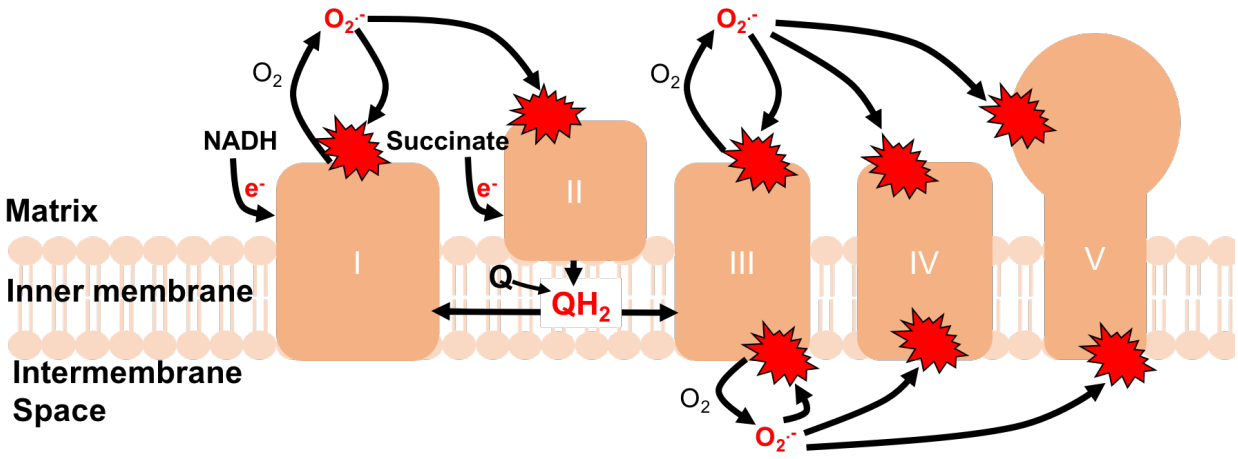

Figure 5: ETS during reperfusion. Upon reperfusion, electrons from NADH and succinate enter Complexes I and II, respectively. Since electron binding sites of complexes III and IV are fully occupied electrons from complex II are transferred to complex I wherein the react with molecular oxygen to form superoxide. The burst of superoxide during reperfusion overwhelms the endogenous antioxidant systems, and members of the ETS are oxidized, causing them to dysfunction and superoxide continue to be generated by complexes I and III.

In addition to excessive ROS generation and impaired ETS activity, opening of mPTP at the onset of reperfusion occurs in response to mtROS accumulation (67,107), increase in pH as lactic acid is cleared from the tissue (67), and Ca^{2+} overload (67,107). mPTP opening collapses the mitochondrial membrane potential and allows solutes to enter the mitochondria, resulting in mitochondrial swelling, rupture and release pro-apoptotic factors (19,108,109,109). Apoptosis can be activated by release of cytochrome c and apoptosis inducing factor from the mitochondria into the cytosol (110). Mitochondria collected from myofibers treated with N-methyl-4-isoleucine-cyclosporine, an mPTP inhibitor, prior to reperfusion displayed improved viability and decreased edema (81). Thus, prevention of mPTP may be a therapeutic target for prevention of IR injury.

In summary, reperfusion is required for motor nerve fiber and myofiber survival, however, it activates a number of deleterious events that cause cell dysfunction and may result in cell death. Mitochondrial dysfunction plays a fundamental role in initiating IR injury by generating superoxide and activating apoptotic pathways. Despite efforts dedicated to designing therapeutics to specifically target the mitochondria, there is currently no effective treatment available. Additionally, as IR events are often not anticipated, it is critical to develop interventions that can be administered at the time of injury. It is therefore imperative for researchers and clinicians to gain a better understanding of the underlying mechanisms that cause IR injury, particularly mitochondrial impairments, in order to overcome therapeutic barriers.

1.2. Neuromuscular junction

Fundamental life tasks, including breathing and locomotion, require coordination between the nervous and skeletal muscle systems. The functional site of neuromuscular communication is neuromuscular junction (NMJ), a specialized chemical synapse formed between the axon terminal of an α-motor nerve fiber and skeletal muscle fiber (myofiber). NMJ are the location and means, by which motor nerve action potentials are transduced into myofiber for inducing muscle contractions. Mature NMJ persevere throughout life in a state of dynamic equilibrium, responsive to physical activity, damage and disease. Defects in NMJ maintenance as a function of pre- or post-synaptic alterations will result in debilitating neuromuscular disorders (111,112).

Research stemming from the discovery of chemical synapses to the characterization of NMJ has been ongoing for nearly a century. In the early 1900s, Professor John Newport Langley discovered that myofibers possessed 'substances' that receive and transmit stimuli when combined with nicotine, and these processes were blocked by the poisonous drug curare (113). His findings offered the first suggestion that myofibers have synaptic contacts and specialized receptors, which were later identified as acetylcholine receptors (114). A few years later, Sir Henry Dale and colleagues discovered that acetylcholine displayed chemical transmitter properties between nerve and muscle, overturning the accepted dogma that synaptic transmission occurred only by direct electrical propagation (115). In 1936, Dale and Professor Otto Loewi were awarded the Nobel Prize in Physiology or Medicine for their discoveries in chemical neurotransmission. Dale's work was later complemented by studies conducted by Professor Bernard Katz and colleagues who revealed that acetylcholine is released from a motor nerve fiber by vesicular exocytosis as multi-molecular quanta that cause a brief depolarizing

transmembrane current on a myofiber (116–119). A contemporary of Professor Bernard Katz, Sir John Eccles and his team elucidated the spinal circuit of feedback inhibition, the mechanism preventing two antagonizing muscle groups from contracting at the same time (120,121). Furthermore, Eccles's group made the pivotal discovery that synapses are plastic, altered by use and disuse as a function of environmental, behavioral and neural changes (122). These seminal studies provided the basis of understanding of neurochemical transmission, which has underscored the importance of NMJ for neuromuscular function.

Neuromuscular biologists have since made tremendous strides dissecting the steps and molecular modulators involved in NMJ development during embryogenesis (123–127), as well as identifying pre- and post synaptic perturbations that effect neuromuscular function in a number congenital diseases and disorders (128–130) . Despite these appreciable advances, there remains a paucity of information regarding the mechanisms that mediate maintenance or degradation of mature NMJ under physiological and pathological conditions. Recently, maintenance of mitochondrial function in neuromuscular stability has come to forefront due to several points of evidence showing that patients with neuromuscular disorders also have mitochondrial abnormalities (e.g. amylotrophic lateral sclerosis, aging and traumatic spinal cord injury) (85,131–133). Deterioration in mitochondrial function has been suggested to be causal to the development of neuromuscular disorders (134–136). However, much is left to be uncovered concerning mitochondrial-mediated neuromuscular pathology.

1.2.1. Neuromuscular Transmission

Transduction of an action potential from a α-motor nerve fiber terminal to a myofiber in order to produce a contraction is a multi-step process. When an action potential reaches the

motor nerve fiber terminus, P/Q-type voltage-dependent calcium (Ca^{2+}) channels open to allow Ca^{2+} into the cell (137). The influx of Ca^{2+} triggers fusion of docked synaptic vesicles containing acetylcholine to the presynaptic plasma membrane and release of acetylcholine into the synaptic cleft, the narrow space between the pre- and post-synaptic regions (138). Free acetylcholine binds to nicotinic acetylcholine receptors on the post-synaptic membrane that open to allow sodium ions (Na^{+}) to flow into the motor end-plate of the myofiber (139). This cation exchange across thousands of acetylcholine receptors causes a local depolarization called an end-plate potential (54). When depolarization exceeds the contraction threshold value (~-50mV), voltage-dependent Na^{+} channels open causing an influx of Na^{+} and conversion of the end-plate potential to an action potential (+40mV) that is distributed deep into myofiber along T-tubules (54). T-tubules are invaginations of myofiber membrane containing voltage sensitive dihydropyridine receptors that are closely associated with ryanodine receptors on the sarcoplasmic reticulum (137,140). Upon arrival of an action potential, dihydorpyridine receptors induce physiochemical changes of the ryanodine receptors causing them to release Ca^{2+} from the sarcoplasmic reticulum, increasing intracellular, cytoplasmic Ca^{2+} levels (141). Ca^{2+} then binds to troponin C of the thin filament causing a conformational rotation of tropomyosin away from the cleavage furrows on the actin filaments, exposing the myosin binding sites (142). The myosin head of the thick filament then binds to the uncovered sites on actin and, upon the release of adenosine diphosphate (ADP) and inorganic phosphate (Pi), 'pulls' actin to generate force (143,144). At the end of contraction, the myosin head binds adenosine triphosphate (ATP) and detaches from the actin molecule (143,144). This series, termed cross-bridge cycling, continues until the loss of the elevation of Ca^{2+} level in the sarcoplasm, resulting in the cessation of skeletal muscle contraction.

When the synaptic endings of an axon returns to resting potential, acetylcholine release stops, and residual acetylcholine is quickly degraded (>1ms) by acetylcholinesterases that reside on the basal lamina of the motor end-plate. Closing of Na^+ channels and opening of potassium channels repolarize the postsynaptic membrane. In the absence of voltage-mediated stimuli, dihydropyridine receptors and ryanodine receptors become deactivated. Within ~30 ms after action potential is terminated, intracellular [Ca^{2+}] returns to baseline as Ca^{2+} is pumped back into the sarcoplasmic reticulum by sarcoplasmic/endoplasmic reticulum Ca^{2+} ATPase (SERCA), and myosin-bindings sites on actin are covered once more by tropomoycin.

Execution of muscle contraction and relaxation involves several steps, any of which can be affected by various diseases and disorders and compromise neuromuscular function. Clinical manifestations of disruption of neuromuscular coupling include muscle weakness and atrophy and/or partial to complete paralysis and may be a manifestation of neuropathies, myopathies or both. A number of diagnostic techniques are used in parallel to identify whether the source of neuromuscular perturbations are pre- and/or post-synaptic, to exclude other coexisting neuromuscular disorders, monitor disease progression, or oversee the effects of treatment (145,146). These include but are not limited to electro-diagnostic approaches, such as nerve conduction studies and electromyography (147,148), magnetic resonance imaging (149), quantitative and repetitive strength testing and immunohistochemistry (150), all of which are recommended to be done in parallel (147). While these techniques are not sufficient to identify the underlying molecular mechanisms that contribute to pathology, they help guide clinicians and researchers to appropriate sites for further investigation and treatment administration (145).

1.2.2. Presynaptic motor nerve terminal

Execution of planned or reflexive muscle contractions requires conduction of neural signals from the central nervous system to a target skeletal muscle through an α-motor nerve fiber, which will henceforth be referred to as a motor nerve fiber. Motor nerve cell bodies are located in the brainstem or ventral horn of the spinal cord and pass through a plexus of peripheral nerves to a single muscle in the periphery. Anatomically, motor nerve fibers have a large cell body (~35-80 μm in diameter) that gives off a large single axon (6-20 μm in diameter) (151). Due to the size and the thickness of the electrically insulating myelin sheath, motor nerve fibers have high conduction velocities (~80-120 m/s) that allows for skeletal muscle to respond rapidly to changing stimuli (152).

As the axon of a motor nerve fiber approaches skeletal muscle it branches into 10-200 un-myelinated, knob-shaped presynaptic terminals that extend into shallow synaptic troughs on the myofiber membrane (153,154) **(Figure 6)**. Presynaptic terminals and postsynaptic specializations align directly across from one another and interact via trophic factors and structural proteins (155). The nerve-muscle contact is covered by thin Schwann cell processes everywhere except at the immediate interface with the muscle. This structural feature plays a critical role in NMJ development, maintenance and remodeling following nerve injury (156,157). It is important to note that each pre-synaptic branch forms a synapse with a single myofiber. The collection of myofibers innervated by a motor nerve constitutes a motor unit, and the myofibers contract simultaneously when the motor unit is sufficiently activated (158,159).

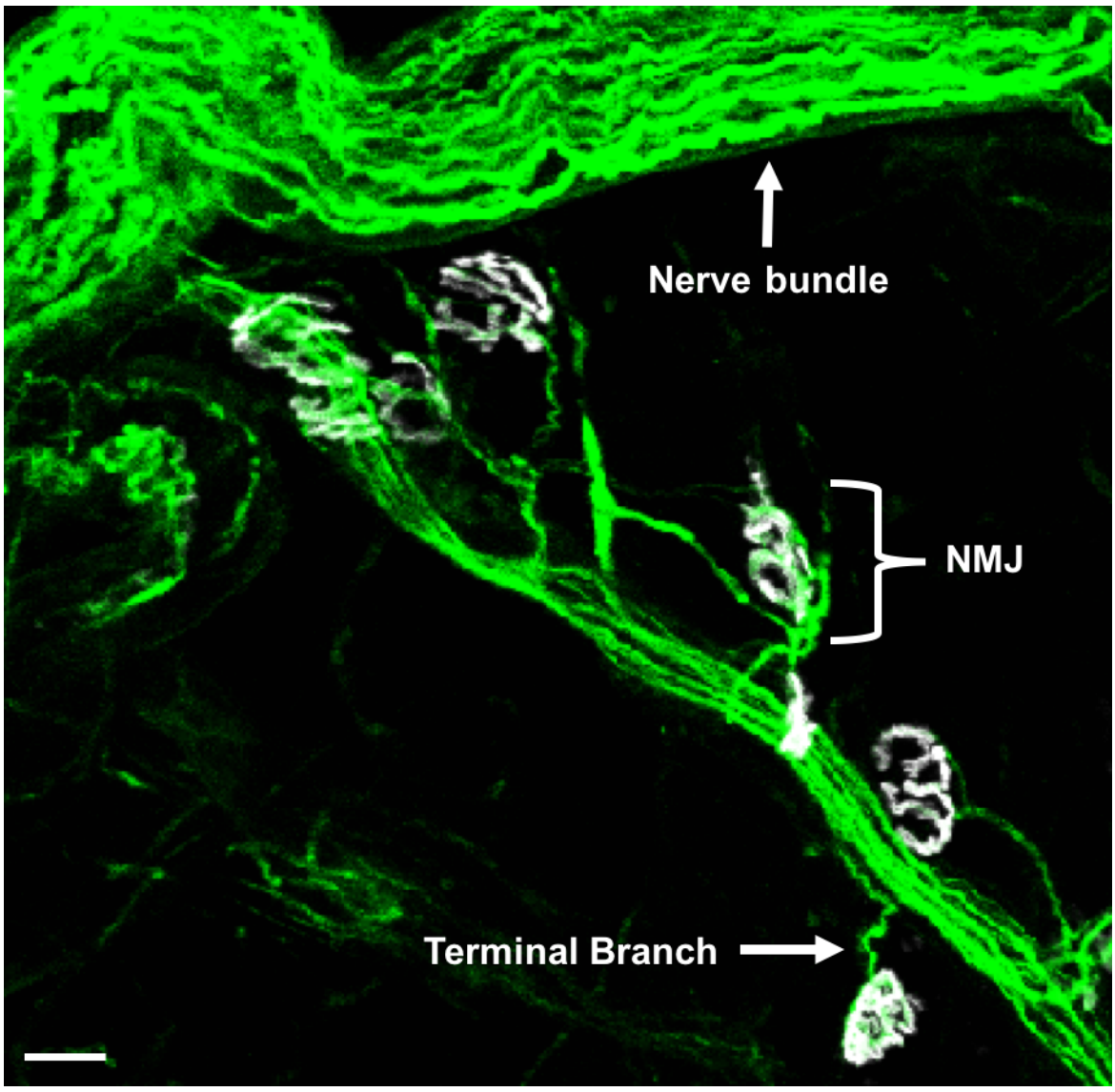

Figure 6: Innervation at NMJ. A representative confocal image of NMJ innervation. Motor nerve bundles enter the skeletal muscle, and individual motor nerve fibers branch off forming a single terminal branch with a myofiber. Green=motor nerve fiber, white=acetylcholine receptors on myofiber end-plate. Scale Bar = 20 μm.

Fundamental features of presynaptic terminals are consistent across different species of adult vertebrates (160,161). In particular, presynaptic terminals contain a large number of synaptic vesicles located in active zones and numerous mitochondria at a high density. Presynaptic terminals are readily identifiable with electron microscopy by synaptic vesicles, a presynaptic thickening of the plasma membrane, which is formed by macromolecules in the active zones and elongated mitochondria amassed in the central cytosolic core (160,162,163). Both active zones and mitochondria are critical for conversion of an action potential into a chemical signal in a precise spatial-temporal manner (164–166). Mitochondria play a particularly important role in synaptic transmission by providing energy and buffering ions needed for active zone proteins, as well as supporting remodeling and regeneration **(Figure 7).**

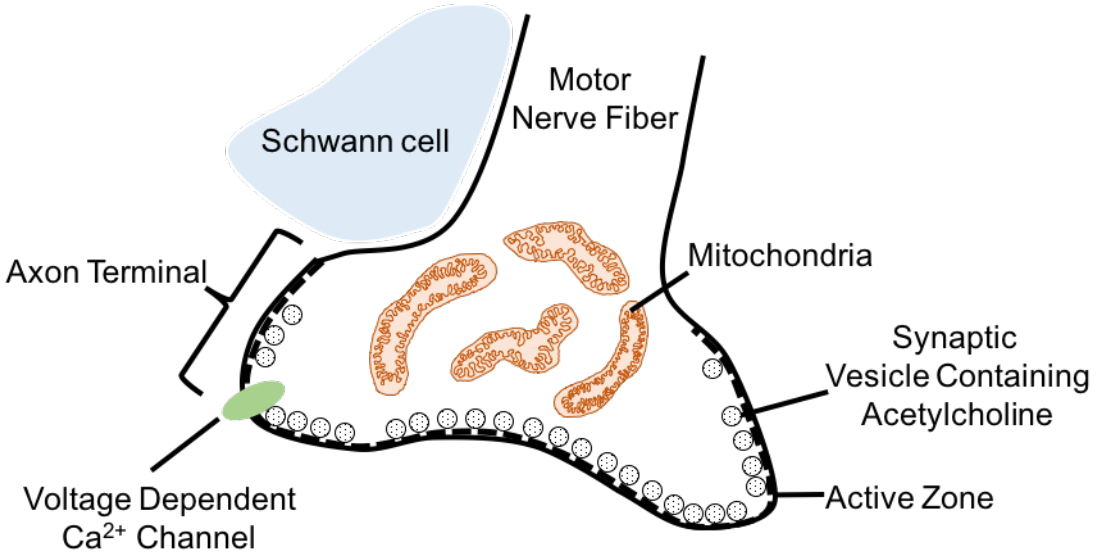

Figure 7: Presynaptic terminal. As the motor nerve fiber approaches a myofiber, the terminal engorges into a 'bulb' shaped structure. Mitochondria are found at a high density in the cytosolic regions of the presynaptic terminal. Electron dense regions along the presynaptic terminal membrane, called active zones, feature docked synaptic vesicles loaded with acetylcholine as well as voltage dependent Ca^{2+} channels. The axon terminal is covered by Schwann cells everywhere except the interface between pre- and post-synaptic specializations.

Active zones are electron dense regions of the presynaptic membrane that align postsynaptic specializations and function as synaptic vesicle fusion and acetylcholine release sites (167). Active zones consist of hundreds of synaptic vesicles connected together or directly tethered to the plasma membrane by filaments, synaptic vesicle releasing machinery, voltage dependent Ca^{2+} channels and cytoskeletal matrix proteins (165,166,168). Evaluation of human and mouse NMJ revealed approximately 200 active zones at a density of 2.3-2.7 active zones /μm^2 in each presynaptic terminal (169). The architecture and distribution of active zones along the membrane is regimented to ensure fast, synchronous excitation and vesicular release in addition to properly aligning with postsynaptic specializations (170).

Formation and maintenance of active zones is mediated by a trans-synaptic mechanism. Extracellular domains of presynaptic voltage-dependent Ca^{2+} channels and the postsynaptic organizer protein laminin β2 interact directly to position the presynaptic protein complex in front of the postsynaptic specialization (171). Moreover, voltage-dependent Ca^{2+} channels and laminin β2 interaction facilitates clustering of voltage-dependent Ca^{2+} channels, which in turn recruit other presynaptic components (172). NMJ in voltage-dependent Ca^{2+} channel knockout mice have a normal size, but have significantly reduced numbers of active zones and docked vesicles as well as less presynaptic cytoplasmic matrix and postsynaptic laminin β2 proteins (173). Furthermore, NMJ in mice with genetic deletion of voltage-dependent Ca^{2+} channels or laminin β2 display disassembled active zones (173). These studies suggest that active zone formation and synaptic vesicle accumulation in the presynaptic terminal are based on cell adhesion and/or retrograde signaling between presynaptic terminal and postsynaptic end-plate.

Specific proteins are recruited to active zones and work in concert to coordinate the cycling of synaptic vesicles, which is required for rapid and repeated rounds of acetylcholine

release (166,174). At any given time, active zones have 2-3 synaptic vesicles docked at the plasma membrane and a pool of ~200-300 positioned nearby (175). The pools are categorized as a release-ready pool, vesicles that are immediately available to release acetylcholine upon arrival of action potential, and a reserve pool that are only exocytosed during prolonged stimulation (175–177).

When an action potential reaches the motor nerve fiber terminal, voltage-dependent Ca^{2+} channels open and allow Ca^{2+} to enter the cell, rapidly triggering synaptic vesicles exocytosis (< 1 ms) (178). Release of >10,000 acetylcholine molecules from a single synaptic vesicle causes a miniature end-plate potential (~0.4-1 mV) on the postsynaptic membrane (179,180). Continued release of acetylcholine causes summation of miniature end-plate potentials that leads to action potential firing when the threshold is reached (181). Importantly, the amount of acetylcholine released is several fold higher than the minimum amount needed to trigger a postsynaptic action potential (170,181). Following exocytosis, synaptic vesicles are endocytosed, wherein they are locally recycled, refilled with acetylcholine, and returned to active zones (182). On account of advancements in fluorescence imaging, for example FM1-43 dye, which labels the membranes of recycled synaptic vesicles, the behavior and localization of synaptic vesicle cycling can be readily monitored *in vivo* over time (177,183,184). These techniques have aided the discovery that synaptic activity is maintained by a relatively small pool (1-5%) of synaptic vesicles that are repeatedly recycled and mixed with reserve vesicles in a matter of hours (185).

1.2.2.1. Motor nerve fiber mitochondria

Mitochondria play a critical role in synaptic function as well as motor nerve adaptability and stability by providing energy needed for the synaptic vesicle cycling, intracellular remodeling and Ca^{2+} buffering in response to depolarization-induced Ca^{2+} uptake. Mitochondria are also a dominant source for ROS generation that induces apoptosis, which contributes to the pathogenesis of a number of motor nerve degenerative disorders (85,132,136,186,187).

In order to locally respond to energetic and Ca^{2+} buffering demands, mitochondria are transported bi-directionally along cytoskeletal tracts from the cell body where they are synthesized, to the presynaptic terminal where they accumulate (188). Presynaptic mitochondria are positioned next to active zones, ~200 nm away from the plasma membrane (164). ATP is required to support a number of processes in the presynaptic terminal. For example, in the process of synaptic vesicle cycling, energy provided by ATP hydrolysis is required for exocytosis and refilling (189,190) as well as acetylcholine synthesis (191,192). Insufficient mitochondrial ATP production causes dramatic decrease in synaptic vesicle mobilization, which can be improved by stimulation of glycolysis (193) or administration of exogenous ATP (194). Similarly, ATP hydrolyzing activity of plasma membrane ATPases is necessary for maintenance of membrane stability and integrity, and intracellular ion homeostasis (195). In metabolically intact synapses, ATP synthesis reaches a steady state to maintain ~10^6 ATP molecules in each presynaptic terminal (196). Despite the presence of this reserve, important properties of presynaptic function are severely impaired following even momentary interruption in ATP synthesis (196).

Mitochondria are also important for synaptic transmission by sequestering and releasing Ca^{2+} to maintain Ca^{2+} homeostasis (197,198) and stimulate ATP production (199). Increases in

[Ca^{2+}] in the cytosol upon depolarization causes a rapid uptake of Ca^{2+} into the mitochondria (188,200). This buffering diminishes the probability of synaptic vesicle release, accelerating acetylcholine recovery after nerve stimulation and is most important during repetitive activity (189). Mitochondria serve as ideal Ca^{2+} buffers during neurotransmission as the rate of Ca^{2+} uptake far exceeds the rate of release, netting in greater [Ca^{2+}] accumulation (201). During recovery from terminal firing, Ca^{2+} is released from the mitochondria via the Na^{+}/Ca^{2+} exchanger in order to restore basal Ca^{2+} homeostasis (200). Furthermore, increase in mitochondria [Ca^{2+}] stimulates ATP production by activation of the tricarboxylic acid cycle (TCA) enzymes; pyruvate dehydrogenase, α-ketogluterate dehydrogenase, and isocitrate dehydrogenase (202,203). Together, sequestration of Ca^{2+} in the mitochondria couples activity-driven energy demands to local ATP synthesis (196). Mishandling of Ca^{2+} by mitochondria leads to abnormally high intracellular Ca^{2+} (204), and hyper-activation (205). Furthermore, excessive accumulation of mitochondrial Ca^{2+} leads to opening of the permeability transition pore (206), which depolarizes mitochondria, reducing ATP output, and can induce mitochondrial-mediated apoptosis (207).

Beyond morphological and functional assessments, alterations in mitochondrial dynamics and axonal transport are critical for motor nerve adaptation and recovery from damage (208–210). Approximately 20-30% of mitochondria are motile and able to be trafficked along cytoskeletal tracts from the cell body to areas of high ATP and Ca^{2+} demands (211,212). Trafficking is particularly important during recovery from neural damage (212). Indeed, damage intrinsically stimulates transport of healthy mitochondria, and removal of damaged mitochondria, in order to provide ATP needed to reseal damaged membranes, rearrange cytoskeletal structures, and activate synthesis of macromolecules needed for regrowth (212). Studies in sciatic nerve

found that mitochondria undergo dynamin-1-like protein dependent fission and migrate toward the area of injury following sciatic nerve transection (213). Prevention of fission, trafficking, or anchoring of mitochondria to injured areas hampers recovery (212,213), thus emphasizing the importance of mitochondrial motility to areas of high energy demands.

Dysregulation of mitochondrial function, including impaired ATP production and heightened ROS production, is implicated in the pathogenesis of multiple motor nerve degenerative diseases characterized by loss of motor nerve fibers and muscle weakness (44,85,134,164,214–217). For example, superoxide dismutase-1 mutant mice, which develop familial amylotrophic lateral sclerosis (ALS) in a manner akin to humans (218), have an increased susceptibility to tourniquet-induced IR degeneration of NMJ (44) and display abnormalities in mitochondrial appearance (e.g. swelling, disorganized cristae, and vacuoles containing mitochondrial remnants) prior to disease development (133,197,219,220). Similarly, mitochondria in motor nerves collected from mice lacking the survival motor neuron gene, a model for spinal muscle atrophy with abnormal changes in genes associated with mitochondrial bioenergetics, have reduced maximal respiration and membrane potential, impaired dynamics, and increased oxidative stress in the pre-symptomatic phase of the disease (217,221). Genetic sequencing of motor nerve fibers from a mouse model of spinal muscle atrophy revealed changes associated with mitochondrial bioenergetics (221). Thus, derangements in mitochondrial function, including reduced ATP production and increased ROS production, are considered to be an early and likely causal event leading to dysfunction and degeneration.

1.2.2. Postsynaptic myofiber

Equally as important to neuromuscular function are the postsynaptic myofibers, which

convert electrochemical impulses into mechanical work. Myofibers are long, fully-excitable, multinucleated cells composed of thousands of myofibrils that can generate force (222,223). End-plates with postsynaptic specializations form near the middle of the myofiber and interface with a presynaptic terminal (181,224). An adult myofiber form a single end-plate, which constitutes only 0.1% of the fiber surface (138) that features a basal lamina, a folded postsynaptic membrane, and an underlying sarcoplasm enriched with mitochondria (170) **(Figure 8**). Each component of the end-plate serves a critical function for neurotransmission that include stabilization of end-plate structures, positioning presynaptic terminals, signal reception, integration and dissemination, and metabolic support needed to accomplish contraction (163,181).

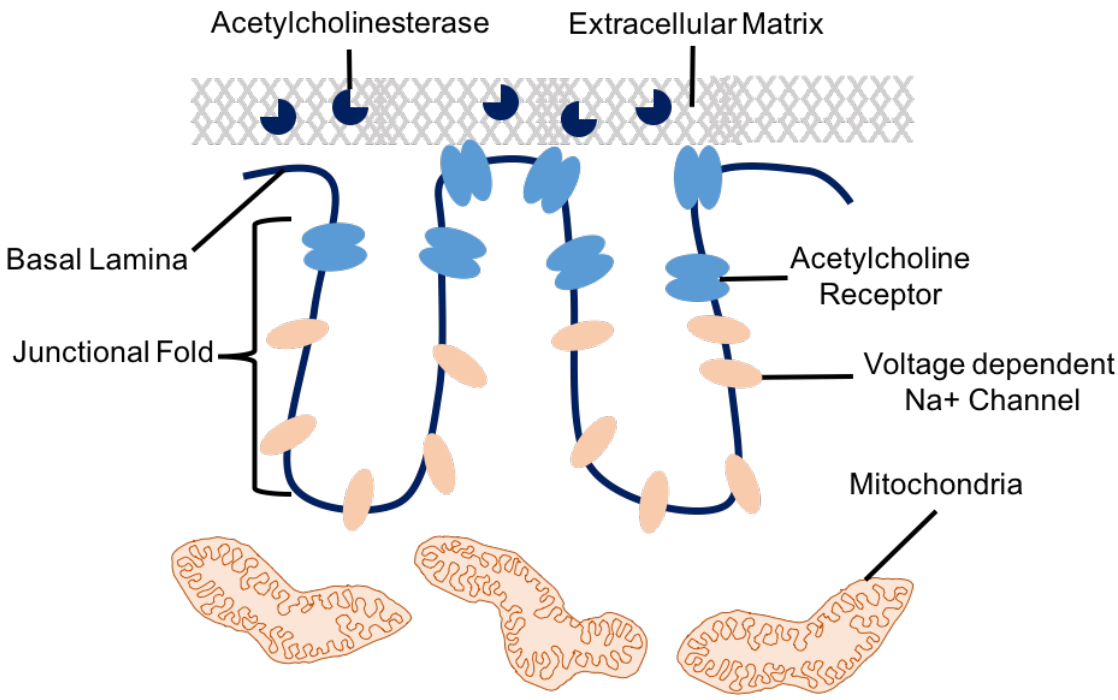

Figure 8: Postsynaptic end-plate. The postsynaptic end-plate features an extracellular matrix with acetylcholinesterases, a basal lamina membrane containing a high density of acetylcholine receptors and voltage-dependent Na+ channels. Unlike other synaptic junctions, the postsynaptic membrane folds in on itself, forming junctional folds. Finally, mitochondria are found at a high density at the end-plate.

The basal lamina is comprised of a complex extracellular matrix (ECM) that shapes an environment to enable intracellular cross-talk (225). Embedded in the ECM are secreted synapse specific structural glycoproteins, proteoglycans and growth factors (226). The basal lamina plays an informative role by providing 'homing signals' that help guide the presynaptic terminal to properly localize with the end-plate as well as direct and stabilize acetylcholine receptor clustering (227). Indeed, following denervation of motor nerve and myofiber destruction, axon reinnervation occurs at the original synaptic basal lamina. Myofiber regeneration also occurs at original synaptic sites on the basal lamina, even in the absence of the axon (172). Thus, the basal lamina both marks the location of NMJ and provides sufficient support that allows regenerating cells to survive even in the absence of a synaptic partner.

The basal lamina is also important for regulating neurotransmission. Acetylcholine esterases concentrated in basal lamina (3,000 per μm^2) rapidly catalyze the hydrolysis of acetylcholine that is not bound to acetylcholine receptor (~25,000 acetylcholine molecules/sec) (228). This is to ensure end-plate activation by acetylcholine does not persist after action potential has ended. Deficiency in acetylcholine esterase expression or activity have devastating consequences on neuromuscular transmission (229). Indeed, humans and mice with genetic deficiency of acetylcholine esterase exhibit altered synaptic structure, where clefts are degenerated and presynaptic terminals are partially demyelinated (230). At high doses chemical inhibitors of acetylcholine esterase, such as nerve gases and insecticides, have lethal consequences (231). Conversely, lower doses of acetylcholine esterase inhibitors have been to treat myasthenic crisis, severe muscle weakness due to poor neuromuscular transmission (231,232).

Unlike any other synapses, end-plate membranes have deep invaginations, called

junctional folds, which maximize surface area and enhance reliability of neuromuscular transmission (181). Within the membrane are the two protein complexes required to initiate and amplify local depolarization into action potential; ligand gated acetylcholine receptors and voltage gated Na^+ channels. Aside from different functions, acetylcholine receptors and voltage gated Na^+ channels are spatially segregated, occupying discrete areas which increases the reliability of neuromuscular transmission (170,172,233).

The crests of the junctional folds feature a high-density acetylcholine receptors clusters (~8700 acetylcholine receptor/μm^2 of postsynaptic membrane) that align with active zones (234). The density of acetylcholine receptors is influenced by trophic factors and volume of activity. Of particular importance, agrin protein secreted from the nerve fiber mediates acetylcholine receptor clustering (235,236). Mice lacking agrin lose acetylcholine receptors and structural proteins on the end-plate and the synaptic cleft (237), which can be reversed by ectopic expression of agrin (238). Acetylchoine receptor dynamics are also very sensitive to activity. In physiological conditions, acetylcholine receptors have a half-life of ~14 days, however, when the acetylcholine binding site is blocked by the competitive inhibitor α-bungarotoxin, the half-life is reduced to ~24 hours and cluster density diminishes (239,240). However, this is reversible by direct muscle stimulation or restoration of synaptic transmission (198).

Voltage gated Na^+ channels accumulate in the depths of the junctional folds and convert local depolarization initiated by acetylcholine receptor opening into a propagating action potential (241,242). Indeed, the Na+ current density at the end-plate is ~5-10 fold larger than extrajunctional membrane effectively lowering the threshold of an action potential (233,243,244). Under pathological conditions (e.g. myasthetic gravis and denervation), density

of voltage gated Na^+ channels is reduced, rendering myofibers weak or paralyzed due to loss of excitability (222). In sum, the structure and molecular organization of postsynaptic membrane facilitates specific and efficient neuromuscular transmission to help ensure that nerve impulses give rise to a myofiber action potential.

1.2.1.1. Myofiber mitochondria

Early electron microscopy studies revealed that like the presynaptic terminal, the junctional sarcoplasm has a high density of mitochondria (170,245). While end-plate membranes are readily identifiable with fluorescent molecules such as α-bungarotoxin, no method exists to isolate resident mitochondria for direct analysis. As a consequence, all mitochondria in the myofiber are analyzed, limiting the ability to elucidate whether mitochondria clustered at the end-plate represent a distinct population with unique biochemical functions (246). Nevertheless, myofiber mitochondria undoubtedly play a critical role in neuromuscular function by supporting basal myofiber processes (54), excitation-contraction coupling (141,247) and by maintaining NMJ stability and adaptability (248). Indeed, NMJ dismantlement seems to be preceded by deranged mitochondrial function (134,197,221). Conversely, augmentation of mitochondrial content in myofibers either by exercise training (249,250) or genetic manipulation (248,251,252) promotes NMJ remodeling and function, which alleviates conditions in which neuromuscular function is reduced.

Efficient muscle contraction and relaxation requires a constant supply of ATP and modulation of intracellular $[Ca^{2+}]$. Mitochondria are the most important sources of ATP and display a large capacity to increase respiration to meet energy demands, which can change up to 100-fold during active contraction (253,254). The majority of ATP is utilized during two cyclical processes during excitation-contraction coupling: the interaction of myosin-actin cross-bridges

and Ca^{2+} uptake by sarcoplasmic/endoplasmic reticulum ATPase (255). Myofiber contraction is initiated by release of Ca^{2+} from the sarcoplasmic reticulum, which induces an increase in Ca^{2+} in the sarcoplasm (69). Ca^{2+} binds to and causes a conformational change of the troponin complex (142,256), which in turn removes tropomyosin from myosin binding sites on actin . Hydrolysis of ATP by myosin ATPase energizes the myosin head to form a cross-bridge with an actin molecule (257). Upon the stepwise release of Pi and ADP, the myosin head changes conformation and exerts a torsional force to 'pull' the actin myofilament (143). The cross-bridge remains intact until another ATP is bound to myosin, at which point myosin detaches from the actin to then bind another. As the cross-bridge cycle continues, the myofiber shortens and generates force. At the end of the stimulus sarcoplasmic endoplasmic reticulum ATPase utilizes the energy from ATP hydrolysis to transport Ca^{2+} against the concentration gradient back into the sarcoplasmic reticulum (258). In the absence of ATP, cross-bridges do not dissociate and cytosolic Ca^{2+} remains elevated causing hypercontracture, which is observed during ischemia and rigor mortis.

The tight coupling of mitochondrial ATP production to the requirements of a contracting muscle is ensured by effects of Ca^{2+} on aerobic metabolism. As mentioned earlier, release of Ca^{2+} from the sarcoplamic reticulum elevates cytosolic Ca^{2+} and triggers Ca^{2} uptake into mitochondria in an electrochemical gradient-dependent fashion (141,259). Indeed, contractile waves, produced by depolarization-induced Ca^{2+} release, are associated with propagating waves of mitochondrial depolarization, consistent with Ca^{2+} entering the mitochondrial matrix (260,261). Furthermore, transient mitochondrial depolarization is directly related to the focal release of Ca^{2+} form sarcoplasmic reticulum (262). Increase in matrix Ca^{2+} activates Ca^{2+}-sensitive dehydrogenases, which are key rate-controlling enzymes in the TCA cycle and help to

prevent quick exhaustion of ATP during contraction (247). Kinetic analysis has revealed electron flux through complexes I, III, and IV of the electron transport system (ETS) and an increase of ATP production in response to Ca^{2+} in a dose-dependent manner (263). Deletion or mutation of the mitochondrial Ca^{2+} uniporter causes reduction in mitochondrial Ca^{2+} and subsequent dysfunction and leads to cellular damage and apoptosis. Patients and mice lacking mitochondrial Ca^{2+} uniporter suffer from ataxia and muscle weakness (264). Similarly, mice lacking MICU1, a myofiber specific component of the mitochondrial Ca^{2+} uniporter, present with multiple neuromuscular abnormalities, including altered balance and reduced muscle mass (264). Thus, like motor nerve fibers, Ca^{2+} uptake into mitochondria functions to maintain energy homeostasis in response to varying energy demands.

Defects in myofiber mitochondrial ATP production, Ca^{2+} buffering and dynamics have been implicated in development and progression of neuromuscular pathologies. Uncoupling of myofiber mitochondria causes muscle atrophy, NMJ dismantlement and degeneration of motor nerve fibers, similar to what is observed in ALS (134) and following IR injury (47,265). Similarly, patients and animals suffering from Duchene muscular dystrophy, caused by the loss of critical cytoskeletal proteins, exhibit abnormal NMJ structure and age-dependent loss of NMJ function (266). Mitochondrial dysfunction, such as abnormal respiration (267), Ca^{2+} signaling (268) and ROS detoxification (269), is evident in dystrophic myofibers. Such changes are thought to stem from down-regulation of metabolic gene expression and dysfunctional mitochondrial enzymes (270). Interestingly, an enhanced expression of the master regulator of mitochondrial biogenesis peroxisome proliferator-activated receptor γ coactivator 1α has been found to alleviate neuromuscular abnormalities from dystrophic mice by increasing the content of mitochondria (251). Aging is also associated with reduced muscle strength and mass, and

denervation (271,272). Comparison of young and aging rats revealed that gene expression and protein content of energy metabolism and neuromuscular function are depressed in aged animals, which is paralleled with a decrease in muscle size as well as mitochondrial respiration (273). These findings, in combination with the observation that promoting mitochondrial biogenesis benefits neuromuscular function, suggest therapies that target mitochondria may be the most efficacious.

Failure to maintain a healthy population of mitochondria in myofibers is partially blamed for functional degeneration. In particular, diminished capacity for mitochondrial removal by autophagy has been found to exacerbate muscle atrophy (274), blunt tissue recovery (275,276) and adaptation (277,278), and accelerate aging (279). Consistently, myofiber specific deletion of upstream autophagy regulatory protein unc-like protein 51 kinase hampers functional regeneration in skeletal muscle following myotoxic and IR injury and is associated with disrupted mitochondrial network remodeling (275,276). Furthermore, mice with depletion of autophagy related protein 7 display mitochondrial defects, myofiber atrophy, NMJ deterioration and accelerated aging (279). Together, these findings underscore the importance of mitochondrial quality for the maintenance of NMJ integrity.

Voluntary movement is dependent on constant exchange of information between nervous and skeletal muscle systems at the NMJ. Derangements in NMJ structure and function are a characteristic of diseases and traumas that cause weakness, muscle atrophy, frailty and/or paralysis. A considerable body of interdisciplinary studies has revealed that mitochondria play a key role in stabilizing NMJ and preserving neuromuscular cross-talk, and mitochondrial abnormalities contribute to the early processes of neuromuscular dysfunction. An in-depth spatial and temporal understanding of mitochondrial function and dynamics *in vivo* is necessary to fully

assess mitochondrial alterations under pathological conditions and will aid in development of preventative and therapeutic strategies to assuage neuromuscular dysfunction caused by disease or injury.

CHAPTER 2. MATERIALS AND METHODS

2.1 Animals

Animal procedures were conducted upon the approval of the Institutional Animal Care and Use Committee of the University of Virginia. All mice were housed in temperature-controlled (21°C) cages in a pathogen free room with a 12:12-h light-dark cycle, and had free access to water and normal chow. Wild type male C57Bl/6 mice between 9 and 12 weeks were obtained from Jackson Laboratory (Bar Harbor, ME). *MitoTimer* transgenic mice were generated by subcloning the *MitoTimer* coding region into an inducible expression vector downstream from LoxP-flanked chloramphenicol acetyltransferase (CAT) coding sequence (280) with a stop codon under the control of CMV early enhancer/chicken β actin (CAG) promoter (281). We called this construct *pCAG-CAT-MitoTimer,* which allows inducible expression of MitoTimer following expression of the Cre recombinase. When we co-transfected *pCAG-CAT-MitoTimer* with *pCMV-Cre*, an expression vector of Cre under the constitutively active *CMV* promoter, we observed MitoTimer expression while co-transfection with an empty vector, *pCI-neo*, showed no expression of MitoTimer. We then used the isolated DNA fragment containing the expression unit for pro-nuclei injection and generated transgenic mouse line in C57BL/6 background, call *CAG-CAT-MitoTimer* mice. After we crossbred the *CAG-CAT-MitoTimer* mice with a global inducible Cre mouse line, *CAG-Cre-ER^{T2}*, we injected the adult global inducible MitoTimer mice (CAG-CAT-MitoTimer;*CAG-Cre-ER^{T2}*) with tamoxifen (40 mg/kg, i.p.) daily for 7 days and observed expression of MitoTimer in the skeletal muscle, heart, lung, liver, kidney and brain (282).

2.2. Endurance Exercise Training

Mice in the exercise group were acclimatized to a cage with a locked running wheel for 3 days. Following acclimation mice were allowed free access to the running wheel, and all mice were provided food and water ad libitum for 5 weeks. Daily running distance was recorded via computer monitoring. Running wheels were locked 24-hours prior to additional experiments as described below.

2.3. Hind limb Ischemia-reperfusion injury

Under anesthesia (isoflurane in 2% oxygen) a 4.0-oz 1/8' orthodontic rubber band (DENTSPLY GAC International Inc 11-102-03) was applied above the greater tronchanter of the right femur using a McGivney Hemmrohidal Ligator as previously described (283) (**Figure 9**). Mice were conscious and monitored during the 1-hour ischemic period followed by tourniquet removal to induce reperfusion. Functional, morphological and biochemical analyses were performed at various time points ranging from 0 h (end of ischemia) to 28 days following IR.

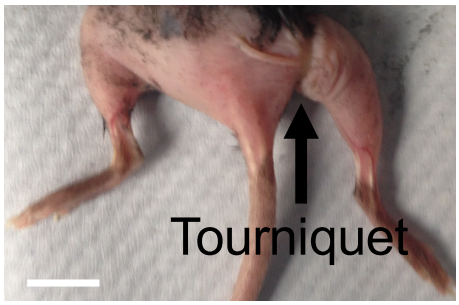

Figure 9: Tourniquet application to hindlimb. An image of shaved mouse hindlimbs with a unilateral rubber band tourniquet placed above the right femur to induced ischemia for 1 hour. Scale = 2 cm

2.4. Creatine Kinase Activity

Creatine kinase activity was measured following the manufacturer's instructions of a commercial kit (Sigma Aldrich MAK116). Blood was collected from the tail, incubated at RT for 30 minutes and then spun at 1,500 x g at 4°C for 30 minutes. The clear supernatant portion

was saved (serum) and the clot was discarded. The samples were aliquoted and stored at -80°C. At the time of the assay, the samples were thawed on ice and diluted 1:10 in dH_2O.

2.5. *In vivo* Muscle Function

Maximal isometric torque of the plantarflexors was assessed as previously described (275). Under anesthesia (1% isoflurane in oxygen) mice were placed on a heated stage in the supine position, and the right foot was secured to a foot-plate attached to a servomotor at 90° relative to the immobilized knee (Model 300C-LR; Aurora Scientific, Ontario, Canada) **(Figure 10)**.

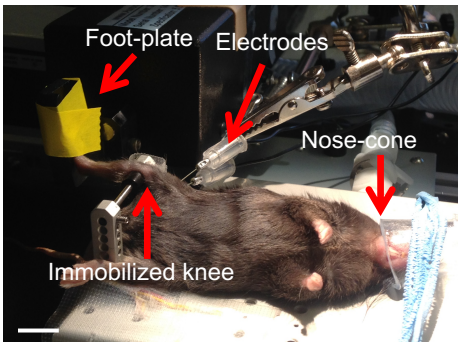

Figure 10:*in vivo* muscle function. An image of *in vivo* muscle contraction set-up for nerve-stimulation. Anesthesia is delivered through a nose-cone.

For nerve stimulated contractions (Nerve Stim), teflon coated electrodes were inserted percutaneously on either side of the sciatic nerve ~1 cm proximal to the knee joint. For direct muscle stimulation (Direct Stim), electrodes were inserted into the proximal and distal ends of the GA muscle. Peak isometric torque (mN●m), which is referred to as force, was achieved by varying the current delivered to the nerve or muscle with the following constant parameters: 10 Volts electric potential, 200 Hz stimulation frequency, 300 ms stimulation duration, and 0.3 ms pulse duration. To account for differences in body size among mice during longitudinal studies, force was normalized by body mass (g), which did not change significantly over the experimental time period. At the end of the experimental period, mice were sacrificed and

hindlimb muscles were collected and weighed. Specific force was calculated by dividing absolute force by plantarflexor muscles (sum of soleus, plantaris and gastrocnemius muscles) wet weight (mg).

2.6. Drug Treatment

MitoSNO and MitoNAP, generous gifts from Michael Murphy (Cambridge University), were dissolved in 0.9% sterile saline, filtered through 2 μM filter, kept on ice and protected from light immediately prior to the experiments. Saline, MitoSNO or MitoNAP were injected into the tibialis anterior (100 μL) and GA (150 μL) after 55 minutes of ischemia.

2.7. MitoTimer Analysis

MitoTimer is a mitochondria targeted fluorescent protein encoded from *MitoTimer* reporter gene that shifts emission from green fluorescent protein (GFP, excitation/emission 489/508 nm) to *Discosoma sp.* red fluorescent protein (DsRed excitation/emission 558/583 nm) upon oxidation. MitoTimer is a useful tool to measure mitochondrial oxidative stress (red:green ratio) (277,284). Images were acquired as previously described (277,284). Briefly, the sciatic nerve and plantaris muscle were harvested from the hindlimb and fixed in 4% paraformaldehyde (PFA) for 20 minutes, washed with PBS, and mounted on a gelatin coated slide with 50/50 PBS glycerol. Images were acquired via confocal microscopy using Olympus Fluoview FV1000. Quantification of the red:green ratio of MitoTimer signals in plantaris muscle and sciatic nerve was performed using a custom-designed Matlab-based algorithm. For MitoTimer and AchR analysis, plantaris muscle were first prepared as described above and then incubated with α-BTX

prior to confocal imaging. Analysis of MitoTimer at NMJ was done manually using ImageJ. All images were acquired with identical acquisition parameters for the respective tissue types.

2.8. NMJ Analysis

NMJ area and occupancy were assessed as previously described (285,286). Briefly, plantaris muscles were fixed in 4% PFA for 20 minutes, permeabilized in 3% Triton-X100 in PBS for 30 minutes and blocked in 1% Triton-X100 + 4% fatty acid-free BSA for 60 minutes at room temperature. The muscles were then incubated with primary antibodies against Tubulin β-III (Tuj1, Covance 801201, 1:100) and synaptic vesicle 2A (SV2, Abcam ab32942, 1:50) overnight at 4°C. The muscles were washed 3 times with PBS and then incubated with Goat-anti-Rabbit-FITC and Goat-anti-Mouse-FITC secondary antibodies for 2 hours at RT. Alexa Fluor 647 conjugated α-bungarotoxin (1μg/mL) (Thermo Scientific B35450) was added to the secondary antibodies after 1.5 hours. At the end of 2 hours, the muscles were rinsed 3 times for 5 minutes with PBS and then mounted on gelatin-coated sides using Vectashield (Vector Laboratories H-1000). Images were acquired using Olympus Fluoview FV1000. To assess the whole NMJ, Z-stacks were acquired using both 20x and 60x objectives. Only NMJ complete *en face* acquired at 60x were analyzed as previously described (PMC4282693, PMC4563167). Maximum intensity Z-stacks were reconstructed in ImageJ (National Institutes of Health) and underwent the following corrections in the order listed: background subtraction (50.0 pixels), despeckling, application of a Gaussian blur (2.0 radius) and conversion to binary. Occupancy was determined by dividing the area of the presynaptic structures by the area of postsynaptic structures (pre μm^2/post μm^2 x 100). Denervation is defined as the percentage of total NMJ in which the occupancy is <5%.

2.9. Immunoblotting

Tissues were homogenized in (1 mg/10 μL) 2x Sample buffer (80 mM Tris HCl pH 6.8, 2% SDS, 10% glycerol, 0.0006% bromophenol blue, 0.1 M DTT) containing 1 protease inhibitor tablet, 100 uL of phosphatase 2 and 3 (Sigma-Aldrich). Equal amount of protein for each sample was loaded on a 10% SDS-PAGE gel. Following electrophoresis, the proteins were transferred onto a nitrocellulose membrane, and the membrane was blocked with 5% dried milk and incubated with primary antibodies followed by incubation with secondary antibodies previously described (277). The primary antibodies used in the studies are: NDUFS1 (Thermo Scientific PA5-28220), Mito OXPHOS cocktail (abcam ab110413), 4-Hydroxynoneanal (ab48506), Calpain-1 (CST2556), Calpain-2 (CST2539), Actin (Sigma-Aldrich A2066).

2.10. Cryosectioning and Immunostaining

Immediately after dissection the plantaris muscle was embedded in a mold filled with Tissue Tek optimal cutting temperature compound (Fischer Scientiic 23-730-571) and then frozen in an isopentane slurry cooled by liquid nitrogen. Transverse sections were cut using a cryostat (5 μm), mounted on positively charged slides, thawed and air dried, then stored at -80°C. Cryosections of plantaris muscle were stained with hematoxylin and eosin (H&E) (287). Three digital images were acquired at 20x magnification, and centralized nuclei and fiber number were counted by a blinded investigator. For immunostaining, slides were removed from the freezer, fixed in 4% PFA for 10 minutes on ice, and then incubated in 0.3% Triton-X100 in PBS for 10 minutes. After rinsing with PBS, sections were circled using a hydrophobic pen and incubated with 5% normal goat serum (NGS) in PBS for 60 minutes. The samples were then

incubated with primary antibodies against Ncam (Abcam, ab9018) and laminin (Chemicon MAB1928) diluted 1:100 in NGS overnight at 4°C in a humidified chamber. The samples were washed and incubated with fluorescently conjugated secondary antibodies that had been diluted 1:100 in NGS for 60 minutes at RT. After a 10-minute incubation with 7.5 nM DAPI and being washed with PBS slides were mounted using Vectashield and glass coverslips. Images were acquired using Olympus Fluoview FV1000 with identical parameters. The number of fibers and fibers with intracellular staining of NCAM was counted by a blinded investigator.

2.11. Biotin-Switch

The biotin switch technique was employed to measure *S*-nitrosylated proteins in the GA and sciatic nerve as previously described (288). Briefly, tissues were homogenized in 1:10 mg tissue/mL lysis buffer (50 mM Tris HCL pH 7.5, 1 mM EDTA, 150 mM NaCl, 0.4% triton X-100, 0.1 mM neocuproine + 1 protease inhibitor tablet in 50 mL) by 3 strokes at medium speed of polytron. Positive and negative controls were created by incubating a muscle *in vitro* with 100 µM MitoSNO with or without 5 mM DTT, respectively, for 10 min at 37°C with shaking,. Lysate was then centrifuged at 4,000 rpm for 15 min at 4°C and the pellet was discarded. Protein concentration was determined using BCA assay (Pierce), and 100 µg of each sample was placed in 4 volumes of blocking buffer (9 volumes HEN + 1 vol 25% SDS containing 20 mM MMTS) for 1h at 55°C with shaking at 400 rpm (note: equal concentrations of each sample were saved to serve as input prior to blocking). Protein was precipitated by adding 2 volumes of ice-cold acetone and placed at -20°C for 30 minutes and spun at maximum followed by discarding the supernatant. Protein was suspended in 25 µL of 4 mM HPDP-biotin and 1 uL of 100 mM sodium ascorbate and incubated for 1 h at RT. HPDP-biotin was removed by precipitation with 2 volumes of acetone at -20°C for 30 minutes and then spun at maximum

speed for 30 minutes. The supernatant was discarded, and the pellet was resuspended in 100 µL HEN buffer (250 mM HEPES pH 7.7, 1 mM EDTA, 0.1 mM neocuproine). Afterwards, 200 µL of neutralization buffer (20 mM HEPES pH 7.7, 10 mM NaCl, 1 mM EDTA, 0.5% Triton X-100) and 50 µL streptavidin agarose (Sigma-Aldrich S1638) were added, and the samples were incubated at RT for 1 hour. The samples were then washed 5 times with neutralization buffer + 600 mM NaCl. The proteins were eluted in 2x Sample buffer (80 mM Tris HCl pH 6.8, 2% SDS, 10% glycerol, 0.0006% bromophenol blue, 0.1 M DTT) containing 1 protease inhibitor tablet, 100 uL of each phosphatase inhibitors. An equal amount of protein for each sample was loaded on a 10% SDS-PAGE gel. Following electrophoresis, the proteins were transferred onto a nitrocellulose membrane, and the membrane was blocked with 5% dried milk and then incubated with Rabbit anti-NDUFS1 (Thermo Scientific PA5-28220, 1:500) or a cocktail of mouse primary antibodies against complexes I, II, III, IV, and V of the ETS (abcam ab110413, 1:500) and Rabbit anti-Actin (sigma A2066, 1:5000).

2.12. Statistical Analysis

Statistical analysis was performed using GraphPad Prism software. All results are presented as means ± standard deviation (SD). Two-tailed t-test was used to compare body weight, creatine kinase, and force production between sedentary and exercise trained mice. One-way analysis of variance (ANOVA) was used to compare creatine kinase, muscle mass, maximum specific force, centralized nuclei, fiber size, NMJ denervation, MitoTimer red:green ratio over a time course. Two-way analysis of variance (Two-way ANOVA) was used to compare force produced by nerve and muscle stimulation at different time points (stimulation vs. time), and force of nerve and muscle stimulation between treatment groups (stimulation vs.

treatment). A significant interaction of 0.05 was required to perform a between-variable post-hoc analysis, in which case Tukey's honestly significance difference test was performed. $p < 0.05$ is considered statistically significant for all the analyses described above.

CHAPTER 3. MITOCHONDRIAL PROTEIN *S*-NITROSYLATION PROTECTS AGAINST ISCHEMIA REPERFUSION-INDUCED DENERVATION AT NEUROMUSCULAR JUNCTIONS IN SKELETAL MUSCLE

3.1. Introduction

Neuromuscular junction (NMJ) is a unique microdomain where a motor nerve fiber and skeletal muscle fiber interface to coordinate voluntary muscle contractions. Conditions in which neuromuscular function is compromised, such as amyotrophic lateral sclerosis (136), aging (285), muscular dystrophies (289) and traumatic injuries (290), are characterized by deterioration of NMJ. In particular, following certain types of surgeries or as a first response to traumatic injury, in which a tourniquet is applied to control blood flow, skeletal muscle and motor nerve fibers are often damaged by ischemia reperfusion (IR), caused by interruption in tissue perfusion and subsequent restoration of blood flow. In addition to muscle weakness and atrophy (291,292), IR injury can cause irreversible nerve and NMJ damage (10,245), all of which hinder functional recovery of the affected skeletal muscle. However, we know little about the underlying mechanism(s) of IR-induced neuromuscular damage, and hence there is currently no reliable and effective intervention (6,293,294).

Mitochondria are enriched on the pre- and post- synaptic sides of NMJ (295,296) and are essential for NMJ development and stability, and neurotransmission (194,297,298). Perturbations that alter mitochondrial energy production, Ca^{2+} buffering, or increase oxidative stress, play a causal role in NMJ degradation and neuromuscular dysfunction (136,299). In the context of IR injury, excessive generation of mtROS, which leads to mitochondrial oxidative stress, are considered central to the initiation and exacerbation of IR pathology (19,78). Mitochondria

transfer electrons through the electron transport system (ETS) to drive the formation of adenosine triphosphate (ATP), which serves as chemical energy storage used directly for all biological processes (23). During normal mitochondrial oxidative respiration, a small percentage of electrons escape the ETS and form superoxide (83), which is rapidly scavenged and detoxified by the resident antioxidant enzymes and molecules (300,301). During ischemia, tissue oxygen supply is discontinued and mitochondrial oxidative respiration suspended (302). Depending on the duration of ischemia, there will be insufficient production of ATP and accumulation of ADP as well as other intermediate metabolites and reducing equivalents, such as NADPH and succinate (50,51). Upon reperfusion, these metabolic buildups cause a surge of mtROS from the ETS (83,303) When the production of mtROS exceeds the capacity of the mitochondrial antioxidant defense system, it results in oxidization of cellular components (e.g. DNA, protein and lipid, etc.), causing tissue damage and dysfunction and/or cell death (75,304). Furthermore, mtROS may further damage mitochondrial structure and impair function (92), leading to a vicious cycle (29,30). Therefore, prevention of mtROS production or neutralization of the reactive molecules may prove be the most efficacious intervention against IR injury.

Nitric oxide (NO) and its derivatives have been found to interact with the mitochondrial proteome, modulating respiration and providing cytoprotective effects (305) in the context of IR injury. In particular, mitochondrial protein *S*-nitrosation (SNO) reversibly inhibits mitochondrial respiration, prevents mtROS production by reverse electron transfer (RET) at complex I of the ETS (50), and shields protein cysteine residues from irreversible oxidation (306,307). Enhancement of mitochondrial SNO either by ischemic preconditioning (308) or treatment with NO donor (94,309–311) has been found to be protective in models of myocardial infarction; however, whether such strategies are applicable for conditions of neuromuscular injuries and

how enhanced mitochondrial SNO might lead to the protection are unknown. In the present study, we utilized a clinically relevant model of tourniquet-induced IR injury in mouse hindlimb to test whether pharmacological augmentation of mitochondrial SNO could preserve muscle and/or motor nerve structural integrity and function into the recovery period. We employed state-of-the-art mitochondrial reporter technology to elucidate the underlying mechanism(s) of the pathology of IR injury with a focus on mitochondrial oxidative stress in both adult skeletal muscles and motor nerve fibers.

3.2. Results

3.2.1. Tourniquet-induced IR in skeletal muscle causes both nerve and muscle damage.

To determine the impact of IR injury on nerve and muscle function, we applied a tourniquet above the right femur of mice to induce ischemia for 1 hour, a duration compatible with the clinical guidelines, followed by removal of tourniquet to initiate reperfusion (312). We performed a longitudinal study, in which we measured the maximal tetanic force production of the planter flexors *in vivo* via nerve stimulation or direct muscle stimulation. These protocols provide insight into neuromuscular transmission and force generating capacity of the muscle, respectively (293,313). In un-injured mice (sham), force production resulting from nerve and muscle stimulations was indistinguishable (**Figure 11a**). However, at day 7 following IR injury, force generated by nerve and muscle stimulations were reduced by 80% and 50%, respectively, compared to the sham (**Figure 11a**). The additional deficit in force production via nerve stimulation is indicative of impaired neuromuscular transmission. At day 14 post injury, nerve stimulation-elicited force production became equal to that produced by muscle stimulation while the latter had not changed. By day 28, force production by muscle and nerve stimulation

significantly increased and had recovered to sham levels when normalized to muscle weight **(Figure 11b)**. These findings demonstrate that IR causes injury to nerve and muscle and neuromuscular transmission recovers prior to functional regeneration of muscle.

To assess muscle injury, we measured serum creatine kinase (CK) activity, a marker of muscle damage (314,315). CK was elevated 4-fold between 3 and 12 hours post-IR compared to the sham before returning to baseline after 1 day (**Figure 11c**). This initial, transient increase in CK activity suggests that a single damaging event had occurred to the muscles. Muscle damage was further confirmed by reduced gastrocnemius (GA) wet weight to 40% of the sham control at day 14 (**Figure 11d**). Furthermore, histological analysis by H&E staining revealed a gradual increase of centrally located myonuclei over the 28-day experimental period (**Figure 11e and 11f**), suggestive of ongoing muscle regeneration (316).

Finally, we examined innervation at neuromuscular junctions (NMJ) in the middle portion of the plantaris muscle. Muscle contraction begins at NMJ where neurotransmitter acetylcholine is released by the motor nerve (pre-synaptic) and binds to its receptor on the muscle (post-synaptic), initiating a cascade of events that lead to contraction and force generation (317). Impairment of structure and/or function on either pre- or post-synaptic side of NMJ will impair muscle contraction (131). We assessed NMJ innervation by measuring the overlap of immunoreactivity of the presynaptic markers β-III tubulin (Tuj1) and synaptic vesicle 2a proteins with the post-synaptic acetylcholine receptor detected by α-bungarotoxin (α-BTX). We found a significant reduction in Tuj1/Synaptic vesicle 2 and α-BTX overlap at 3 hours following IR injury compared to the sham control. This was followed by a partial recovery at day 28 (**Figure 11g and 11h**). Importantly, the reduction in Tuj1/synaptic vesicle 2-α-BTX overlap was due to loss of immunoreactivity of the pre-synaptic structures, indicative of NMJ

denervation. These data suggest that 1-hour tourniquet application followed by reperfusion leads to both muscle and nerve injury and also raises the possibility that functional recovery of skeletal muscle may, at least in part, depend on motor nerve recovery.

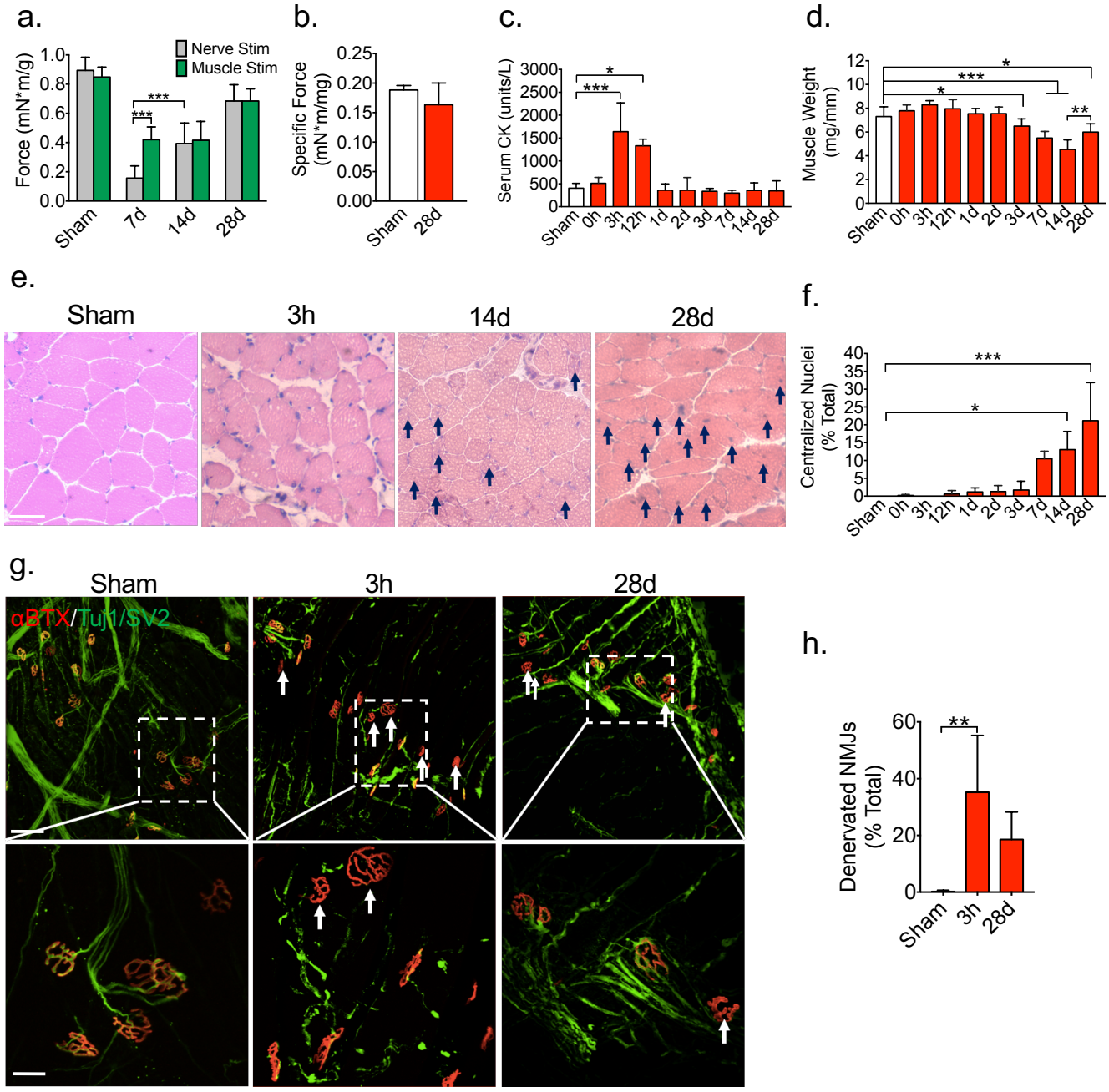

Figure 11. Tourniquet-induced IR in skeletal muscle causes both nerve and muscle damage. To determine the consequence of IR on skeletal muscle and motor nerve fibers a rubber band was applied to induce ischemia and released after 1 hour to initiate reperfusion. Muscle function and muscle injury as well as motor nerve innervation were assed at indicated time points over 28 days. (a) Comparison of tetanic force production of plantar flexors by nerve stimulation or muscle stimulation after IR at multiple time points (** and *** denote $p < 0.01$ and $p < 0.001$, respectively, n = 6). Other statistically significant comparisons are presented in supplemental Table 1. (b) Specific tetanic force 28 days following injury. (c) Serum creatine kinase activity (* and *** denote $p < 0.05$ and $p < 0.001$, respectively, n = 3-5). (d) Wet weight of GA muscle normalized by tibia length (mm). (*, ** and *** denote $p < 0.05$, $p < 0.01$ and $p < 0.001$, respectively, n = 6-8). (e) Representative light microscope images of H&E stained skeletal muscle cross sections and (f) percentage of fibers with centralized nuclei (Scale = 100 μm* and *** denote $p < 0.05$ and $p < 0.001$, n=3-5). (g) Representative confocal images of α-bungarotoxin (α-BTX, red) and beta III-tubulin/synaptic vesicle protein-2 (Tuj1/SV2, green) (Scale = 50 μm and 20 μm for the top panel and bottom enlarged panel, respectively) and (h) percentage of denervated NMJ following IR. (**$p < 0.01$, n = 5-7). Data are represented as mean ± SD.

3.2.2. Ischemia-reperfusion causes mitochondrial oxidative stress in skeletal muscle, motor nerve and NMJ.

Since mtROS production is considered central to IR injury we sought to determine whether tourniquet-induced IR causes mitochondrial oxidative stress within the neuromuscular system. To address this question we crossed *CAG-CAT-MitoTimer* mice with *CAG-CreER*^{T2} mice to obtain *MitoTimer* reporter mice with global inducible expression of a novel redox-sensitive mitochondrial-targeted reporter gene, *MitoTimer* (275,277,284). We observed a significant increase in MitoTimer red:green in plantaris muscle (**Figure 12a and 12b**) and sciatic nerve (**Figure 12c and 12d**) 3 hours following IR injury, emblematic of increased oxidative stress (275,277,284). To assess the mitochondrial oxidative stress at NMJ we utilized α-BTX to identify NMJ and imaged areas where MitoTimer and α-BTX overlapped. (Figure 10e and 10f). In accordance with electron microscopy studies that show an enrichment of mitochondria at NMJ (297), MitoTimer fluorescence was concentrated in a similar pattern as α-BTX. Moreover, MitoTimer red:green in this region was significantly greater 3 hours following IR as compared to the sham control, providing the first quantitative measurement of oxidative stress in the mitochondria of NMJ *in vivo*. Clustering of MitoTimer signal with α-BTX was confirmed to be indicative of mitochondria at the NMJ using MitoTimer with Tuj1 and α-BTX or MitoTracker and α-BTX (**Figure 13a and 13b**). These findings demonstrate that IR causes oxidative stress in plantaris muscle, sciatic nerve and NMJ.

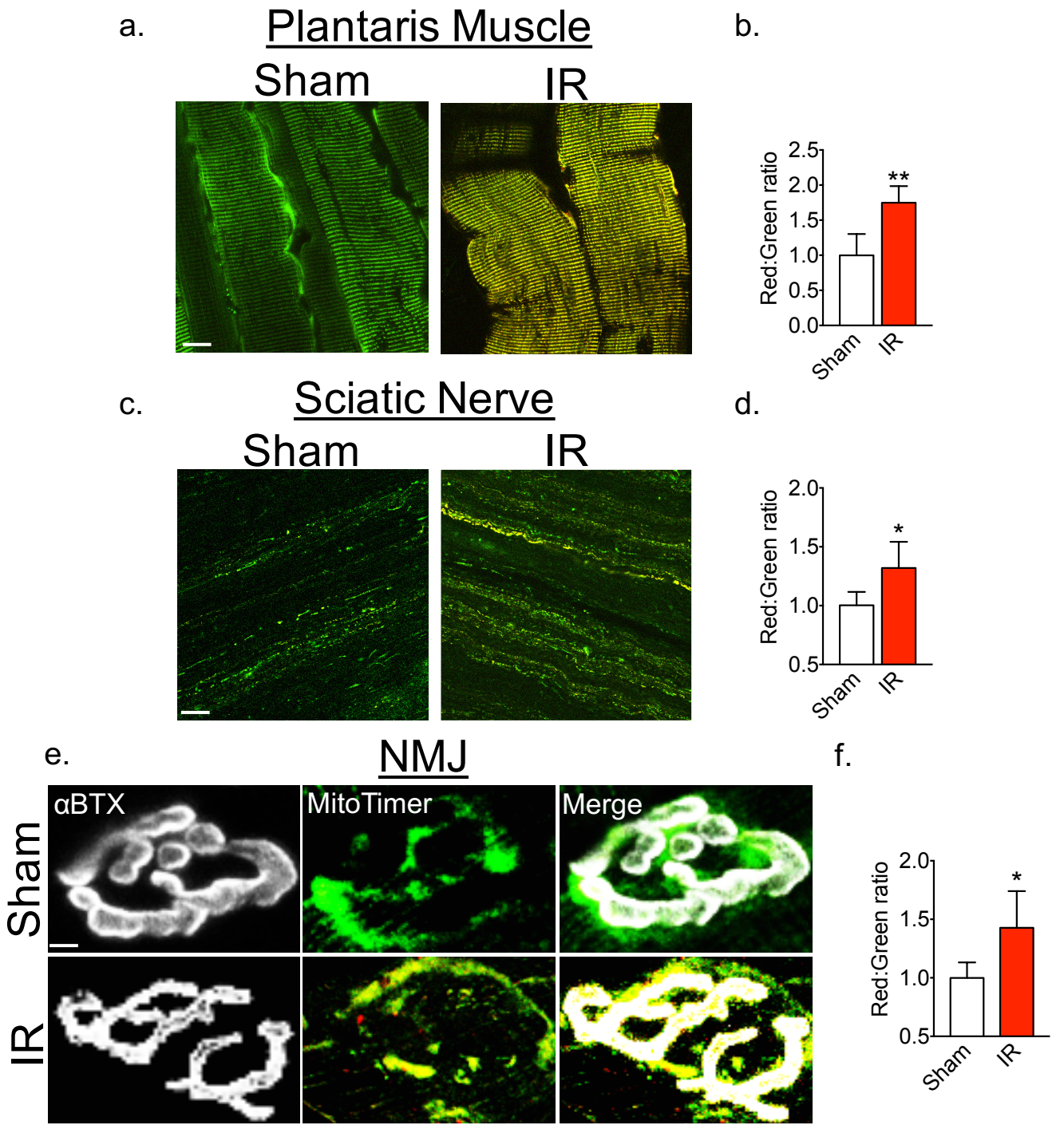

Figure 12: IR injury causes mitochondrial oxidative stress in skeletal muscle, motor nerve and NMJ. To determine the impact of IR on mitochondrial oxidative stress *MitoTimer* Tg mice were subjected to IR followed by 3 hours of reperfusion. Representative confocal images and quantification of MitoTimer red:green in plantaris muscle (PL) (a and b) and sciatic nerve (SN)

(c and d) (*p<0.05, **p<0.01 n=3-4). (e) Representative images of α-BTX (gray) and MitoTimer (green and red) colocalization with NMJ. (f) Quantification of MitoTimer red:green ratio at the NMJ (*p<0.05 n=3). Data are represented as mean ± SD.

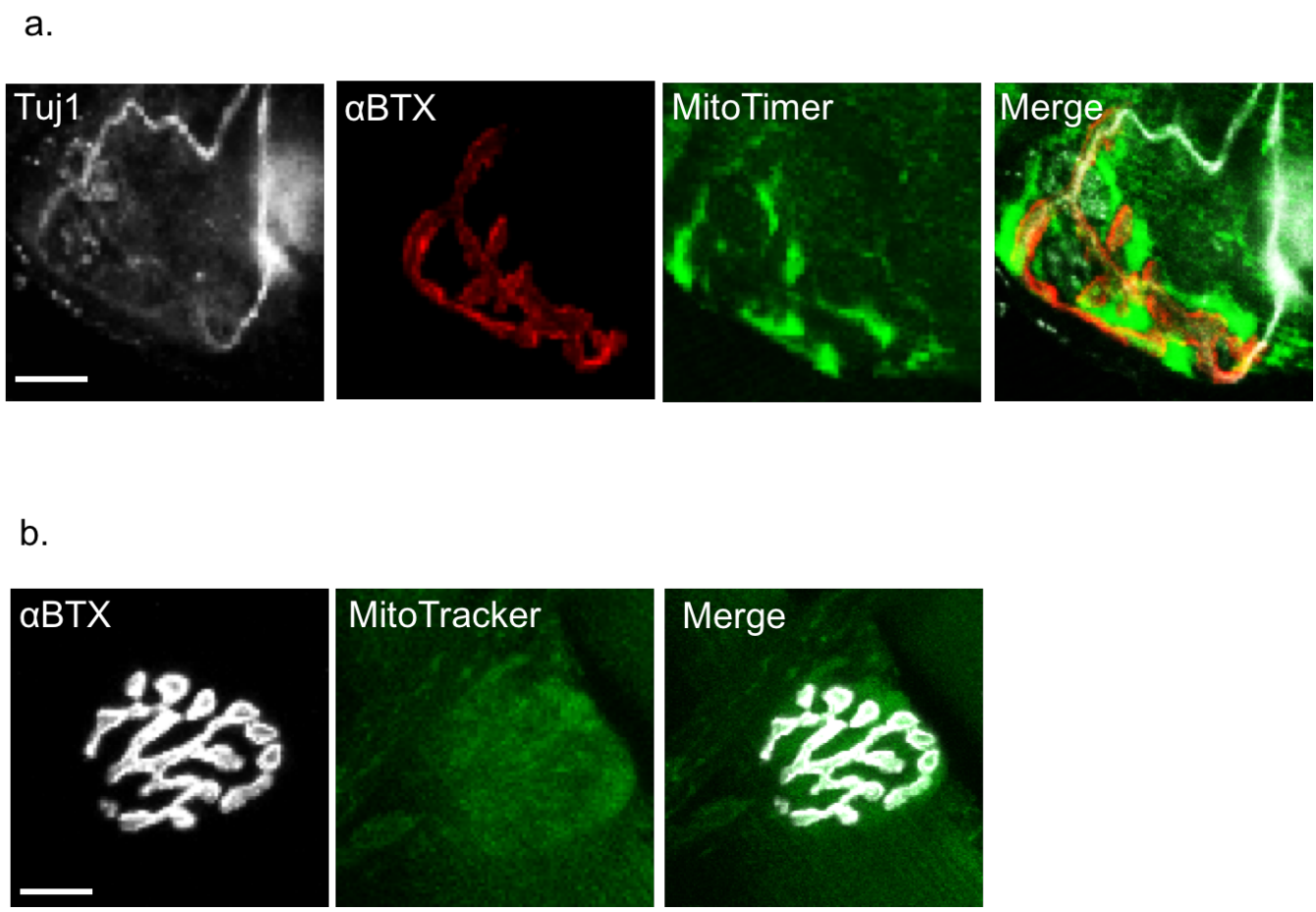

Figure 13: Development of a method to assess mitochondria oxidative stress at NMJ. Skeletal muscle from *MitoTimer* transgenic mice was collected, and motor nerve and NMJ were identified. (a) Representative confocal images of the motor nerve (gray), α-BTX (red), and MitoTimer (green), and merged channels (n=3). (b) Representative confocal images of α-BTX (gray), MitoTracker (green), and merged channels (n=3). Data are represented as mean ± SD

3.2.3. MitoSNO protects motor nerve function leading to improved functional regeneration of skeletal muscle.

Mitochondrial SNO has been found to reversibly depress mitochondrial respiration, reduce mtROS generation and shield cysteine residues from oxidation (96), we investigated whether promoting mitochondrial SNO was sufficient to attenuate muscle and/or nerve damage. We administered saline, MitoSNO (a mitochondrial targeted *S*-nitrosothiol) or MitoNAP (the thiol precursor of MitoSNO included to jettison the non-SNO effects of MitoSNO), which we identified as a critical time point for MitoSNO-mediated effects (38). To determine the consequence of MitoSNO treatment following IR injury, we measured tetanic force production *in vivo* by muscle and nerve stimulations. At day 7 post-IR, force production via nerve stimulation was significantly greater in MitoSNO-treated muscles compared to MitoNAP and saline (**Figure 14a**), providing the first evidence of an intervention to protect motor nerve (293,318). Conversely, force production induced by direct muscle stimulation was reduced similarly in saline-, MitoNAP- and MitoSNO-treated hindlimb muscles compared to the sham control (**Figure 14a**), suggesting an equal level of damage to the muscles under these conditions. At day 14 following injury, neuromuscular transmission had recovered in all groups, but MitoSNO-treated muscles generated significantly greater force, suggesting that MitoSNO treatment promotes functional regeneration of skeletal muscle following IR injury. Importantly, administration of MitoSNO after 10 minutes of reperfusion did not preserve nerve or muscle function following IR injury (**Figure 15a and 15b**).

Next, we assessed muscle mass and found a similar reduction (40%) in of gastrocnemius muscle wet weight in saline-, MitoNAP-, and MitoSNO-treated groups mice compared to the sham at 14 days post-IR (**Figure 14b**). Analysis of specific force revealed that MitoSNO-treated

muscle specific force production was indistinguishable from sham and significantly higher than saline- and MitoNAP- treated muscles (**Figure 14c**). These data indicate that MitoSNO treatment did not lead to a complete recovery of muscle mass but led to complete recovery of muscle contractile function per unit of muscle volume. Additionally, lack of protection provided by administration of MitoNAP suggests that attenuation of injury following MitoSNO treatment is due to the presence of the NO moiety, which transnitrosylates cysteine residues, rather than the antioxidant properties of the free thiol. Thus, we excluded MitoNAP from subsequent experiments.

To confirm that intramuscular injection of MitoSNO during ischemia enhances mitochondrial protein SNO, we assessed mitochondrial protein SNO in gastrocnemius muscle and sciatic nerve using a biotin switch assay (288). The levels of SNO of ETS complex I (NADH oxidoreductase 75 kDa subunit), II (Succinate dehydrogenase iron-sulfur subunit B), III (Cytochrome c oxidase subunit 1), and V (ATP synthase subunit α) were significantly elevated compared to saline-treated muscle and Sham in the muscle (**Figure 14d and 14e**) and nerve (**Figure 14f and 14g**), validating enhanced mitochondrial protein SNO by intramuscularly injection of MitoSNO. Taken together, these findings suggest that MitoSNO treatment enhances SNO of mitochondrial proteins and protects motor nerve and/or NMJ, leading to improved contractile function recovery post-IR injury.

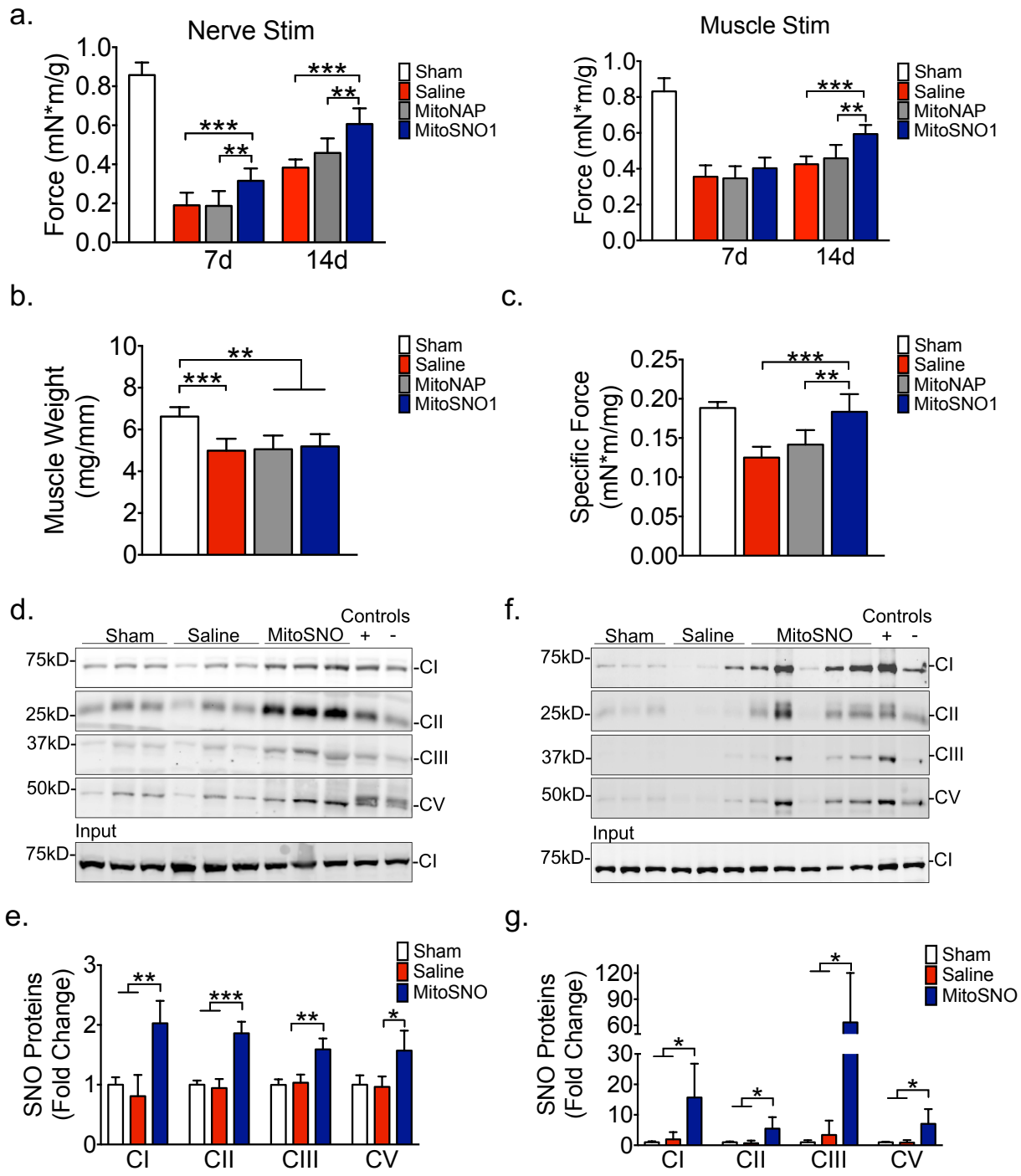

Figure 14: MitoSNO preserves neuromuscular function and facilitates recovery of muscle force. To determine whether enhancement of mitochondrial protein SNO could attenuate IR injury to the nerve and/or skeletal muscle, saline, MitoSNO (a mitochondrial targeted SNO), or MitoNAP (the thiol precursor of MitoSNO) were injected i.m. 5 minutes prior to tourniquet

removal. Mitochondrial protein SNO, nerve and muscle function, and muscle mass were measured at indicated time points. (a) Maximum tetanic force produced by nerve or muscle stimulation at days 7 and 14 following IR (**$p < 0.01$ and ***$p < 0.001$, n = 6-9). (b) Mass of GA at day 14 normalized to tibia length (mm) (***$p < 0.001$, n = 6). (c) Nerve-stimulated specific force at day 14 (***$p < 0.001$, n = 6). Immunoblots of complexes I, II, III, and V of the ETS from GA muscle (d) and sciatic nerve (f) following the biotin switch protocol. Positive and negative controls were generated by incubating respective tissues *in vitro* with either MitoSNO and MitoSNO + Dithiothreitol, which reduces SNO bonds, respectively. Quantification of immnoblot from GA (e) and SN (g) (*$p < 0.05$, **$p < 0.01$ and ***$p < 0.001$, n = 3-5). Data are represented as mean ± SD.

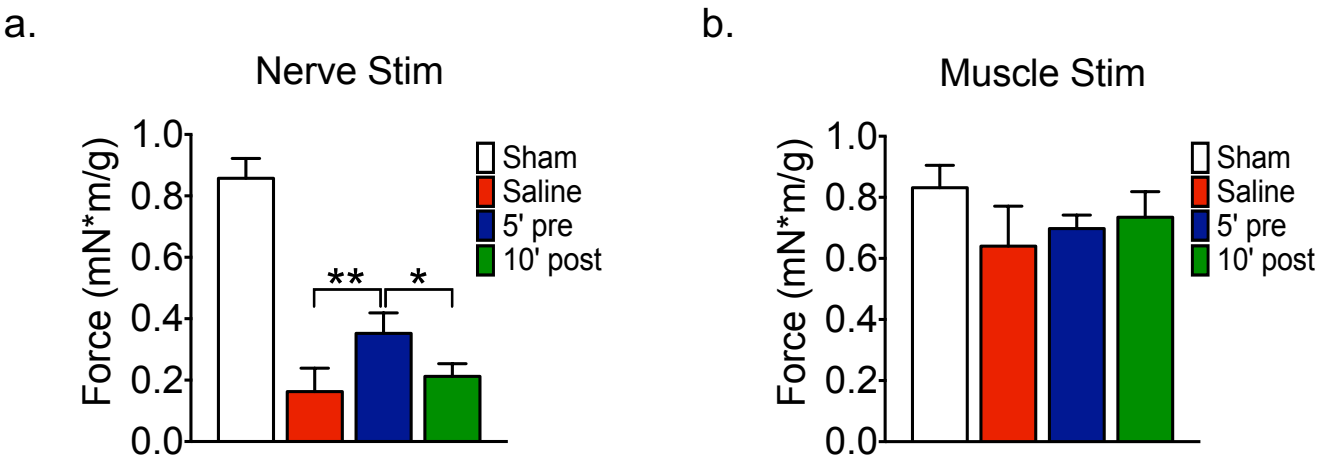

Figure 15: Administration of MitoSNO during reperfusion does not protect nerve or muscle against initial IR injury. To determine whether the timing of MitoSNO administration was of consequence, mice were subjected to IR, and peak force production by motor nerve and direct muscle stimulation was measured 1 day following injury. (*$p < 0.05$ and **$p < 0.01$, n = 4). Data are represented as mean ± SD

3.2.4. MitoSNO treatment preserves innervation at NMJ following IR.

To elucidate the impact of mitochondrial SNO on neuromuscular system, we subjected mice to IR with or without treatment with MitoSNO. Following IR, MitoSNO-treated muscle displayed a preserved overlap of α-BTX and Tuj1/SV2 while saline-treated muscle displayed significant loss of this overlap, suggesting MitoSNO-mediated protection against IR-induced denervation at NMJ (**Figure 16a and 16b**). This difference of innervation at NMJ between saline- and MitoSNO-treated muscles was maintained up to day 14 days post-IR. Additionally, the number of muscle fibers expressing neural cell adhesion molecule (Ncam), a marker of denervation (319), was increased at day 14 in saline-treated muscle compared to sham control, which was profoundly attenuated by MitoSNO treatment (**Figure 16c and 16d**). These findings provide additional evidence for the protective effect of MitoSNO on NMJ from IR injury.

To assess the impact of MitoSNO treatment on muscle damage, we measured serum CK activity 3 hours after IR and observed a 6-fold increase in serum CK activity (**Figure 16e**) in Saline and MitoSNO groups compared with Sham group, suggesting a comparable degree of muscle damage. Histological analysis at day 14 revealed a significant increase in centralized nuclei in Saline compared to Sham group; the increase of central nuclei in the MitoSNO group was not statistically reduced, suggesting the same degree of muscle damage by IR following treatment with MitoSNO (**Figure 16f and 16g**). Together, these data show that enhancing mitochondrial SNO by intramuscular injection of MitoSNO prior to reperfusion protects against IR-induced denervation at NMJ, which leads to overall improved functional recovery of muscle following IR.

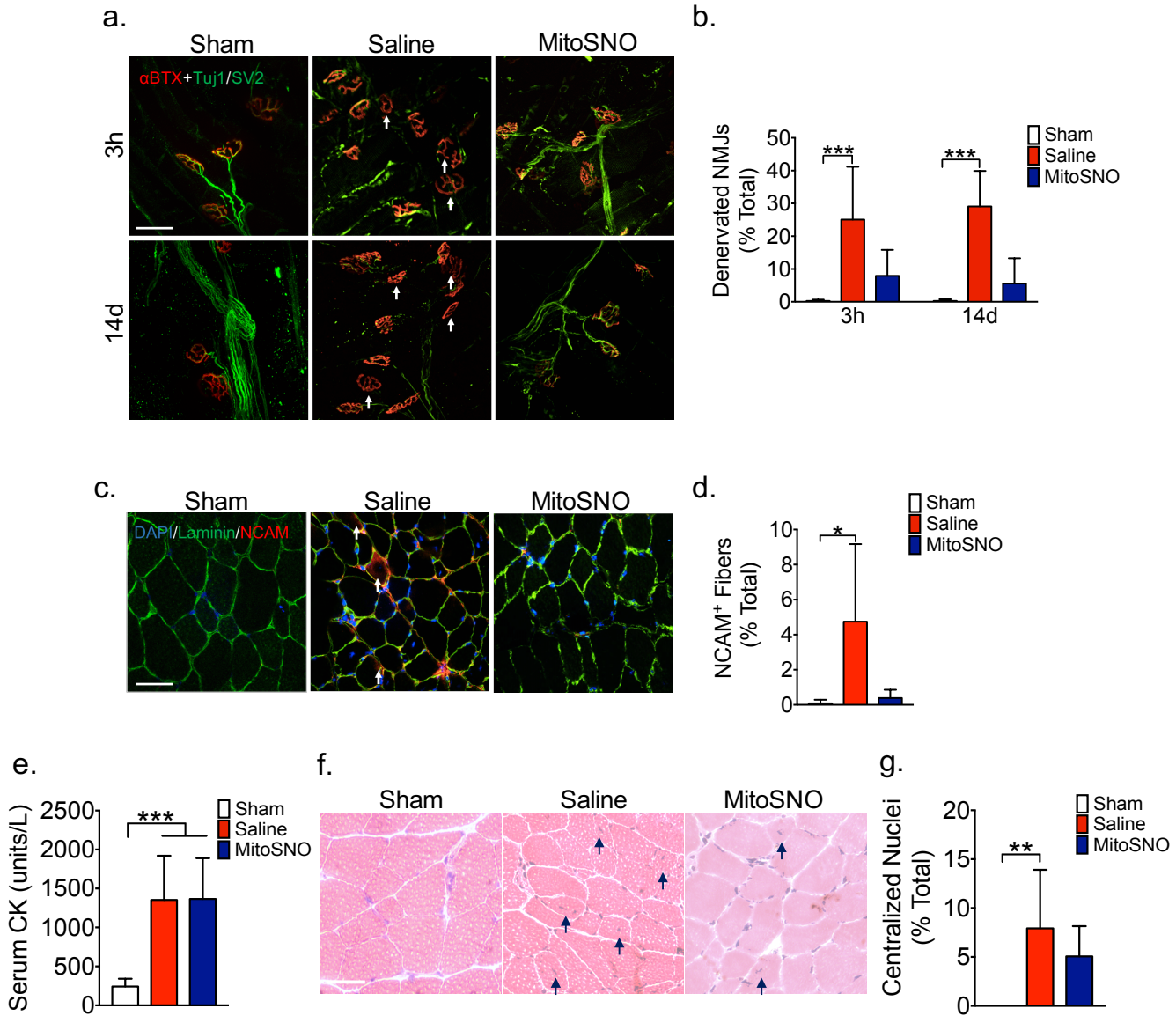

Figure 16: MitoSNO attenuates denervation of NMJ. To elucidate the consequence of MitoSNO treatment on innervation at NMJ and muscle injury, we subjected mice to sham, IR + saline, or IR + MitoSNO procedures. (a) Representative confocal images of denervation at NMJ 3 hours and 14 days following IR; (b) Quantification of the percentage of denervated NMJ (scale = 20 μm, ***$p < 0.001$, n = 5-6); (c) Representative confocal images of transverse sections of skeletal muscle expressing NCAM (red) and laminin (green), and DAPI staining (blue); (d)

Quantification of the percentage of $Ncam^+$ fibers at 14 days following injury (scale = 100 μm, *p < 0.05, n = 4); (e) Serum creatine kinase activity 3 hours following IR (**$p < 0.01$, ***$p < 0.001$, n = 6); (f) Representative images of H&E stained transverse sections of skeletal muscle; and (g) Quantification of percentage of fibers with centralized nuclei 14 days following IR (scale = 100 μm, **$p < 0.05$, $p < 0.001$, n = 4). Data are represented as mean ± SD.

3.2.5. MitoSNO treatment reduces IR-induced mitochondrial oxidative stress in the motor nerve.

To determine whether reduction of mitochondrial oxidative stress underlies MitoSNO-mediated protection of the nerve function and innervation at NMJ, we subjected *MitoTimer* reporter mice to IR injury. IR injury led to a significant increase in MitoTimer red:green ratio in plantaris muscle (**Figure 17a and 17b**), sciatic nerve (**Figure 17c and 17d**) and NMJ (**Figure 17e and 17f**) 3 hours following IR, indicative of increased mitochondrial oxidative stress in these tissue entities in the hindlimb (275,277,284). Treatment with MitoSNO significantly attenuated the increase of MitoTimer red:green ratio in the sciatic nerve and NMJ, but this effect in plantaris muscle was not statistically significant. Since the redox sensitive residue of MitoTimer is tyrosine 67 (320), which cannot undergo SNO, the reduction of MitoTimer red:green ratio following MitoSNO treatment in the sciatic nerve and NMJ is likely a consequence of reduced mtROS rather than direct shielding by SNO. Collectively, these findings suggest that MitoSNO treatment reduces IR-induced mitochondrial oxidative stress in the motor nerve, leading to preservation of motor nerve/NMJ structure and neuromuscular transmission, which facilitate functional rehabilitation of the muscle following IR (**Figure 18**).

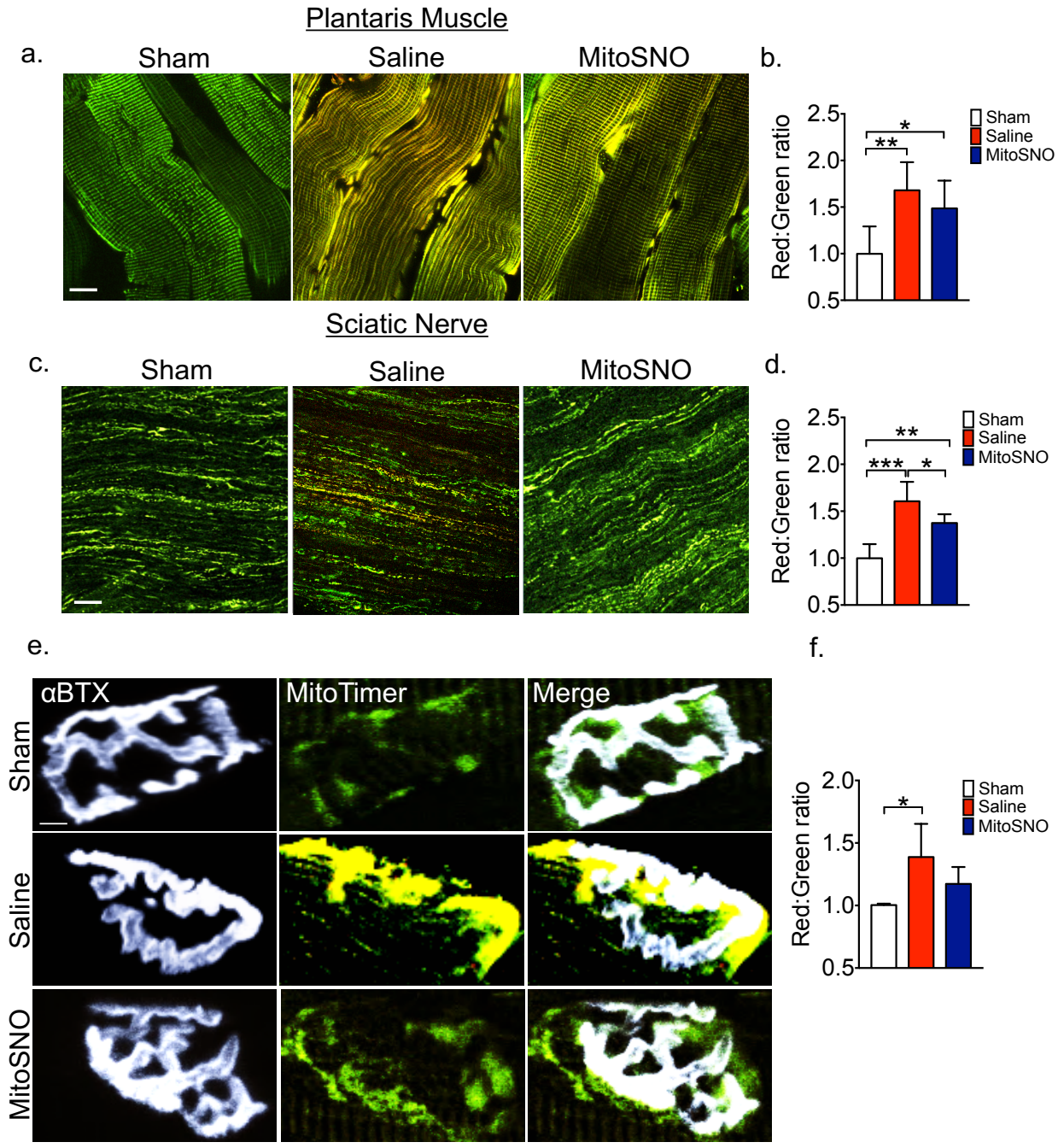

Figure 17: MitoSNO reduces IR induced mitochondrial oxidative stress. To determine the effect(s) of MitoSNO treatment on nerve and muscle mitochondria we subjected whole body inducible *MitoTimer* transgenic mice to IR and collected the PL and SN for whole-mounted confocal imaging at 3 hours following injury. Representative confocal images and quantification

of MitoTimer red:green ratio in plantaris muscle (a and b), sciatic nerve (c and d), and NMJ (e and f), scale bar = 50 μm. (*$p < 0.05$, **$p < 0.01$ and ***$p < 0.001$ n = 4-7). Data are represented as mean ± SD.

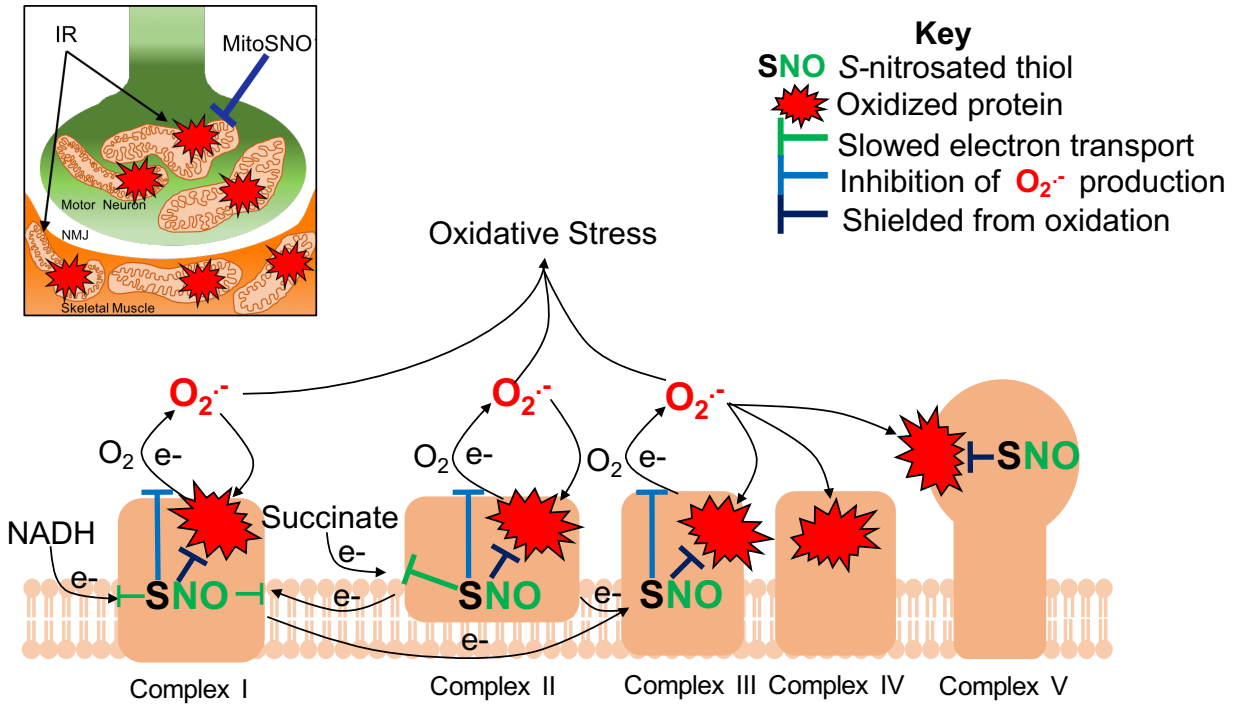

Figure 18: Summary of principal findings. 1-hour IR causes oxidative damage to mitochondria of the motor nerve and skeletal muscle leading to denervation of the NMJ and compromised muscle contractile function. Treatment with MitoSNO preserves innervation at NMJ and motor nerve function by reducing mitochondrial oxidative stress by one or more of the three possible mechanisms: slowing electron transport by inhibiting oxidation of NADH and FADH2 by complex I and II, respectively, preventing the production of superoxide and shielding residues from irreversible oxidation by ROS.

3.3. Discussion

Impaired neuromuscular function, due to NMJ injury, is central to a number of diseases and traumas that affect muscle mass and force production, causing impairments of voluntary movement. While the mechanism(s) underlying deterioration in neuromuscular function and NMJ are still being uncovered, excessive generation of mtROS and consequential oxidative stress predominate (135,136). However, until now, there has been no therapeutics that directly target mitochondria to preserve neuromuscular integrity. In this study, we sought to elucidate the consequence(s) of IR injury on the mitochondrial oxidative status and its impact on skeletal muscle and motor nerve function by employing a model directly relevant to humans following procedures that employ a tourniquet to control blood flow. We obtained functional, morphological, and biochemical evidence that recapitulates many of the consequences of IR injury observed in human skeletal muscle and motor nerve fibers (10,321). Furthermore, we found that treatment with MitoSNO, a mitochondria-targeted molecule that enhances SNO, protected motor nerve fibers against IR injury and improved functional regeneration of the affected skeletal muscle. These findings identify intramuscular injection of MitoSNO as an effective intervention against IR injury and highlight the importance of nerve function on muscle recovery from IR injury.

Accumulation of oxidative stress within the NMJ mitochondria is thought to play a causal role in neuromuscular dysfunction. Despite the recognized importance of mitochondria in neuromuscular function, technologies in which to assess mitochondrial morphology, function, and/or integrity at NMJ have been limited to electron microscopy (297,322), *in vitro* cell culture (323), or extrapolation of studies conducted in separate categories of nerve synapses using a variety of fluorescent probes (194). However, these aforementioned approaches do not provide

insight into mitochondrial oxidative stress in NMJ *in vivo*. Here, we developed and utilized a novel transgenic mouse line, in which *MitoTimer,* a reporter gene for measuring mitochondrial oxidative stress, is inducibly expressed in all tissues of the body. We discovered that IR injury caused a significant increase of mitochondrial oxidative stress in the motor nerve and skeletal muscle. Taking advantage of fluorescently conjugated α-BTX, we could ascertain MitoTimer signal in NMJ, which reports mitochondrial oxidative stress at NMJ. Using this novel approach, we found clear evidence of increased mitochondrial oxidative stress in these discrete areas following IR injury. Together, these findings provide the first direct measurement of mitochondrial oxidative stress in NMJ.

Aberrant mtROS production upon rapid reactivation of mitochondrial respiration during reperfusion is critical for initiation and propagation IR injury (16). Given the proximity to the primary site of mtROS production, mitochondrial macromolecules are especially vulnerable to oxidative damage (324). Accumulation of damaged mitochondrial proteins contributes to mitochondrial dysfunction, which effectively impairs tissue function and recovery (276). Regulation of mitochondrial processes by redox-based modifications on cysteine residues of mitochondrial proteins, particularly enhanced SNO of proteins of ETS, have been found to elicit cytoprotective effects against IR injury (303,310,325). Indeed, studies of myocardial infarction reveal that SNO of Cys39 on the ND3 subunit of complex I by MitoSNO potently protects the heart from IR injury by slowing mitochondrial respiration and mtROS production during reperfusion (94,310). Informed by this precedent, we asked whether administration of MitoSNO could enhance SNO of ETS proteins and attenuate mitochondrial oxidative stress following IR. Our studies revealed that in addition to enhanced SNO of complex I, treatment with MitoSNO increased SNO of complexes II and III in muscle, and, to a greater extent, nerve. These

complexes in ETC are known contributors to mtROS production (50,326). Consistent with this finding, MitoSNO treatment significantly reduced mitochondrial oxidative stress in nerve and NMJ following IR. Of note, previous reports in the heart have identified that enzymes of the tricarboxylic acid cycle (TCA), including α-ketoglutarate dehydrogenase and pyruvate dehydrogenase, are significant sources of mtROS during reperfusion (302), which can be attenuated by SNO of key residues (308). Although we did not probe for these aforementioned enzymes, we speculate that MitoSNO enhances SNO of these proteins, possibly reducing production of ROS. In addition to reversible modulation of enzyme activity, SNO shields cysteine residues from irreversible oxidation, which has been shown to protect proteins that are vulnerable to oxidant-mediated inactivation in the heart (327). Thus, it is likely that MitoSNO mediated protection to the nerve is a synergistic effect of SNO of multiple sites of the ETS ultimately reducing mitochondrial oxidative stress and preserving mitochondrial function. Further studies are necessary to confirm this latter assertion.

Loss of tissue viability and function are among the consequences of IR, and thus, attenuation of mitochondrial oxidative stress should curb these abnormalities. Indeed, we obtained substantial evidence that treatment with MitoSNO preserved nerve function following IR injury, as determined by the discrepancies between the forces elicited by nerve and direct muscle stimulation. This is most likely attributable to the aforementioned reduction in mitochondrial oxidative stress, which would maintain nerve function extending from the axon to the NMJ. Such reasoning is bolstered by other studies in models of diabetic neuropathy and ALS, in which administration of antioxidants or antioxidant gene mimetics attenuated loss of motor nerve conduction (328) and enhanced survival of motor nerve fibers (329), respectively.

However, additional studies are needed to parse the precise mechanism, by which mitochondrial oxidative stress abrogates nerve function upon IR injury.

Despite the potent protection of motor nerve by MitoSNO treatment, initial damage to skeletal muscle was not prevented. This lack of protection against skeletal muscle injury *per se* suggests that muscle damage may be mediated by a mechanism(s) independent of mtROS, such as ROS production from non-mitochondrial sources (330), and/or enhanced calpain activity (331). Other studies have shown that necrotic and apoptotic cell death pathways in skeletal muscle are rapidly initiated during ischemia, and the degree of activation of cell death pathway is proportional to the duration of ischemia (332). Thus, MitoSNO, which we administered immediately prior to reperfusion, would not likely affect damage occurred during ischemia. Importantly, our data that functional regeneration of muscles that were treated with MitoSNO exceeded that of the other groups suggests that the protection is mediated by a process other than direct protection against initial muscle injury.

Both the maintenance of muscle mass and contractile function under normal conditions and the recovery following injury are highly affected by neuromuscular activity as well as neurotrophic factors. The influences of nerve on muscle functional regeneration are multifold, impacting muscle metabolism (333), sarcomeric organization (334), and muscle fibrillation (335). Indeed, functional recovery of muscle following nerve crush injury has been previously shown to only be accomplished, albeit gradually, after neural input recovers (336). We found that nerve function and NMJ innervation was preserved 7 days following treatment with MitoSNO when compared to MitoNAP and saline-treated groups. Of great interest is that MitoSNO treated muscles led to a more rapid recovery of contractile function without an appreciable reinnervation of the NMJ at day 14. These data suggest the increase in force

production between day 7 and 14 in MitoSNO treated muscles is due to functional regeneration of the muscle. It is therefore likely that the accelerated improvement in muscle function is attributable to the preserved NMJ innervation and function during the initial phase of IR. Therefore, preservation of NMJ accelerates the functional regeneration of skeletal muscle from IR injury.

In conclusion, our studies demonstrate that treatment with mitochondria-targeted *S*-nitrosothiol MitoSNO prior to reperfusion attenuates IR-induced denervation at NMJ and preserves neuromuscular function, which facilitate functional regeneration. Our findings highlight a here unto unappreciated role of the physiological consequences of enhanced SNO of mitochondrial proteins at NMJ and prove the feasibility of intramuscular injection of MitoSNO as a highly effective intervention against IR injury.

CHAPTER 4. EXERCISE TRAINING PROTECTS AGAINST NEUROMUSCULAR DYSFUNCTION FOLLOWING HINDLIMB ISCHEMIA-REPERFUSION INJURY

4.1. Introduction

Ischemia-reperfusion (IR) injury due to temporary loss of blood flow is common to many debilitating diseases and a corollary to some clinical procedures. Skeletal muscle as an organ with fundamentally important function is particularly relevant since, as a common practice in certain types of surgery or as a first response to traumatic injury, a tourniquet is often used to prohibit hemorrhage, exsanguination, or provide a bloodless operating field (337,338). The negative consequences of this procedure include muscle weakness and atrophy as well as temporary or irreversible nerve damage, all of which hinder functional recovery (8,10,291,339,340).

The compounding of cellular alterations accrued during ischemia and reperfusion determines the extent of pathology. This includes intracellular ion imbalance, destabilization of the plasma membrane (16,17,341), and accumulation of metabolic intermediates (50) during ischemia, as well as excessive generation of ROS, plasma membrane rupture, activation of inflammatory cascades, and necropoptosis during reperfusion. Given the diversity of deleterious pathways activated by IR, the best intervention(s) is likely to be the one that could assuage multiple rather than one component of the pathways. Indeed, remote pre-conditioning before ischemia has been found to attenuate IR injury in experimental models in a multi-faceted manner, the efficacy of pre-conditioning is far from optimal (293,318,342). Thus, it is of the upmost importance to develop more effective therapeutics that targets multiple components of IR injury.

Exposure to repeated, low-grade stress provokes adaptations that enhance cell resiliency to future and more potent insults, a phenomenon called hormesis (343–345). In line with this biological phenomenon, endurance exercise training involves and requires transient energetic, oxidative and/or mechanical stress to elicit favorable adaptations both locally and systemically (344,346,347). Certainly, endurance exercise training has been shown to lessen IR injury in the heart (348–350), liver (351), and lungs (347), whereas the underlying mechanisms are varied and include enhancement of antioxidant (352–356) and damage repair enzyme expression (278,357–359) and activity increased Ca^{2+} buffering capacity (360–362), and improved mitochondrial quality and function (284,362,363). However, there have not been studies investigating the impact of endurance exercise training on the susceptibility of recruited, adapted skeletal muscle to IR injury. If this endurance exercise training indeed leads to less IR injury in skeletal muscle, the next question would be whether the protection occurs during the ischemic or reperfusion phases and whether the muscle or the motor nerve components are protected. The purpose of this study was to determine whether endurance exercise training is sufficient to protect motor nerve fibers, the neuromuscular junction (NMJ) and/or myofibers, which populate skeletal muscle, against IR injury. These studies would significantly improve our understanding of the utility and underlying mechanism of endurance exercise training as a therapeutic intervention to attenuate/prevent IR injury.

4.2. Results

4.2.1. Exercise training significantly preserves hindlimb function following IR.

To ascertain if endurance exercise training leads to protection against IR injury to myofibers and motor nerve fibers, we subjected exercise trained mice (following 5 weeks of voluntary running) to 1-hour to ischemia by unilateral application of a rubber band tourniquet above the femur followed by releasing the tourniquet with reperfusion with sedentary mice receiving the same experimental procedure and mice receiving sham operation as controls. Myofiber and motor nerve functions were assessed based on total force generated by plantar flexor muscles following direct muscle or sciatic nerve stimulation, respectively. These approaches provide insight into the force generating capacity of muscle and neuromuscular transmission, indicative of myofiber and motor nerve function, respectively (293).

Prior to the injury, body weight (**Figure 19a**), direct and nerve stimulated force production (**Figure 19b and 19c**), and serum creatine kinase (data not shown) were indistinguishable between sedentary and exercised mice. At 7 days following IR, gastrocnemius muscle mass from sedentary and exercise-trained mice was reduced by 22% and 29%, respectively, compared to sham, suggesting an equal level of myofiber atrophy (**Figure 19d**). Next, we evaluated specific force by normalizing absolute force produced to the mass of plantar flexor muscles (gastrocnemius, soleus and plantaris muscles), which accounted for differences in muscle size. Plantar flexor muscles of exercise-trained mice generated significantly greater specific force than sedentary mice in response to both direct muscle (**Figure 19e**) and nerve stimulation (**Figure 19f**). Together these suggest that exercise training preserves myofiber and motor nerve function.

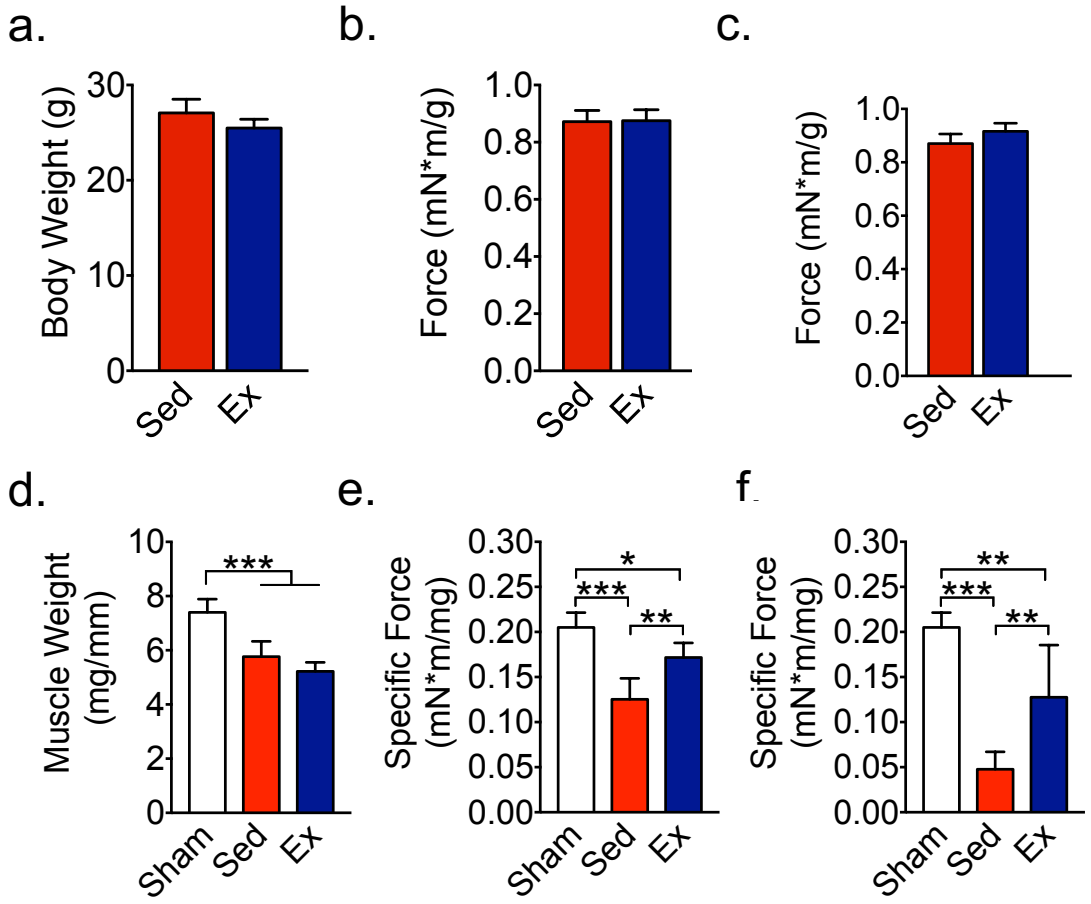

Figure 19: Exercise training preserves neuromuscular function following IR. In order to determine whether exercise provides protection against IR injury, mice were subjected to IR, and muscle weight and, muscle and nerve function were measured 7 days following the injury. (a) Comparison of body weight between Sed and Ex groups prior to IR (n = 6). Maximum tetanic force of plantar flexors prior to injury elicited by direct muscle (b) and nerve (c) stimulation (n = 6); (d) Gastrocnemius muscle wet weight normalized to tibia length to account for differences in body size (***$p < 0.001$ n = 6); Specific force elicited by (e) direct muscle stimulation and (f) nerve stimulation (** and *** denote $p < 0.01$ and $p < 0.001$, respectively, n = 6). Data are represented as mean ± SD.

4.2.2. Endurance exercise training attenuates skeletal muscle damage following IR.

To assess injury to myofibers, we performed morphological analysis for transverse sections of the plantaris muscle by H&E staining. At 3 hours post-IR, skeletal muscle from sedentary mice showed many rounded myofibers with increased interstitial space and exhibited a significant increase of cross sectional area, suggestive of edema, necrosis and hypercontraction (**Figure 20a and 20b**). Exercise-trained mice had significant less severe damage in these aforementioned parameters. To obtain biochemical evidence of the protection by exercise, we measured the activity of creatine kinase (CK) in the serum, a clinically relevant marker of muscle damage. Compared to sham control, serum CK activity increased 6-fold in sedentary mice, which was attenuated to 3.5-fold in exercise-trained mice (**Figure 20c**). We then assessed muscle morphology 7 days following injury (**Figure 20d**). In accordance with a reduction in gastrocnemius mass, IR resulted in significantly reduced myofiber cross-sectional area in plantaris muscles (**Figure 20e**) in both sedentary and exercise-trained mice, suggesting equal muscle atrophy in these two groups. However, myofibers from sedentary mice displayed a significant increase in centralized myonuclei, a marker for ongoing muscle regeneration, when compared to sham control (**Figure 20f**), while there is a trend of increased number of centralized myonuclei in exercise-trained mice, but it is not statistically significant. This morphological data combined with serum CK activity data suggests exercise training led to a reduced muscle injury.

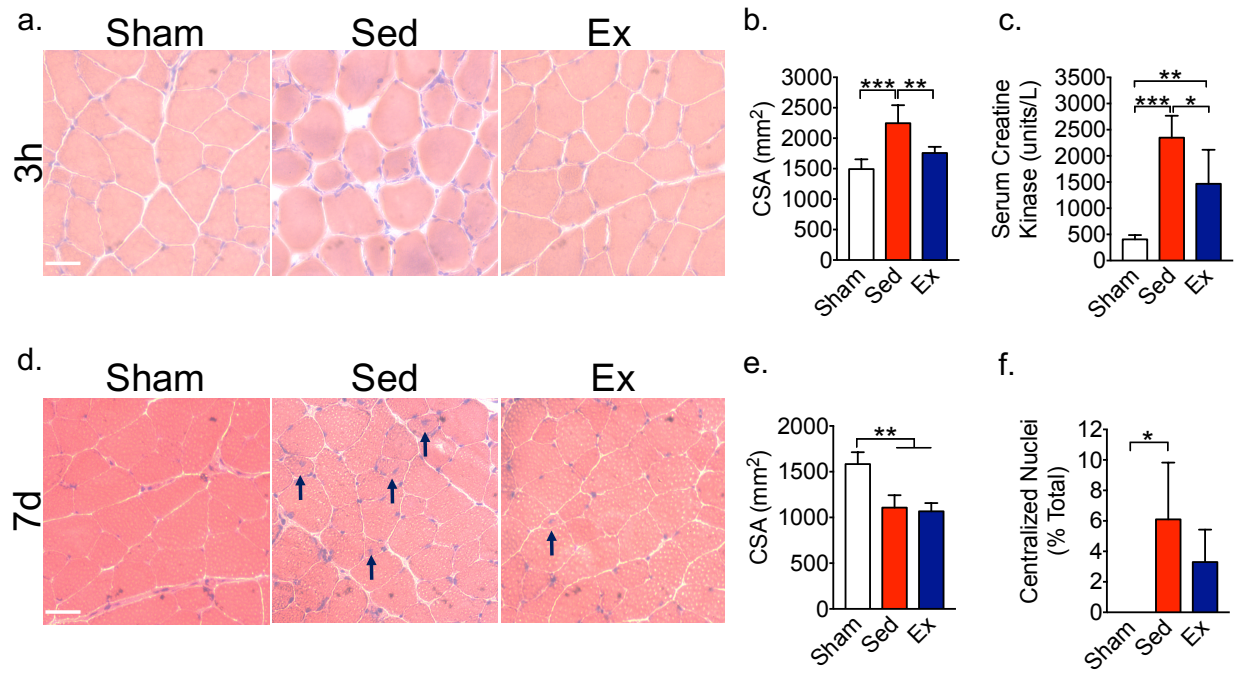

Figure 20: Exercise training renders skeletal muscle more resistant to IR. Morphological and biochemical evaluation of muscle damage was conducted following IR. (a) Representative images of H&E-stained transverse sections of skeletal muscle 3 hours after IR, scale bar = 50 μm; (b) Cross-sectional area of myofibers 3 hours after IR (** and *** denote $p < 0.01$ and $p < 0.001$, respectively n = 6). (c) Serum creatine kinase activity 3 hours after injury (*, **, and *** denote $p < 0.05$, $p < 0.01$, and $p < 0.001$, respectively n = 6); (d) Representative images of H&E-stained transverse sections of plantaris muscle 7 days after IR**.** Scale bar = 50 μm (n = 6); (e) Cross-sectional area of myofibers 7 hours after injury (** denote $p < 0.01$, n = 6); (f) Percentage of total myofibers displaying centralized nuclei (* denote $p < 0.05$ n = 6). Data are represented as mean ± SD.

4.2.3. Exercise training preserves innervation at NMJ following IR.

Patients exposed to tourniquet-induced IR can experience temporary or permanent motor nerve damage which contributes to post-procedure muscle weakness and delayed functional recovery (10,364,365). Neuromuscular junctions (NMJ) are specialized chemical synapses formed between motor nerve and myofiber that serves as the nexus of neuromuscular transmission. Previous studies have revealed that NMJ are vulnerable to IR injury; we, therefore, asked whether endurance exercise training could preserve NMJ integrity. To evaluate NMJ, we quantified the fluorescent overlap of the presynaptic neuron-specific class III β–tubulin (Tuj1) with the postsynaptic acetylcholine receptors (AchR) in the plantaris muscle. At 3 hours after IR Tuj1 florescence that overlap with AchR was profoundly decreased compared to the sham control, indicative of denervation at NMJ (**Figure 21a and 21b**). However, significantly fewer NMJ showed this kind of denervation in skeletal muscle collected from exercise-trained mice. To further ascertain long-term denervation, we measured the intercellular expression of neuronal cell adhesion marker (Ncam), a marker of denervation and muscle regeneration (319,366,367), in transverse sections of the plantaris muscle. At day 7 following IR, expression of NCAM in myofibers from sedentary mice showed a clear trend of increase compared to the sham control ($p=0.053$), but not in exercise-trained mice (**Figure 21c and 21d**). In summary, these data demonstrate that exercise training attenuates denervation at NMJ following IR.

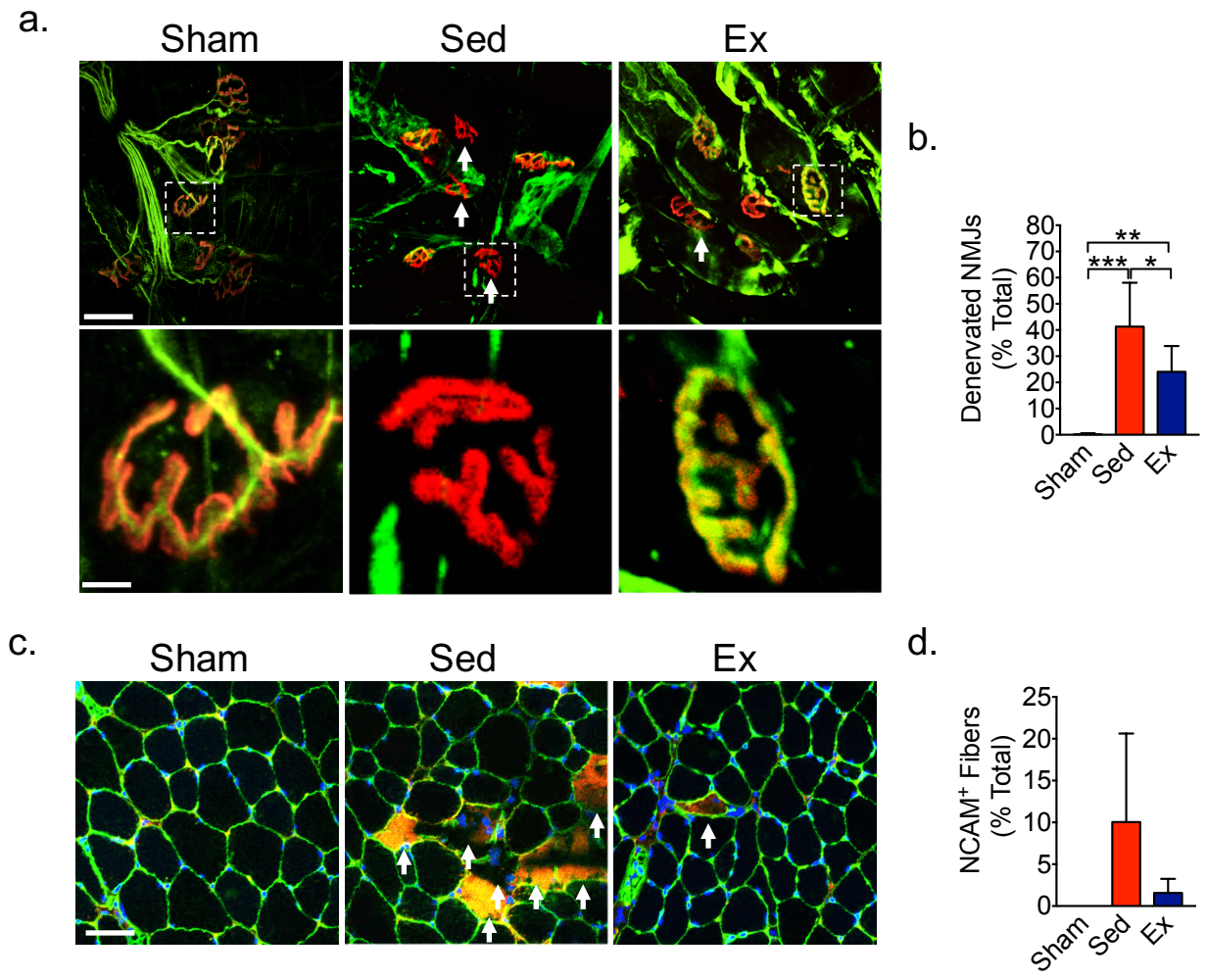

Figure 21: Exercise training attenuates denervation of skeletal muscle following IR. To elucidate the consequence of endurance exercise training on skeletal muscle innervation sedentary and exercise-trained mice were exposed to IR. (a) Representative confocal images NMJ and presynaptic motor nerve fibers identified by Tuj1 (red) and postsynaptic acetylcholine receptors detected with α-bungarotoxin (red) 3 hours after injury, scale = 20 μm and 5 μm, respectively (n=8); (b) Quantification of denervated NMJ 3 hours after injury (*, *** denote $p <$ 0.05 and 0.001, respectively n=8); (c) Representative confocal images of transverse sections of plantaris muscle expressing Ncam (red) and laminin (green), and DAPI staining (blue) 7 days after injury; and (d) quantification of the percentage of $Ncam^{+}$ myofibers at 7 days following

injury. Mice in the sedentary group had a trend of increase toward significant ($p = 0.053$) (scale = 100 μm). Data are represented as mean ± SD.

4.2.4. Exercise training does not prevent IR-induced oxidative stress.

Oxidative stress and consequent damage to cellular components is a hallmark of IR injury. Reduction in the production or enhanced detoxification of oxidants has been found to reduce IR injury across a number of tissues. Endurance exercise training has been reported to promote antioxidant defense systems in skeletal muscle (356,368), which might lead to increase resistance to IR injury. Indeed, we found that expression of superoxide dismutase isoforms 1, 2 and 3 as well as catalase were significantly increased following voluntary running in myofibers (**Figure 22a**) but such an enhancement of the antioxidant enzyme defense system was not robust in sciatic nerve (**Figure 22b**). Encouraged by these findings we hypothesized that exercise training mediated protection against IR injury was through a reduction in oxidative stress at least in myofibers.

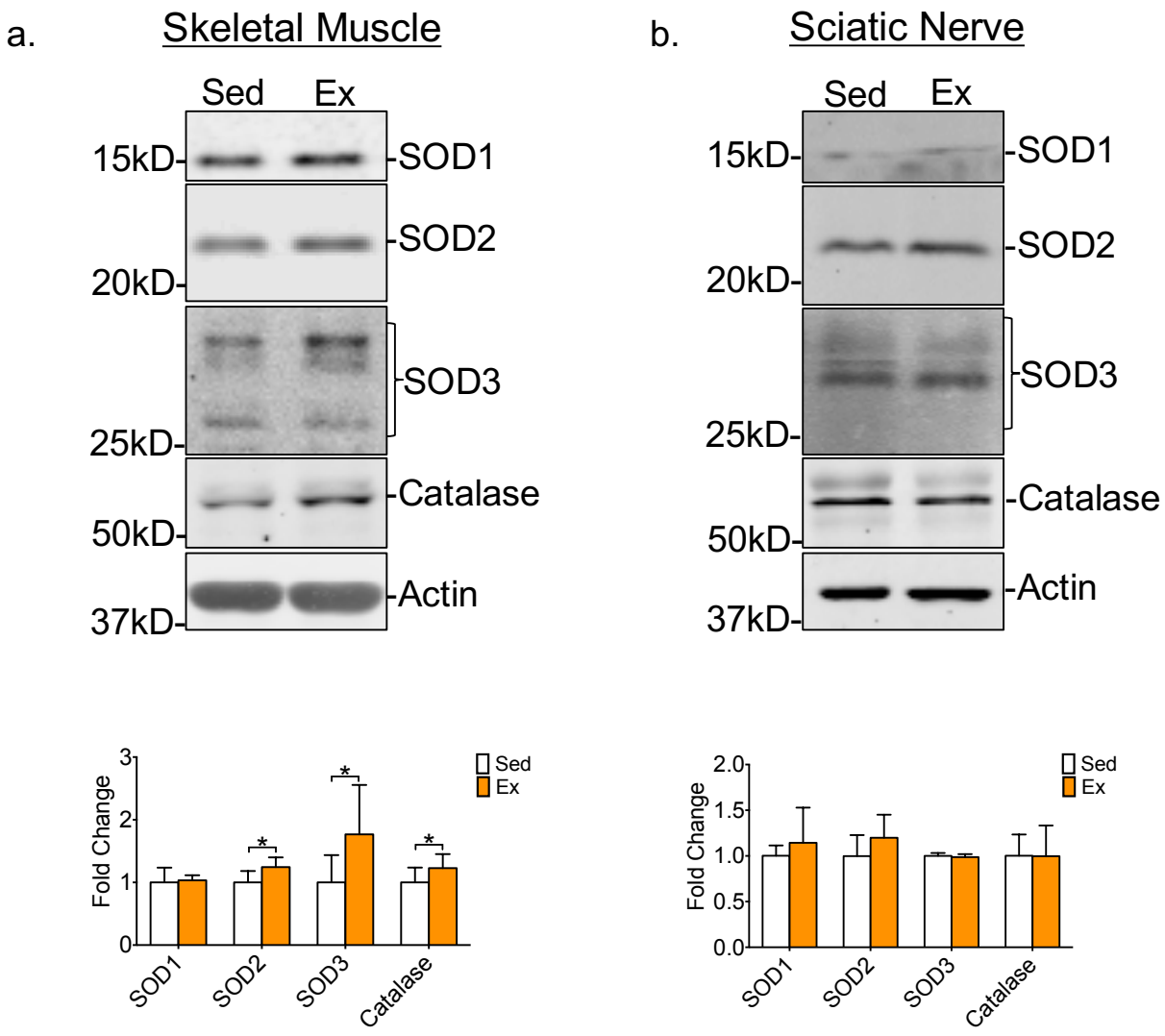

Figure 22: Exercise training increases antioxidant protein expression in skeletal muscle. Comparison of basal antioxidant protein expression in skeletal muscle and sciatic nerve collected from Sed and Ex mice. Representative immunoblots and quantification of relative expression of antioxidant proteins SOD1, SOD2, SOD3 and Catalase normalized to actin in (a) skeletal muscle and (b) sciatic nerve (* denotes $p < 0.05$ n = 5). Data are represented as mean ± SD.

We first evaluated mitochondrial oxidative stress *in vivo* by using a novel transgenic mouse model with a globally induced expression of the mitochondria reporter gene *MitoTimer* (MitoTimer-Tg). Our lab developed this novel mitochondrial reporter gene to encode a mitochondrial targeted green fluorescent protein, which irreversibly switches to Discosoma sp. red fluorescent protein upon oxidation (284,369). Computer assistance ratiometric analysis of MitoTimer red:green fluorescence ratio provides a quantifiable measure of mitochondrial oxidative stress (284,357,370). We subjected sedentary and exercise-trained MitoTimer-Tg mice to IR and collected tissues after at 3 hours. Unexpectedly, MitoTimer red:green in myofibers (**Figure 23a and 23b**) and motor nerve fibers (**Figure 23c and 23d**) from sedentary and exercise-trained mice was indistinguishably higher than the sham control mice, indicating that exercise training does not attenuate IR-induced mitochondrial oxidative stress. Since other sources of ROS also contribute to IR injury (16,17,31,330), we measured 4-hydroxynoneal, a stable product of lipid peroxidation brought on by oxidative stress (371,372), in whole cell lysates. Similarly to the findings of MitoTimer, we observed significant but indistinguishable increases of 4-Hydroxynoneanal in myofibers and motor nerve fibers 3 hours after IR in both sedentary and exercise-trained mice (**Figure 23e and 23f).** Together, these data suggest that the main protective effect of endurance exercise training against IR is not through an enhanced antioxidant defense with reduced oxidative stress.

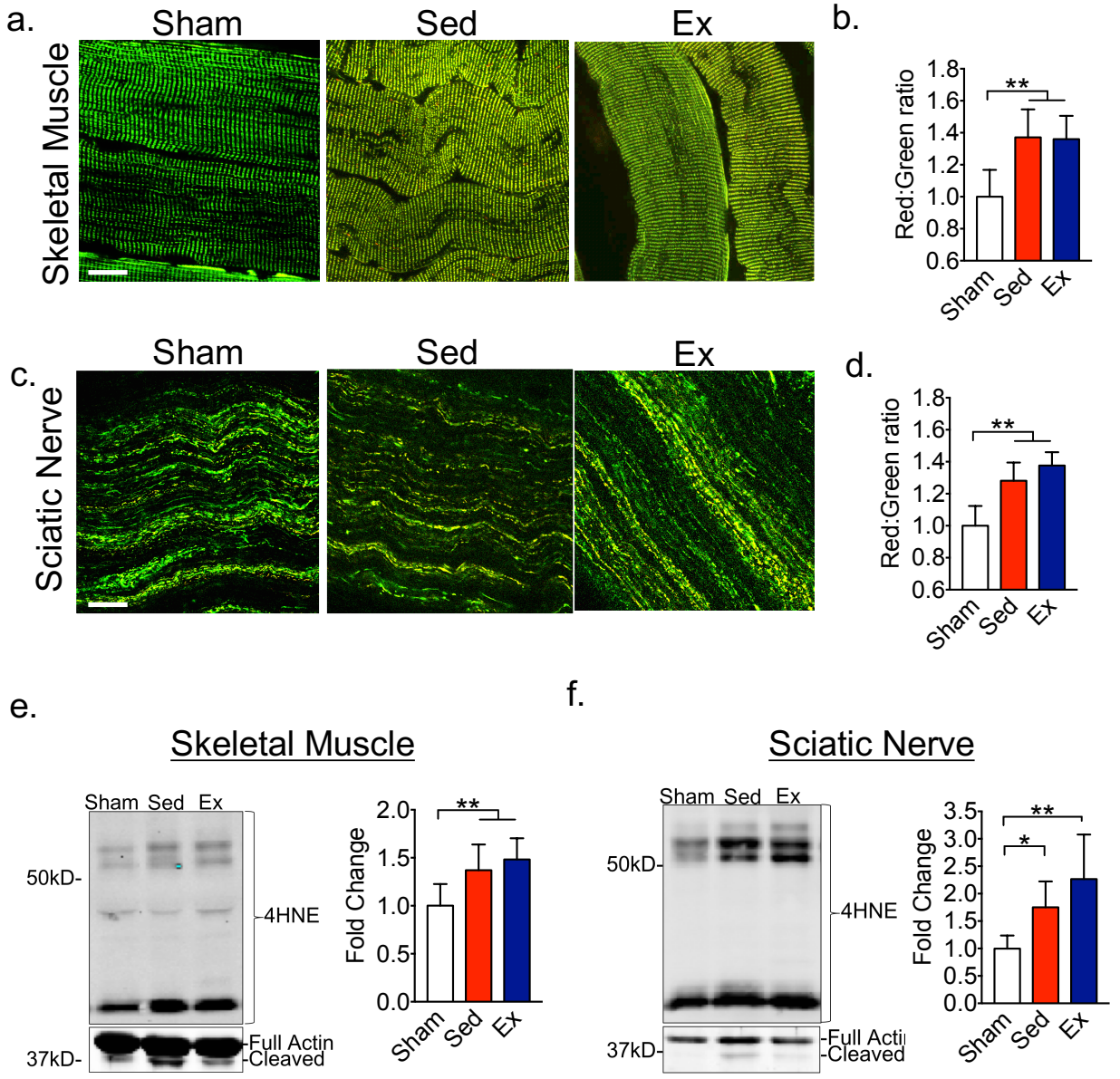

Figure 23: IR-induced oxidative stress is not attenuated with exercise training. Comparison of mitochondrial and whole cell oxidative stress between Sed and Ex after IR. Representative confocal images of MitoTimer in skeletal muscle (a) and sciatic nerve (c) collected 3 hours after IR, scale = 25 μm. Quantification of MitoTimer red:green ratio in skeletal muscle (b) and sciatic nerve (d) (** denotes $p < 0.01$, n = 4-7). Representative immunoblot images and quantification of 4-Hydroxynoneanal (4HNE) in skeletal muscle and sciatic nerve 3 hours after IR (* and ** denote $p < 0.05$ and $p < 0.01$, respectively n = 6). Data are represented as mean ± SD.

4.2.5. Exercise training reduces cytoskeletal protein degradation following IR.

Activation of proteases, including calpains (109,373–375) and caspases (376–378), has been speculated to contribute to IR pathology in multiple tissues by promoting protein degradation. However, little is known about whether these proteases contribute to protein degradations in myofibers and/or motor nerve in hindlimb IR injury. Under the condition of Ca^{2+} overload, such as IR, the Ca^{2+}-sensitive proteases, μ–calpain and m-calpain, are activated and undergo autolysis (379,380). Here, we found that at 3h following IR, μ–calpain and m-calpain cleavage was undetectable in myofibers (**Figure 24a and 24b**), nor in sciatic nerve (**Figure 24d and 24e**). Furthermore, fodrin, which is a substrate of calpain, was not cleaved (data not shown). These findings suggest that calpain proteases were not activated in myofibers and motor nerve fibers following IR. Interestingly, IR did lead to an increase of total μ–calpain to a greater extent in myofibers from sedentary mice compared to exercise-trained mice, suggesting that μ-calpain expression is responsive to IR injury. However, whether this increase of total μ–calpain contributed to the exercise-mediated protection was questionable. It has recently come to light cleavage of actin causes cytoskeletal degeneration and also acts as a sensor and mediator of apoptosis (377,381–383). Mechanistic studies of neurodegeneration and tumorigenesis have found that actin cleavage is mediated by caspases (377,382). We, therefore, measured actin cleavage and observed a significant increase in cleaved actin in myofibers and motor nerve fibers from sedentary mice 3h post IR injury, which was prevented by exercise training (**Figure 24c and 24f**). These findings provide the first insight into the possible mechanism by which exercise training attenuates myofiber and motor nerve fibers damages in a clinically relevant animal model of IR injury in skeletal muscle.

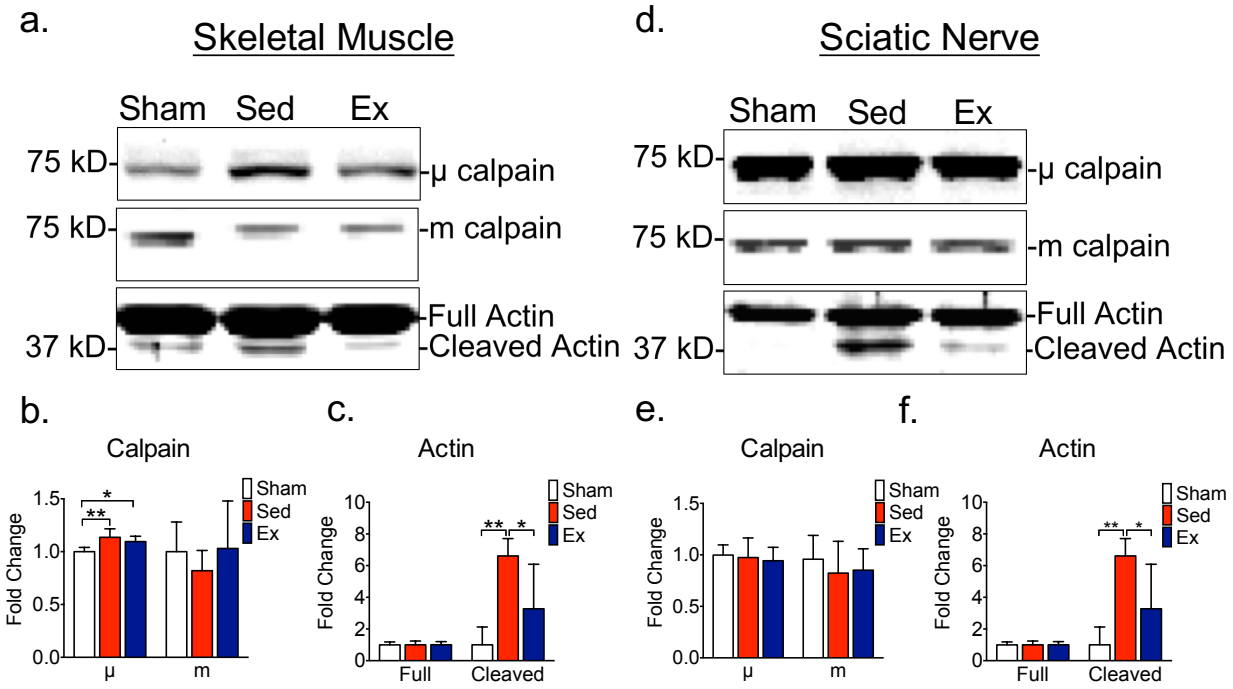

Figure 24: Exercise training reduces cleavage of cytoskeletal proteins after IR injury. Representative immunoblot images of μ-caplain, m-calpain and full and cleaved actin in skeletal muscle (a) and sciatic nerve (d) 3 hours after IR. Quantification of μ-caplain and m-calpain in skeletal muscle (b) and sciatic nerve (e) (* and ** denote $p < 0.05$ and $p < 0.01$, respectively n = 6). Quantification of full length and cleaved actin in skeletal muscle (c) and sciatic nerve (f) (* and ** denote $p < 0.05$ and $p < 0.01$, respectively n = 6). Data are represented as mean ± SD.

4.3. Discussion

Impairment of neuromuscular function is an inherent risk in procedures that employ tourniquets to modulate blood flow. The clinical manifestations of IR injury in this context are myofiber atrophy, weakness, limb numbness, and temporary or permanent paralysis, all of which jeopardize the quality of life and amplify the incidence of morbidity and mortality. Although we have recently demonstrated IR injury, particularly to NMJ, can be attenuated by targeting mitochondria, there has always been a need to develop an effective and accessible physiological intervention, where endurance exercise training is one of the most feasible candidates. Endurance exercise has been shown to improve myocardial tolerance to IR injury in a manner that is analogous to preconditioning (348,350,384,385). However, whether endurance exercise training confers such benefits to skeletal muscle remains unaddressed. This study provides the first evidence that endurance exercise training attenuates IR induced neuromuscular derangement, which is evident on functional, morphological, cellular and molecular levels.

Impairments in force generation in response to direct muscle stimulation reveal that the force generating capacity of the muscle is reduced due to activation of intrinsic myopathies. We observed clear evidence of concurrent myofiber edema (increased myofiber cross sectional area and interstitial space) and increased serum creatine kinase, both of which were attenuated by exercise training. These findings indicate that the sedentary mice experienced substantially greater IR injury to myofibers than exercise-trained mice. Moreover, the percentage of centralized nuclei in myofibers from sedentary mice was significantly increased 7 days after IR, whereas this increase was not statistically significant in exercise-trained mice. Considering these findings in sum, we conclude that endurance exercise training resulted in fewer damaged myofibers by IR. Alternatively, the same number of myofibers were effected, but to a lesser

degree in exercise-trained mice, or a mixture of both. Future studies are necessary to determine which phenomena predominate.

Assessment of force production in response to sciatic nerve stimulation and innervation at NMJ provide insight into motor nerve function. The former assesses neuromuscular transmission, the mechanism whereby nerve impulses initiate muscle contraction, and the latter reveals structural changes that might underlie impaired neuromuscular transmission. We observed a dramatic decrease in nerve-stimulated force production that was paralleled by denervation at NMJ denervation, supporting the notion of compromised neuromuscular transmission following IR. Nerve stimulation-mediated force production in exercise-trained mice following IR, on the other hand, was significantly greater than IR challenged sedentary mice. This exercise training-mediated protection was accompanied by attenuated denervation at NMJ. These data suggest that exercise training preserves motor nerve function, at least in part, by preserving innervation at NMJ.

Acute bout(s) of exercise causes transient stress in skeletal muscle and other remote tissue/organs, which could initiate adaptive responses and ultimately render the effected tissues/organs more resistant to ensuing stresses (please see reviews (363,385,386)). A seemingly important adaptation induced by endurance exercise training is increased expression of antioxidant enzymes in the antioxidant defense system. Consistent with the findings by our and other groups (356,387), we found that long-term voluntary running led to modest increases of antioxidant enzyme content in myofibers. However, IR-induced cytosolic and mitochondrial oxidative stresses were not attenuated in myofibers from exercise trained mice. The most straightforward conclusion is that endurance exercise training-induced increases in antioxidant enzymes are not sufficient to prevent oxidative stress induced by IR.

Protein degradation and cytoskeletal dismantlement are part of the pathological processes activated by IR injury. Multiple pathways could be involved including activation of proteases, ubiquitin-proteasome system and autophagy, among which calpain-mediated cleavage has been reported in myocardial IR (388,389). Interestingly, we detected increased total μ–calpain in skeletal muscle following IR, but we were unable to detect an increase autoclaved μ–calpain or m-calpain in skeletal muscle or motor nerve fibers. These findings suggest that calpains were not activated although the expression of μ–calpain is enhanced by IR. Actin is a major constituent of the cytoskeleton of motor nerve fibers and skeletal muscle and is required for pre- and post-synaptic formation and maintenance, as well as skeletal muscle force production. It has been shown that actin is vulnerable to cleavage by caspases, and cleaved actin could serve as both mediator and marker of apoptosis. Following IR, skeletal muscle and motor nerve from sedentary mice had significant increases in cleaved actin, which was completely prevented by long-term voluntary running before the IR procedure. The conservation of actin may underlie the better maintenance of motor nerve, NMJ, and skeletal muscle following IR in exercise-trained mice, which is supported by our morphological and functional data. In addition, preservation of actin in muscle and motor nerve from exercise-trained mice could be indicative of reduced apoptosis under the condition of IR injury.

In conclusion, this study provides the first evidence that endurance exercise training is sufficient to attenuate IR injury in motor nerve and myofibers, thus preserving neuromuscular function. Collectively, our findings support a new application of endurance exercise training with strong clinical implications where endurance exercise regime could be prescribed in preparation for surgeries or procedures that will employ a tourniquet. Finally, these discoveries provide a foundation for future studies to elucidate the precise mechanism(s) of exercise training

mediated protection against IR injury, which may be relevant to other IR-related injuries or diseases.

CHAPTER 5. CONCLUDING REMARKS AND FUTURE DIRECTIONS

IR injury to motor nerve fibers and myofibers, a consequence of tourniquet use, aortic aneurism, and peripheral arterial disease, compromises neuromuscular function, manifesting as weakness and/or paralysis (47,75,390). Until now, there has been a paucity of practical and effective strategies to alleviate neuromuscular dysfunction following IR injury (318,391,392). The work presented in this thesis identifies two distinct interventions that preserve neuromuscular function in the context of tourniquet-induced IR injury: pharmacological administration of MitoSNO and endurance exercise training. These findings have high translatable value, which may assist in improving clinical practice(s) and also raise a number of avenues for future biomedical research, both of which will be detailed herein.

Perhaps the most exciting finding from these studies is the profound protection that both MitoSNO treatment and exercise training had on neuromuscular function following tourniquet-induced IR injury, which has never before been accomplished through other interventions. For example, ischemic preconditioning, which involves short repeated bouts of ischemia prior to sustained ischemia, alleviates myofiber damage but does not protect motor nerve function (293). Regional hypothermia has been marginally successful in preserving motor nerve and myofiber function; however, the effective hypothermic temperature has not been clearly defined, and the intervention can lead to undesirable pathological consequences, such as metabolic acidosis, microvascular permeability, and vasoconstriction (294,393,394). Treatment with antioxidants before, but not during IR, has had marginal success in reducing oxidative stress in animal models and humans, but it is unclear whether both motor nerve fiber and myofiber functions are preserved (75,395–397).

We found that administration of MitoSNO, which enhances mitochondrial protein SNO, and exercise training effectively preserved neuromuscular function following IR injury. Furthermore, we discovered that the mechanism(s) of MitoSNO and exercise training mediated protection against IR injury are distinct from one another. It is therefore possible that combining MitoSNO treatment with endurance exercise training could abolish IR injury altogether. Alternatively, if we uncover the mechanism of exercise training-mediated protection, we could design a mimetic that could be administered in conjunction with MitoSNO to achieve the same combinatory benefit. Furthermore, these approaches could be even more effective if we were to identify a dose of MitoSNO that could also attenuate myofiber injury. A possible scenario in which combinational therapy could be applied is in certain time period leading up to a planned surgery. For instance, a physician could prescribe a pre-surgical exercise regimen, and then administer MitoSNO during surgery. Not only could this reduce post-IR complications, which include weakness and paralysis (398,399), but could also lessen risk of the need of amputation (338). In support of this proposal, pre-surgery exercise training is now being explored in a clinical trial as a pre-rehabilitative strategy to improve functional outcomes for patients following total knee arthroplasty, which utilizes a tourniquet; however, no results have been reported (400). Taken together, these findings could have broad implications on clinical practice(s) in preventing IR injury.

In addition to the possible clinical implications of our findings, we have addressed a number of exciting fundamental research questions that could advance the fields of reduction-oxidation biology, mitochondrial bioenergetics, neuromuscular physiology and exercise physiology. Administration of MitoSNO during ischemia reduced mitochondrial oxidative stress and potently protected motor nerve function and myofiber innervation in the wake of IR injury.

The mechanism by which enhancing mitochondrial protein SNO protects against IR is not entirely clear, particularly because SNO has been found to shield critical cysteine thiols from irreversible oxidation and alter protein activity (96,308,325). Determining whether this protection is due to SNO of a single protein or many proteins is important for understanding the pathology of IR injury and for development of effective therapeutics. For instance, we found that MitoSNO increases SNO of complexes I, II, III and V of the ETS. It is likely that more targets within the mitochondria were modified, especially because ~1% of the mitochondrial proteome is available for SNO (94,325), which may be important for MitoSNO mediated protection. Identification of other mitochondrial proteins targets of MitoSNO and determination of whether SNO of those proteins prevents oxidation is of particular interest. This can be accomplished by simultaneous identification of cysteine residues that are oxidized or S-nitrosylated using tandem mass spectrometry as previously described by Kohr et al. (96). The information provided by this approach could be valuable by: 1) providing insight into whether MitoSNO confers protection by shielding cysteine residues from oxidation; and 2) identifying novel proteins that can be S-nitrosylated, leading to future studies where those residues can be mutated to determine the consequence of the redox modification. Identification of critical cysteine residues could help in developing targeted therapeutics.

Previous studies performed for myocardium in the context of myocardial infarction found that MitoSNO-mediated protection specifically reduced ROS production by complex I by preventing reverse electron transport (310). Hence, another possible future direction is to determine the mechanism by which MitoSNO protects motor nerve fibers. We found that the most dramatic increase in SNO with MitoSNO treatment in the sciatic nerve was of Complex III, a known source of ROS production during IR (105,401–403). Korge et al., found that treatment

of cardiomyocytes with antimycin A, a drug that mimics IR-induced damage of complex III, causes a profound burst of ROS production from complex III as well as opening of mPTP, thus dissipating the electrochemical gradient (67,81). They proposed that the predominant source of ROS in contexts where the mitochondrial membrane potential is not fully intact, such as during ischemia and at the onset of reperfusion (404,405), is complex III (403). Future studies should measure the mitochondrial membrane potential in the sciatic nerve during ischemia and reperfusion as well as site-specific ROS generation in the presence and absence of MitoSNO. This can be accomplished by administering targeted inhibitors and specific substrates to isolated mitochondria and measuring fluorescence of resurofin, the product of Amplex red oxidation by the ROS hydrogen peroxide (102,406,407). For instance, to assess the rate of ROS production by complex I due to reverse electron transport, isolated mitochondria would need to be treated with succinate and complex I inhibitor rotenone, which drives electrons from the ubiquinone to form ROS (408,409). Identification of tissue specific differences in sources of ROS as well as effects of SNO are important for understanding the pathology of IR injury and would also aid in developing targeted therapeutics.

Beyond identifying interventions for IR injury, we developed a novel method to interrogate mitochondrial oxidative stress in nerve fibers and myofibers using *pMitoTimer*, a state-of-the-art mitochondria targeted reporter gene encoding a mitochondria-targeted protein that irreversibly switches fluorescence from green to red upon oxidation (275,282,284,357,370). We created global, inducible MitoTimer transgenic mice and found that IR injury causes an increase in mitochondrial oxidative stress in nerve fibers and myofibers, which may be attenuated in only the nerve by MitoSNO treatment but not by exercise training. Using this tool, we were further able to visualize a distinct population of mitochondria clustered at the NMJ that

were similarly vulnerable to IR-induced mitochondrial oxidative stress. However, since we used global MitoTimer mice, we were technologically limited in resolving whether the MitoTimer signal was from mitochondria in the motor nerve fiber or myofiber. Generation of motor nerve fiber- and myofiber-specific MitoTimer mice would provide the necessary capability for determining whether there are tissue-specific differences in susceptibility to injury or response to treatment of the mitochondria following IR injury. Insights gained from these studies would further be helpful in evaluation of the biology of NMJ mitochondria. This would not only be helpful for IR research, but could also be applied to studying mitochondria in other neuromuscular pathologies, such as ALS, myasthenia gravis and muscular dystrophies.

Endurance exercise training is a highly accessible and potent stimulus for skeletal muscle and systemic adaptations and has the added benefit of increasing tissue resiliency to pathological insults (252,410–412). Our studies revealed the utility of exercise training to reduce IR injury to motor nerve fibers and myofibers; however, the underlying mechanism(s) remain largely unknown. Unexpectedly, we found that exercise training did not attenuate mitochondrial oxidative stress in the motor nerve fibers or myofibers, even though there was evidence of improved antioxidant defenses in myofibers. We did notice the appearance of an actin cleavage product following IR, which was prevented by exercise training in both motor nerve fibers and myofibers. Additional experiments are necessary to confirm that the cleavage fragment is indeed actin, and if so, this finding reveals a completely novel effect of exercise training on cytoskeletal degradation in the context of IR.

These findings lead to further questions as to what mediates actin cleavage and whether there is a biological consequence of actin cleavage. Perhaps the disappearance of cleaved actin in exercise trained tissues is due to greater capacity to clear damaged macromolecules, such as

enhanced autophagy (277,278,363), rather than reduced actin degradation. Lastly, it is unclear whether protective adaptations are active during the ischemic and/or reperfusion phase. It is possible that exercise trained tissues have a greater ability to maintain ATP levels, which may provide one explanation as to why we observe less tissue damage in this group. Indeed, exercise trained myofibers have been found to have greater glycogen storage, which can be broken down to glucose for glycolysis (413–415); whether this is the case for motor nerve fibers has yet to be ascertained. All of these questions could significantly advance our understanding of the cytoprotective effects of exercise training for IR, and possibly other pathologies.

Collectively, we have found that treatment with MitoSNO, which enhances SNO of mitochondrial proteins, and exercise training attenuate neuromuscular dysfunction and preserved NMJ innervation following hindlimb IR injury through distinct mechanisms. These studies uncovered valuable strategies to attenuate IR injury to motor nerve fibers and myofibers and preserve neuromuscular function, which could be employed in trauma and surgical situations when tourniquets are applied. The interventions detailed in this thesis may also be extended to other causes of IR injury that compromise neuromuscular function, such as spinal cord ischemia caused by an aortic aneurism and/or ischemia caused by PAD. Furthermore, we have begun to uncover unique, tissue-specific mechanisms involved in pathology and prevention of IR injury, which will facilitate the development of targeted therapeutics.

CHAPTER 6: REFERENCES

1. Carter WO, Bull C, Bortolon E, Yang L, Jesmok GJ, Gundel RH. A murine skeletal muscle ischemia-reperfusion injury model: differential pathology in BALB/c and DBA/2N mice. JApplPhysiol. 1998;85(5):1676–83.
2. Aivatidi C, Vourliotakis G, Georgopoulos S, Sigala F, Bastounis E, Papalambros E. Oxidative stress during abdominal aortic aneurysm repair - Biomarkers and antioxidant's protective effect: A review. Eur Rev Med Pharmacol Sci. 2011;15(3):245–52.
3. Pipinos II, Judge AR, Selsby JT, Zhu Z, Swanson SA, Nella AA, et al. The myopathy of peripheral arterial occlusive disease: part 1. Functional and histomorphological changes and evidence for mitochondrial dysfunction. Vasc Endovascular Surg. 2008;41(6):481–9.
4. Laghi Pasini F, Pastorelli M, Beermann U, de Candia S, Gallo S, Blardi P, et al. Peripheral neuropathy associated with ischemic vascular disease of the lower limbs. Angiology. 1996 Jun;47(6):569–77.
5. Blaisdell FW. The pathophysiology of skeletal muscle ischemia and the reperfusion syndrome: a review. Cardiovasc Surg. 2002 Dec;10(6):620–30.
6. Duehrkop C, Rieben R. Refinement of tourniquet-induced peripheral ischemia/reperfusion injury in rats: comparison of 2 h vs 24 h reperfusion. Lab Anim. 2014;48(2):143–54.
7. Low PA, Ward K, Schmelzer JD, Brimijoin S. Ischemic conduction failure and energy metabolism in experimental diabetic neuropathy. AmJPhysiol. 1985;248(0002–9513):E457–62.
8. Dash RK, Li Y, Kim J, Beard D a, Saidel GM, Cabrera ME. Metabolic dynamics in skeletal muscle during acute reduction in blood flow and oxygen supply to mitochondria: in-silico studies using a multi-scale, top-down integrated model. PLoS One. 2008

Jan;3(9):e3168.

9. Olivecrona C, Lapidus LJ, Benson L, Blomfeldt R. Tourniquet time affects postoperative complications after knee arthroplasty. Int Orthop. 2013;37(5):827–32.

10. Olivecrona C, Blomfeldt R, Ponzer S, Stanford BR, Nilsson BY. Tourniquet cuff pressure and nerve injury in knee arthroplasty in a bloodless field. Acta Orthop. 2013;84(2):159–64.

11. Diehm N, Schillinger M, Minar E, Gretener S, Baumgartner I. TASC II section E3 on the treatment of acute limb ischemia: commentary from European interventionists. J Endovasc Ther. 2008;15(1):126–8.

12. Salhotra R, Sharma J. Tourniquets in orthopedic surgery. Indian J Orthop. 2012;46(4):377.

13. Sapega AA, Heppenstall RB, Chance B, Park YS, Sokolow D. Optimizing tourniquet application and release times in extremity surgery. A biochemical and ultrastructural study. J Bone Joint Surg Am. 1985 Feb;67(2):303–14.

14. Vaughan A, Hardwick T, Gaskin J, Bendall S. Tourniquet use in orthopaedic surgery. Orthop Trauma. 2017;31(5):312–5.

15. Nikolaou VS. Common controversies in total knee replacement surgery: Current evidence. World J Orthop. 2014;5(4):460.

16. Kalogeris T, Baines C. Cell biology of ischemia/reperfusion injury. Int Rev Cell Mol Biol Mol Biol. 2012;298:229–317.

17. Kalogeris T, Baines CP, Krenz M, Korthuis RJ. Ischemia/Reperfusion. Compr Physiol. 2016;7(1):113–70.

18. Zweier JL, Talukder MAH. The role of oxidants and free radicals in reperfusion injury. Cardiovasc Res. 2006;70(2):181–90.

19. Tran TP, Tu H, Liu J, Muelleman RL, Li Y-L. Mitochondria-derived superoxide links to tourniquet-induced apoptosis in mouse skeletal muscle. PLoS One. 2012 Jan;7(8):e43410.

20. Chouchani ET, Pell VR, James AM, Work LM, Saeb-Parsy K, Frezza C, et al. A unifying mechanism for mitochondrial superoxide production during ischemia-reperfusion injury. Cell Metab. 2016;23(2):254–63.

21. Roseborough G, Gao D, Chen L, Trush MA, Zhou S, Williams GM, et al. The mitochondrial K-ATP channel opener, diazoxide, prevents ischemia-reperfusion injury in the rabbit spinal cord. Am J Pathol. 2006;168(5):1443–51.

22. Wilson DF, Harrison DK, Vinogradov SA. Oxygen, pH, and mitochondrial oxidative phosphorylation. J Appl Physiol. 2012;113(12):1838–45.

23. Fillingame RH. Coupling H+ transport and ATP synthesis in F1F0-ATP synthases: Glimpses of interacting parts in a dynamic molecular machine. J Exp Biol. 1997;200(2):217–24.

24. Tahara EB, Navarete FDT, Kowaltowski AJ. Tissue-, substrate-, and site-specific characteristics of mitochondrial reactive oxygen species generation. Free Radic Biol Med. 2009;46(9):1283–97.

25. Galante YM, Hatefi Y. Purification and molecular and enzymic properties of mitochondrial NADH dehydrogenase. Arch Biochem Biophys. 1979 Feb;192(2):559–68.

26. Yu C, Yu L. Preparations and properties of high purity succinate dehydrogenase and ubiquinol-cytochrome c reductase. Biochim Biophys Acta. 1980;591:409–20.

27. Crofts AR. The Cytochrome *bc* $_1$ Complex: Function in the Context of Structure. Annu Rev Physiol. 2004;66(1):689–733.

28. Perry SW, Norman JP, Barbieri J, Brown EB, Harris A. Mitochondrial membrane

potential probes and the proton gradient: a practical usage guide. Biotechniques. 2011;50(2):98–115.

29. Dimroth P, Kaim G, Matthey U. Crucial role of the membrane potential for ATP synthesis by F(1)F(o) ATP synthases. J Exp Biol. 2000;203(1):51–9.

30. Salin K, Auer SK, Rey B, Selman C, Metcalfe NB. Variation in the link between oxygen consumption and ATP production, and its relevance for animal performance. Proc Biol Sci. 2015;282(1812):20151028.

31. Lindsay TF, Liauw S, Romaschin AD, Walker PM. The effect of ischemia/reperfusion on adenine nucleotide metabolism and xanthine oxidase production in skeletal muscle. J Vasc Surg. 1990;12(1):8–15.

32. Eliason JL, Wakefield TW. Metabolic Consequences of Acute Limb Ischemia and Their Clinical Implications. Semin Vasc Surg. 2009;22(1):29–33.

33. Takeda Y, Pérez-Pinzón MA, Ginsberg MD, Sick TJ. Mitochondria consume energy and compromise cellular membrane potential by reversing ATP synthetase activity during focal ischemia in rats. J Cereb Blood Flow Metab. 2004;24(9):986–92.

34. Iijima T, Mishima T, Tohyama M, Akagawa K, Iwao Y. Mitochondrial membrane potential and intracellular ATP content after transient experimental ischemia in the cultured hippocampal neuron. Neurochem Int. 2003;43(3):263–9.

35. Harris K, Walker PM, Mickle D a, Harding R, Gatley R, Wilson GJ, et al. Metabolic response of skeletal muscle to ischemia. Am J Physiol. 1986;250(2 Pt 2):H213-20.

36. Haljamäe H, Enger E. Human skeletal muscle energy metabolism during and after complete tourniquet ischemia. Ann Surg. 1975;182(1):9–14.

37. Pedowitz RA. Tourniquet-induced neuromuscular injury. A recent review of rabbit and

clinical experiments. Acta Orthop Scand Suppl. 1991;245:1–33.

38. Zhang P, Liang Y, He J, Fang Y, Chen P, Wang J. Timing of tourniquet release in total knee arthroplasty. Medicine (Baltimore). 2017 Apr;96(17):e6786.

39. Kalla TP, Younger A, McEwen JA, Inkpen K. Survey of tourniquet use in podiatric surgery. J Foot Ankle Surg. 2003;42(2):68–76.

40. Wagers AJ, Conboy IM. Cellular and molecular signatures of muscle regeneration: Current concepts and controversies in adult myogenesis. Cell. 2005;122(5):659–67.

41. Strupp M, Jund R, Schneider U, Grafe P. Glucose availability and sensitivity to anoxia of isolated rat peroneal nerve. AmJPhysiol. 1991;261(3 Pt 1):E389–94.

42. Sladky JT, Greenberg JH, Brown MJ. Enhanced 2-deoxyglucose incorporation in peripheral nerve during ischemia. 1987;414:323–9.

43. Hagberg H. Intracellular pH during ischemia in skeletal muscle: relationship to membrane potential, extracellular pH, tissue lactic acid and ATP. Pflugers Arch. 1985 Aug;404(4):342–7.

44. David G, Nguyen K, Barrett EF. Early vulnerability to ischemia/reperfusion injury in motor terminals innervating fast muscles of SOD1-G93A mice. Exp Neurol. 2007 Mar;204(1):411–20.

45. Zollman PJ, Awad O, Schmelzer JD, Low PA. Effect of ischemia and reperfusion in vivo on energy metabolism of rat sciatic-tibial and caudal nerves. Exp Neurol. 1991;114(3):315–20.

46. Iida H, Schmelzer JD, Schmeichel AM, Wang Y, Low PA. Peripheral nerve ischemia: Reperfusion injury and fiber regeneration. Exp Neurol. 2003;184(2):997–1002.

47. Tu H, Zhang D, Corrick RM, Muelleman RL, Wadman MC, Li Y-L. Morphological

Regeneration and Functional Recovery of Neuromuscular Junctions after Tourniquet-Induced Injuries in Mouse Hindlimb. Front Physiol. 2017;8(April):207.

48. Quiñones-Baldrich WJ, Chervu a, Hernandez JJ, Colburn M, Moore WS. Skeletal muscle function after ischemia: “no reflow” versus reperfusion injury. J Surg Res. 1991 Jul;51(1):5–12.

49. Burwell LS, Brookes PS. Mitochondria as a target for the cardioprotective effects of nitric oxide in ischemia-reperfusion injury. Antioxid Redox Signal. 2008 Mar;10(3):579–99.

50. Chouchani ET, Pell VR, Gaude E, Aksentijević D, Sundier SY, Robb EL, et al. Ischaemic accumulation of succinate controls reperfusion injury through mitochondrial ROS. Nature. 2014;515(7527):431–5.

51. Neely JR, Grotyohann LW. Role of glycolytic products in damage to ischemic myocardium. Dissociation of adenosine triphosphate levels and recovery of function of reperfused ischemic hearts. Circ Res. 1984;55(6):816–24.

52. Fuller W, Parmar V, Eaton P, Bell JR, Shattock MJ. Cardiac ischemia causes inhibition of the Na/K ATPase by a labile cytosolic compound whose production is linked to oxidant stress. Cardiovasc Res. 2003;57(4):1044–51.

53. Marcinek DJ, Kushmerick MJ, Conley KE. Lactic acidosis in vivo: testing the link between lactate generation and H+ accumulation in ischemic mouse muscle. J Appl Physiol. 2010;108(6):1479–86.

54. Lodish H, Berk A, Zipursky S, Matsudaira P, Baltimore D, Darnell J. Molecular Cell Biology. 4th ed. New York: W.H. Freeman and Co.; 2000.

55. Acharya AP, Rafi M, Woods EC, Gardner AB, Murthy N. Metabolic engineering of lactate dehydrogenase rescues mice from acidosis. Sci Rep. 2014;4:1–5.

56. Bünger R, Mallet RT, Hartman D a. Pyruvate-enhanced phosphorylation potential and inotropism in normoxic and postischemic isolated working heart. Eur J Biochem. 1989 Mar 1;180(1):221–33.

57. Stecker MM, Stevenson M. Effects of pH on the response of peripheral nerve to anoxia. Int J Neurosci. 2015 Mar;125(3):221–7.

58. Heerlein K, Schulze A, Hotz L, Bärtsch P, Mairbäurl H. Hypoxia decreases cellular ATP demand and inhibits mitochondrial respiration of A549 cells. Am J Respir Cell Mol Biol. 2005;32(1):44–51.

59. Nakamura M, Jang IS. Acid modulation of tetrodotoxin-resistant Na+ channels in rat nociceptive neurons. Neuropharmacology. 2015;90:82–9.

60. Ivanics T, Miklós Z, Ruttner Z, Bátkai S, Slaaf DW, Reneman RS, et al. Ischemia/reperfusion-induced changes in intracellular free Ca2+ levels in rat skeletal muscle fibers--an in vivo study. Pflugers Arch. 2000 Jun;440(2):302–8.

61. Thaveau F, Zoll J, Bouitbir J, Ribera F, Di Marco P, Chakfe N, et al. Contralateral Leg as a Control During Skeletal Muscle Ischemia-Reperfusion1. J Surg Res. 2009;155(1):65–9.

62. Vosler P, Brennan C, Chen J. Calpain-Mediated Signaling Mechanisms in Neuronal Injury and Neurodegeneration. Mol Neurobiol. 2008;38(1):78–100.

63. Ma L, Chu W, Chai J, Shen C, Li D, Wang X. ER stress and subsequent activated calpain play a pivotal role in skeletal muscle wasting after severe burn injury. PLoS One. 2017;12(10):1–15.

64. López-Vales R, Navarro X, Shimizu T, Baskakis C, Kokotos G, Constantinou-Kokotou V, et al. Intracellular phospholipase A2 group IVA and group VIA play important roles in Wallerian degeneration and axon regeneration after peripheral nerve injury. Brain.

2008;131(10):2620–31.

65. van der Vusse GJ, van Bilsen M, Reneman RS. Ischemia and reperfusion induced alterations in membrane phospholipids: an overview. Ann N Y Acad Sci. 1994 Jun 17;723:1–14.

66. Griffiths EJ, Halestrap AP. Mitochondrial non-specific pores remain closed during cardiac ischaemia, but open upon reperfusion. Biochem J. 1995;307 (Pt 1:93–8.

67. Seidlmayer LK, Juettner V V., Kettlewell S, Pavlov E V., Blatter LA, Dedkova EN. Distinct mPTP activation mechanisms in ischaemia-reperfusion: Contributions of Ca^{2+}, ROS, pH, and inorganic polyphosphate. Cardiovasc Res. 2015;106(2):237–48.

68. Honda HM, Korge P, Weiss JN. Mitochondria and ischemia/reperfusion injury. Ann N Y Acad Sci. 2005 Jun;1047:248–58.

69. Tupling R, Green H, Senisterra G, Lepock J, McKee N. Effects of ischemia on sarcoplasmic reticulum Ca(2+) uptake and Ca(2+) release in rat skeletal muscle. Am J Physiol Endocrinol Metab. 2001;281(2):E224-32.

70. Bushell A, Klenerman L. Ischaemic preconditioning of skeletal muscle #2 Inbvestigation of the potential mechanisms involved. J Bone Jt Surg. 2002;84(8):1189–93.

71. Klenerman L, Lowe NM, Miller I, Fryer PR, Green CJ, Jackson MJ. Dantrolene sodium protects against experimental ischemia and reperfusion damage to skeletal muscle. Acta Orthop Scand. 1995 Aug;66(4):352–8.

72. Charles A-L, Guilbert A-S, Bouitbir J, Goette-Di Marco P, Enache I, Zoll J, et al. Effect of postconditioning on mitochondrial dysfunction in experimental aortic cross-clamping. Br J Surg. 2011 Apr;98(4):511–6.

73. Mansour Z, Charles AL, Bouitbir J, Pottecher J, Kindo M, Mazzucotelli JP, et al. Remote

and local ischemic postconditioning further impaired skeletal muscle mitochondrial function after ischemia-reperfusion. J Vasc Surg. 2012;56(3):774–782.e1.

74. Pipinos II, Judge AR, Zhu Z, Selsby JT, Swanson SA, Johanning JM, et al. Mitochondrial defects and oxidative damage in patients with peripheral arterial disease. Free Radic Biol Med. 2006;41(2):262–9.

75. Tran TP, Tu H, Pipinos II, Muelleman RL, Albadawi H, Li Y-L. Tourniquet-induced acute ischemia-reperfusion injury in mouse skeletal muscles: Involvement of superoxide. Eur J Pharmacol. 2011 Jan 10;650(1):328–34.

76. Addison PD, Neligan PC, Ashrafpour H, Khan A, Zhong A, Moses M, et al. Noninvasive remote ischemic preconditioning for global protection of skeletal muscle against infarction. Am J Physiol Heart Circ Physiol. 2003;285(4):H1435–43.

77. Kuzon WM, Walker PM, Mickle DA, Harris KA, Pynn BR, McKee NH. An isolated skeletal muscle model suitable for acute ischemia studies. J Surg Res. 1986 Jul;41(1):24–32.

78. Lejay A, Meyer A, Schlagowski A-I, Charles A-L, Singh F, Bouitbir J, et al. Mitochondria: mitochondrial participation in ischemia-reperfusion injury in skeletal muscle. Int J Biochem Cell Biol. 2014 May;50:101–5.

79. Sayan H, Ozacmak VH, Ozen OA, Coskun O, Arslan SO, Sezen SC, et al. Beneficial effects of melatonin on reperfusion injury in rat sciatic nerve. J Pineal Res. 2004;37(3):143–8.

80. Pottecher J, Kindo M, Chamaraux-Tran TN, Charles AL, Lejay A, Kemmel V, et al. Skeletal muscle ischemia-reperfusion injury and cyclosporine A in the aging rat. Fundam Clin Pharmacol. 2016;30(3):216–25.

81. Garbaisz D, Turoczi Z, Aranyi P, Fulop A, Rosero O, Hermesz E, et al. Attenuation of skeletal muscle and renal injury to the lower limb following ischemia-reperfusion using mPTP inhibitor NIM-811. PLoS One. 2014;9(6):1–12.

82. Fang H, Zhang J-C, Yang M, Li H-F, Zhang J-P, Zhang F-X, et al. Perfusion of gastrodin in abdominal aorta for alleviating spinal cord ischemia reperfusion injury. Asian Pac J Trop Med. 2016;9(7):688–93.

83. Murphy MP. How mitochondria produce reactive oxygen species. Biochem J. 2009 Jan 1;417(1):1–13.

84. Pisarenko O, Studneva I, Khlopkov V. Metabolism of the tricarboxylic acid cycle intermediates and related amino acids in ischemic guinea pig heart. Biomed Biochim Acta. 1987;46(8–9):S568-71.

85. Bendotti C, Calvaresi N, Chiveri L, Prelle A, Moggio M, Braga M, et al. Early vacuolization and mitochondrial damage in motor neurons of FALS mice are not associated with apoptosis or with changes in cytochrome oxidase histochemical reactivity. J Neurol Sci. 2001;191(1–2):25–33.

86. Pottecher J, Guillot M, Belaidi E, Charles AL, Lejay A, Gharib A, et al. Cyclosporine A normalizes mitochondrial coupling, reactive oxygen species production, and inflammation and partially restores skeletal muscle maximal oxidative capacity in experimental aortic cross-clamping. J Vasc Surg. 2013;57(4):1100–1108.e2.

87. Takhtfooladi HA, Takhtfooladi MA, Karimi P, Asl HA, Mousavi Nasab Mobarakeh SZ. Influence of tramadol on ischemia-reperfusion injury of rats' skeletal muscle. Int J Surg. 2014 Jul 22;(July):1–6.

88. Land WG. The role of damage-associated molecular patterns (DAMPs) in human diseases

part II: DAMPs as diagnostics, prognostics and therapeutics in clinical medicine. Sultan Qaboos Univ Med J. 2015;15(2):e157–70.

89. Hu Q, Wood CR, Cimen S, Venkatachalam AB, Alwayn IPJ. Mitochondrial damage-associated molecular patterns (MTDs) are released during hepatic ischemia reperfusion and induce inflammatory responses. PLoS One. 2015;10(10):1–17.

90. Appell H-J, Glöser S, Soares JMC, Duarte JA. Structural Alterations of Skeletal Muscle Induced by Ischemia and Reperfusion. Basic Appl Myol. 1999;9(5):263–8.

91. Wang Y, Kawamura N, Schmelzer JD, Schmeichel AM, Low PA. Decreased peripheral nerve damage after ischemia-reperfusion injury in mice lacking TNF-alpha. J Neurol Sci. 2008;267(1–2):107–11.

92. Sheu SS, Nauduri D, Anders MW. Targeting antioxidants to mitochondria: A new therapeutic direction. Biochim Biophys Acta - Mol Basis Dis. 2006;1762(2):256–65.

93. Walters AM, Porter GA, Brookes PS. Mitochondria as a drug target in ischemic heart disease and cardiomyopathy. Circ Res. 2012;111(9):1222–36.

94. Prime T a, Blaikie FH, Evans C, Nadtochiy SM, James AM, Dahm CC, et al. A mitochondria-targeted S-nitrosothiol modulates respiration, nitrosates thiols, and protects against ischemia-reperfusion injury. Proc Natl Acad Sci U S A. 2009 Jun 30;106(26):10764–9.

95. Huang C, Andres AM, Ratliff EP, Hernandez G, Lee P, Gottlieb RA. Preconditioning involves selective mitophagy mediated by parkin and p62/SQSTM1. PLoS One. 2011;6(6).

96. Kohr MJ, Sun J, Aponte A, Wang G, Gucek M, Murphy E, et al. Simultaneous measurement of protein oxidation and S-nitrosylation during preconditioning and

ischemia/reperfusion injury with resin-assisted capture. Circ Res. 2011 Feb 18;108(4):418–26.

97. Heusch G, Boengler K, Schulz R. Cardioprotection: nitric oxide, protein kinases, and mitochondria. Circulation. 2008 Nov 4;118(19):1915–9.

98. Hori K, Tsujii M, Iino T, Satonaka H, Uemura T, Akeda K, et al. Protective effect of edaravone for tourniquet-induced ischemia-reperfusion injury on skeletal muscle in murine hindlimb. BMC Musculoskelet Disord. 2013;14(1):113.

99. Mohler LR, Pedowitz RA, Ohara WM, Oyama BK, Lopez MA, Gershuni DH. Effects of an antioxidant in a rabbit model of tourniquet- induced skeletal muscle ischemia-reperfusion injury. J Surg Res. 1996;60(1):23–8.

100. Mitsui Y, Schmelzer JD, Zollman PJ, Mitsui M, Tritschler HJ, Low PA. Alpha-lipoic acid provides neuroprotection from ischemia- reperfusion injury of peripheral nerve. J Neurol Sci. 1999;163(1):11–6.

101. Zhou YF, Li L, Feng F, Yuan H, Gao DK, Fu LA, et al. Osthole attenuates spinal cord ischemiaereperfusion injury through mitochondrial biogenesiseindependent inhibition of mitochondrial dysfunction in rats. J Surg Res. 2013;185(2):805–14.

102. Quinlan CL, Orr AL, Perevoshchikova I V., Treberg JR, Ackrell BA, Brand MD. Mitochondrial complex II can generate reactive oxygen species at high rates in both the forward and reverse reactions. J Biol Chem. 2012;287(32):27255–64.

103. Starkov A a, Fiskum G, Chinopoulos C, Lorenzo BJ, Browne SE, Patel MS, et al. Mitochondrial alpha-ketoglutarate dehydrogenase complex generates reactive oxygen species. J Neurosci. 2004 Sep 8;24(36):7779–88.

104. Starkov AA. The Role of Mitochondria in Reactive Oxygen Species Metabolism and

Signaling. Ann N Y Acad Sci. 2008 Dec 8;1147(1):37–52.

105. Chen Q, Vazquez EJ, Moghaddas S, Hoppel CL, Lesnefsky EJ. Production of reactive oxygen species by mitochondria: Central role of complex III. J Biol Chem. 2003;278(38):36027–31.

106. Guzy RD, Hoyos B, Robin E, Chen H, Liu L, Mansfield KD, et al. Mitochondrial complex III is required for hypoxia-induced ROS production and cellular oxygen sensing. Cell Metab. 2005;1(6):401–8.

107. Rao VK, Carlson EA, Yan SS. Mitochondrial permeability transition pore is a potential drug target for neurodegeneration. Biochim Biophys Acta - Mol Basis Dis. 2014;1842(8):1267–72.

108. Troitzsch D, Moosdorf R, Hasenkam JM, Nygaard H, Vogt S. Effects of cyclosporine pretreatment on tissue oxygen levels and cytochrome oxidase in skeletal muscle ischemia and reperfusion. Shock. 2013 Feb;39(2):220–6.

109. Shintani-Ishida K, Yoshida KI. Mitochondrial m-calpain opens the mitochondrial permeability transition pore in ischemia-reperfusion. Int J Cardiol. 2015;197:26–32.

110. SOUSSI B, IDSTRÖM J-P, SCHERSTÉN T, BYLUND-FELLENIUS A-C. Cytochrome c oxidase and cardiolipin alterations in response to skeletal muscle ischaemia and reperfusion. Acta Physiol Scand. 1990 Feb;138(2):107–14.

111. Kaya C, Ustun YB, Atalay YO. Physiology of the neuromuscular junction and related disorders. J Exp Clin Med. 2014;31(3):149–53.

112. Gonzalez-Freire M, de Cabo R, Studenski SA, Ferrucci L. The neuromuscular junction: Aging at the crossroad between nerves and muscle. Front Aging Neurosci. 2014;6(AUG).

113. Maehle A-H. “Receptive substances”: John Newport Langley (1852-1925) and his path to

a receptor theory of drug action. Med Hist. 2004;48(2):153–74.

114. Changeux JP. The nicotinic acetylcholine receptor: The founding father of the pentameric ligand-gated ion channel superfamily. J Biol Chem. 2012;287(48):40207–15.

115. Tansey EM. Henry Dale and the discovery of acetylcholine. C R Biol. 2006 May;329(5–6):419–25.

116. Baret M, Katz R, Lamy JC, Pénicaud A, Wargon I. Evidence for recurrent inhibition of reciprocal inhibition from soleus to tibialis anterior in Man. Exp Brain Res. 2003;152(1):133–6.

117. Fatt, P, Katz B. Spontaneous subthreshold activity at motor nerve endings. J Physiol. 1952;117:109–28.

118. Del Castillo J, Katz B. Quantal Components of the End-Plate Potential. J Physiol. 1954;124:560–73.

119. Augustine GJ, Kasai H. Bernard Katz, quantal transmitter release and the foundations of presynaptic physiology. J Physiol. 2007;578(3):623–5.

120. Eccles JC, Eccles RM, Iggo a, Ito M. Distribution of recurrent inhibition among motoneurones. J Physiol. 1961;159:479–99.

121. Buller AJ, Eccles JC, Eccles RM. Interactions between motoneurones and muscles in respect of the characteristic speeds of their responses. J Physiol. 1960;150(2):417–39.

122. Burke RE. John Eccles' pioneering role in understanding central synaptic transmission. Prog Neurobiol. 2006;78(3–5):173–88.

123. Yampolsky P, Pacifici PG, Lomb L, Giese G, Rudolf R, Röder I V., et al. Time lapse in vivo visualization of developmental stabilization of synaptic receptors at neuromuscular junctions. J Biol Chem. 2010;285(45):34589–96.

124. Rohrbough J, Rushton E, Woodruff E, Fergestad T, Vigneswaran K, Broadie K. Presynaptic establishment of the synaptic cleft extracellular matrix is required for post-synaptic differentiation. Genes Dev. 2007;21(20):2607–28.

125. Ferraro E, Molinari F, Berghella L. Molecular control of neuromuscular junction development. J Cachexia Sarcopenia Muscle. 2012;3(1):13–23.

126. Witzemann V. Development of the neuromuscular junction. Cell Tissue Res. 2006;326(2):263–71.

127. Wu H, Xiong WC, Mei L. To build a synapse: signaling pathways in neuromuscular junction assembly. Development. 2010;137(7):1017–33.

128. Ryten M, Koshi R, Knight GE, Turmaine M, Dunn P, Cockayne DA, et al. Abnormalities in neuromuscular junction structure and skeletal muscle function in mice lacking the P2X2 nucleotide receptor. Neuroscience. 2007;148(3):700–11.

129. Lin S, Landmann L, Ruegg MA, Brenner HR. The role of nerve- versus muscle-derived factors in mammalian neuromuscular junction formation. J Neurosci. 2008;28(13):3333–40.

130. van der Pijl EM, van Putten M, Niks EH, Verschuuren JJGM, Aartsma-Rus A, Plomp JJ. Characterization of neuromuscular synapse function abnormalities in multiple Duchenne muscular dystrophy mouse models. Eur J Neurosci. 2016;43(12):1623–35.

131. Nishizawa T, Tamaki H, Kasuga N, Takekura H. Degeneration and regeneration of neuromuscular junction architecture in rat skeletal muscle fibers damaged by bupivacaine hydrochloride. J Muscle Res Cell Motil. 2003;24(8):527–37.

132. Martin LJ, Gertz B, Pan Y, Price AC, Molkentin JD, Chang Q. The mitochondrial permeability transition pore in motor neurons: Involvement in the pathobiology of ALS

mice. Exp Neurol. 2009;218(2):333–46.

133. Kong J, Xu Z. Massive mitochondrial degeneration in motor neurons triggers the. J Neurosci. 1998;18(9):3241–50.

134. Dupuis L, Gonzalez de Aguilar JL, Echaniz-Laguna A, Eschbach J, Rene F, Oudart H, et al. Muscle mitochondrial uncoupling dismantles neuromuscular junction and triggers distal degeneration of motor neurons. PLoS One. 2009;4(4).

135. Jang YC, Lustgarten MS, Liu Y, Muller FL, Bhattacharya A, Liang H, et al. Increased superoxide in vivo accelerates age-associated muscle atrophy through mitochondrial dysfunction and neuromuscular junction degeneration. FASEB J. 2010;24(5):1376–90.

136. Pollari E, Goldsteins G, Bart G, Koistinaho J, Giniatullin R. The role of oxidative stress in degeneration of the neuromuscular junction in amyotrophic lateral sclerosis. Front Cell Neurosci. 2014 May 13;8(May):131.

137. Rosato Siri MD, Uchitel OD. Calcium channels coupled to neurotransmitter release at neonatal rat neuromuscular junctions. J Physiol. 1999;514(2):533–40.

138. Sanes JR. The synaptic cleft of the neuromuscular junction. Semin Dev Biol. 1995;6(3):163–73.

139. Fambrough DM. Control of acetylcholine receptors in skeletal muscle. Physiol Rev. 1979;59(1):165–227.

140. Anderson K, Meissner G. T-tubule depolarization-induced SR Ca 2+ release is controlled by dihydropyridine receptor- and Ca 2+ -dependent mechanisms in cell homogenates from rabbit skeletal muscle. J Gen Physiol. 1995;105(March 1995):363–83.

141. Maack C, O'Rourke B. Excitation-contraction coupling and mitochondrial energetics. Basic Res Cardiol. 2007;102(5):369–92.

142. Spudich J a., Watt S. The Regulation of Rabbit Skeletal Muscle Contraction. J Biol Chem. 1971;245(15):4866–71.

143. Offer G, Ranatunga KW. A cross-bridge cycle with two tension-generating steps simulates skeletal muscle mechanics. Biophys J. 2013;105(4):928–40.

144. Podolsky RJ. The rate-limiting step in muscle contraction. Basic Res Cardiol. 1980;75(1):34–9.

145. McDonald CM. Clinical Approach to the Diagnostic Evaluation of Hereditary and Acquired Neuromuscular Diseases. Phys Med Rehabil Clin N Am. 2012 Aug;23(3):495–563.

146. Chouhan S. Normal motor and sensory nerve conduction velocity of radial nerve in young adult medical students. J Clin Diagnostic Res. 2016;10(1):CC01-CC03.

147. Howard JF. Electrodiagnosis of Disorders of Neuromuscular Transmission. Phys Med Rehabil Clin N Am. 2013;24(1):169–92.

148. Tassinary LG, Cacioppo JT, Vanman EJ. The skeletomotor system: surface electromyography. Handb Psychophysiol. 2000;(January):267–99.

149. Morrow JM, Sinclair CDJ, Fischmann A, Machado PM, Reilly MM, Yousry TA, et al. MRI biomarker assessment of neuromuscular disease progression: a prospective observational cohort study. Lancet Neurol. 2016;15(1):65–77.

150. Dvm OP, Dvm SP. Histochemical and immunohistological approach to comparative neuromuscular diseases. 2009;47(2):143–52.

151. Burke RE, Strick PL, Kanda K, Kim CC, Walmsley B. Anatomy of medial gastrocnemius and soleus motor nuclei in cat spinal cord. J Neurophysiol. 1977;40(3):667–80.

152. Dawson G. D. The relative excitability and conduction velocity of sensory and motor

nerve fibres in man. JPhysiol. 1956;131:436–51.

153. Schmalbruch H. Fiber composition of the rat sciatic nerve. Anat Rec. 1986;215(1):71–81.

154. Nishimune H, Valdez G, Jarad G, Moulson CL, Müller U, Miner JH, et al. Laminins promote postsynaptic maturation by an autocrine mechanism at the neuromuscular junction. J Cell Biol. 2008;182(6):1201–15.

155. Seidl AH. Regulation of conduction time along axons. Neuroscience. 2014;276:126–34.

156. Barik A, Li L, Sathyamurthy A, Xiong W-C, Mei L. Schwann Cells in Neuromuscular Junction Formation and Maintenance. J Neurosci. 2016;36(38):9770–81.

157. Kang H, Tian L, Mikesh M, Lichtman JW, Thompson WJ. Terminal Schwann Cells Participate in Neuromuscular Synapse Remodeling during Reinnervation following Nerve Injury. J Neurosci. 2014;34(18):6323–33.

158. Burke RE, Levine DN, Tsairis P, Zajac FE. Physiological types and histochemical profiles in motor units of the cat gastrocnemius. J Physiol. 1973;234(3):723–48.

159. Rafuse VF, Pattullo MC, Gordon T. Innervation ratio and motor unit force in large muscles: a study of chronically stimulated cat medial gastrocnemius. J Physiol. 1997;499 (Pt 3:809–23.

160. Slater CR. Structural determinants of the reliability of synaptic transmission at the vertebrate neuromuscular junction. J Neurocytol. 2003;32(5–8):505–22.

161. Hall ZW, Sanes JR. Synaptic structure and development: The neuromuscular junction. Cell. 1993;72(1001):99–121.

162. Slater CR. The structure of human neuromuscular junctions: Some unanswered molecular questions. Int J Mol Sci. 2017;18(10).

163. Slater CR. Structural factors influencing the efficacy of neuromuscular transmission. Ann

N Y Acad Sci. 2008;1132:1–12.

164. Torres-Benito L, Neher MF, Cano R, Ruiz R, Tabares L. SMN requirement for synaptic vesicle, active zone and microtubule postnatal organization in motor nerve terminals. PLoS One. 2011;6(10).

165. Kittel RJ, Heckmann M. Synaptic vesicle proteins and active zone plasticity. Front Synaptic Neurosci. 2016;8(APR):1–8.

166. Ackermann F, Waites CL, Garner CC. Presynaptic active zones in invertebrates and vertebrates. EMBO Rep. 2015;16(8):1–16.

167. GRAY EG. Electron microscopy of presynaptic organelles of the spinal cord. J Anat. 1963;97(Pt 1):101–6.

168. Harlow ML, Ress D, Stoschek A, Marshall RM, McMahan UJ. The architecture of active zone material at the frog's neuromuscular junction. Nature. 2001;409(6819):479–84.

169. Chen J, Mizushige T, Nishimune H. Active zone density is conserved during synaptic growth but impaired in aged mice. J Comp Neurol. 2012 Feb 1;520(2):434–52.

170. Wood SJ, R. Slater C. Safety factor at the neuromuscular junction. Vol. 64, Progress in Neurobiology. 2001. 393-429 p.

171. Nishimune H. Molecular Mechanism of Active Zone Organization at Vertebrate Neuromuscular Junctions. Mol Neurobiol. 2012 Feb 2;45(1):1–16.

172. Singhal N, Martin P. Role of extracellular matrix proteins and their receptors in the development of the vertebrate neuromuscular junction. Dev Neurobiol. 2011;71(11):982–1005.

173. Nishimune H, Sanes JR, Carlson SS. A synaptic laminin-calcium channel interaction organizes active zones in motor nerve terminals. Nature. 2004;432(7017):580–7.

174. Laßek M, Weingarten J, Volknandt W. The Proteome of the Murine Presynaptic Active Zone. Proteomes. 2014;2(2):243–57.

175. Nagwaney S, Harlow ML, Jung JH, Szule JA, Ress D, Xu J, et al. Macromolecular connections of active zone material to docked synaptic vesicles and presynaptic membrane at neuromuscular junctions of mouse. J Comp Neurol. 2009;513(5):457–68.

176. Ruiz R, Cano R, Casanas JJ, Gaffield MA, Betz WJ, Tabares L. Active Zones and the Readily Releasable Pool of Synaptic Vesicles at the Neuromuscular Junction of the Mouse. J Neurosci. 2011;31(6):2000–8.

177. Verstreken P, Ohyama T, Bellen HJ. FM 1-43 labeling of synaptic vesicle pools at the drosophila neuromuscular junction. Methods Mol Biol. 2008;440:349–69.

178. KATZ B, MILEDI R. The measurement of synaptic delay, and the time course of acetylcholine release at the neuromuscular junction. Proc R Soc London Ser B, Biol Sci. 1965 Feb 16;161:483–95.

179. Kuffler SW, Yoshikami D. The number of transmitter molecules in a quantum: an estimate from iontophoretic application of acetylcholine at the neuromuscular synapse. J Physiol. 1975;251:465–82.

180. Katz B, Miledi R. The binding of acetylcholine to receptors and its removal from the synaptic cleft. J Physiol. 1973;231(3):549–74.

181. Ruff RL. Endplate contributions to the safety factor for neuromuscular transmission. Muscle and Nerve. 2011;44(6):854–61.

182. Heuser JE, Reese TS. Evidence for recycling of synaptic vesicle membrane during transmitter release at the frog neuromuscular junction. J Cell Biol. 1973;57(2):315–44.

183. Henkel A, Lübke J, Betz W. FM1-43 dye ultrastructural localization in and release from

frog motor nerve terminals. Cell Biol. 1996;93(March):1918–23.

184. Gaffield MA, Betz WJ. Imaging synaptic vesicle exocytosis and endocytosis with FM dyes. Nat Protoc. 2007;1(6):2916–21.

185. Denker A, Bethani I, Krohnert K, Korber C, Horstmann H, Wilhelm BG, et al. A small pool of vesicles maintains synaptic activity in vivo. Proc Natl Acad Sci. 2011;108(41):17177–82.

186. Dimauro S, Bonilla E, Davidson M, Hirano M, Schon EA. Mitochondria in neuromuscular disorders. Biochim Biophys Acta - Bioenerg. 1998;1366(1–2):199–210.

187. Xu C-C, Denton KR, Wang Z-B, Zhang X, Li X-J. Abnormal mitochondrial transport and morphology as early pathological changes in human models of spinal muscular atrophy. Dis Model Mech. 2015;dmm.021766.

188. Chouhan AK, Zhang J, Zinsmaier KE, Macleod GT. Presynaptic Mitochondria in Functionally Different Motor Neurons Exhibit Similar Affinities for Ca2+ But Exert Little Influence as Ca2+ Buffers at Nerve Firing Rates In Situ. J Neurosci. 2010 Feb 3;30(5):1869–81.

189. Calupca M a, Hendricks GM, Hardwick JC, Parsons RL. Role of mitochondrial dysfunction in the Ca2+-induced decline of transmitter release at K+-depolarized motor neuron terminals. J Neurophysiol. 1999;81(2):498–506.

190. Ivannikov M V., Harris KM, Macleod GT. Mitochondria: Enigmatic stewards of the synaptic vesicle reserve pool. Front Synaptic Neurosci. 2010;2(OCT):2–3.

191. Vaca K, Pilar G. Mechanisms controlling choline transport and acetylcholine synthesis in motor nerve terminals during electrical stimulation. J Gen Physiol. 1979;73(5):605–28.

192. Unsworth CD. Acetylcholine and ATP are coreleased from the electromotor nerve

terminals of Narcine brasiliensis by an exocytotic mechanism. 1990;87(January):553–7.

193. Calupca MA, Prior C, Merriam LA, Hendricks GM, Parsons RL. Presynaptic function is altered in snake K+-depolarized motor nerve terminals containing compromised mitochondria. J Physiol. 2001;532(1):217–27.

194. Verstreken P, Ly C V., Venken KJT, Koh TW, Zhou Y, Bellen HJ. Synaptic mitochondria are critical for mobilization of reserve pool vesicles at Drosophila neuromuscular junctions. Neuron. 2005;47(3):365–78.

195. Kurnellas MP, Nicot A, Shull GE, Elkabes S. Plasma membrane calcium ATPase deficiency causes neuronal pathology in the spinal cord: a potential mechanism for neurodegeneration in multiple sclerosis and spinal cord injury. Cell Death Differ. 2005;19(2):298–300.

196. Rangaraju V, Calloway N, Ryan TA. Activity-driven local ATP synthesis is required for synaptic function. Cell. 2014 Feb;156(4):825–35.

197. Barrett EF, Barrett JN, David G. Dysfunctional mitochondrial Ca2+ handling in mutant SOD1 mouse models of fALS: integration of findings from motor neuron somata and motor terminals. Front Cell Neurosci. 2014;8(July):1–5.

198. Nanou E, Yan J, Whitehead NP, Kim MJ, Froehner SC, Scheuer T, et al. Altered short-term synaptic plasticity and reduced muscle strength in mice with impaired regulation of presynaptic CaV2.1 Ca2+ channels. Proc Natl Acad Sci U S A. 2016;113(4):1068–73.

199. Chouhan AK, Ivannikov M V., Lu Z, Sugimori M, Llinas RR, Macleod GT. Cytosolic Calcium Coordinates Mitochondrial Energy Metabolism with Presynaptic Activity. J Neurosci. 2012 Jan 25;32(4):1233–43.

200. Colegrove SL, Albrecht MA, Friel DD. Quantitative analysis of mitochondrial Ca2+

uptake and release pathways in sympathetic neurons - Reconstruction of the recovery after depolarization-evoked Ca2+ (i) elevations. J Gen Physiol. 2000;115(3):371–88.

201. Colegrove SL, Albrecht MA, Friel DD. Dissection of mitochondrial Ca2+ uptake and release fluxes in situ after depolarization-evoked Ca2+ (i) elevations in sympathetic neurons. J Gen Physiol. 2000;115(3):351–69.

202. McCormack JG, Halestrap AP, Denton RM. Role of calcium ions in regulation of mammalian intramitochondrial metabolism. Physiol Rev. 1990;70(2):391–425.

203. Traaseth N, Elfering S, Solien J, Haynes V, Giulivi C. Role of calcium signaling in the activation of mitochondrial nitric oxide synthase and citric acid cycle. Biochim Biophys Acta - Bioenerg. 2004;1658(1–2):64–71.

204. Kawamata H, Manfredi G. Mitochondrial dysfunction and intracellular calcium dysregulation in ALS. Mech Ageing Dev. 2010 Jul;131(7–8):517–26.

205. Kruman II, Pedersen WA, Springer JE, Mattson MP. ALS-Linked Cu/Zn–SOD Mutation Increases Vulnerability of Motor Neurons to Excitotoxicity by a Mechanism Involving Increased Oxidative Stress and Perturbed Calcium Homeostasis. Exp Neurol. 1999;160(1):28–39.

206. Kirkinezos IG, Hernandez D, Bradley WG, Moraes CT. An ALS mouse model with a permeable blood-brain barrier benefits from systemic cyclosporine A treatment. J Neurochem. 2004;88(4):821–6.

207. Takeuchi H, Kobayashi Y, Ishigaki S, Doyu M, Sobue G. Mitochondrial localization of mutant superoxide dismutase 1 triggers caspase-dependent cell death in a cellular model of familial amyotrophic lateral sclerosis. J Biol Chem. 2002;277(52):50966–72.

208. Ikenaka K, Katsuno M, Kawai K, Ishigaki S, Tanaka F, Sobue G. Disruption of axonal

transport in motor neuron diseases. Int J Mol Sci. 2012;13(1):1225–38.

209. Miller CC, Villa MA, Achouh P, Estrera AL, Azizzadeh A, Coogan SM, et al. Intraoperative skeletal muscle ischemia contributes to risk of renal dysfunction following thoracoabdominal aortic repair. Eur J Cardio-thoracic Surg. 2008;33(4):691–4.

210. Chang DTW, Reynolds IJ. Mitochondrial trafficking and morphology in healthy and injured neurons. Prog Neurobiol. 2006;80(5):241–68.

211. Cai Q, Zakaria HM, Simone A, Sheng ZH. Spatial parkin translocation and degradation of damaged mitochondria via mitophagy in live cortical neurons. Curr Biol. 2012;22(6):545–52.

212. Zhou B, Yu P, Lin MY, Sun T, Chen Y, Sheng ZH. Facilitation of axon regeneration by enhancing mitochondrial transport and rescuing energy deficits. J Cell Biol. 2016;214(1):103–19.

213. Kiryu-Seo S, Tamada H, Kato Y, Yasuda K, Ishihara N, Nomura M, et al. Mitochondrial fission is an acute and adaptive response in injured motor neurons. Sci Rep. 2016;6:1–14.

214. Vos M, Lauwers E, Verstreken P. Synaptic mitochondria in synaptic transmission and organization of vesicle pools in health and disease. Front Synaptic Neurosci. 2010;2(SEP):1–10.

215. Shi P, Gal J, Kwinter DM, Liu X, Zhu H. Mitochondrial dysfunction in amyotrophic lateral sclerosis. Biochim Biophys Acta - Mol Basis Dis. 2010;1802(1):45–51.

216. Meital LT, Sandow SL, Calder PC, Russell FD. Abdominal aortic aneurysm and omega-3 polyunsaturated fatty acids: Mechanisms, animal models, and potential treatment. Prostaglandins Leukot Essent Fat Acids. 2017;118(October 2016):1–9.

217. Xu W, Chi L, Xu R, Ke Y, Luo C, Cai J, et al. Increased production of reactive oxygen

species contributes to motor neuron death in a compression mouse model of spinal cord injury. Spinal Cord. 2005;43(4):204–13.

218. Julien J-P, Kriz J. Transgenic mouse models of amyotrophic lateral sclerosis. Biochim Biophys Acta - Mol Basis Dis. 2006;1762(11–12):1013–24.

219. Higgins CMJ, Jung C, Xu Z. ALS-associated mutant SOD1G93A causes mitochondrial vacuolation by expansion of the intermembrane space and by involvement of SOD1 aggregation and peroxisomes. BMC Neurosci. 2003;4:16.

220. Tang J, Hu Z, Tan J, Yang S, Zeng L. Parkin Protects against Oxygen-Glucose Deprivation/Reperfusion Insult by Promoting Drp1 Degradation. Oxid Med Cell Longev. 2016;2016.

221. Miller N, Shi H, Zelikovich AS, Ma Y-C. Motor neuron mitochondrial dysfunction in spinal muscular atrophy. Hum Mol Genet. 2016;25(16):3395–406.

222. Rich MM, Teener JW, Raps EC, Schotland DL, Bird SJ. Muscle is electrically inexcitable in acute quadriplegic myopathy. Neurology. 1996;46(3):731–6.

223. Abmayr SM, Pavlath GK. Myoblast fusion: lessons from flies and mice. Development. 2012;139(4):641–56.

224. Lin W, Burgess RW, Dominguez B, Pfaff SL, Sanes JR, Lee KF. Distinct roles of nerve and muscle in postsynaptic differentiation of the neuromuscular synapse. Nature. 2001;410(6832):1057–64.

225. Patton BL. Basal lamina and the organization of neuromuscular synapses. J Neurocytol. 2003;32(5–8):883–903.

226. Sanes JR. The basement membrane/basal lamina of skeletal muscle. J Biol Chem. 2003;278(15):12601–4.

227. Rushton E, Rohrbough J, Broadie K. Presynaptic secretion of mind-the-gap organizes the synaptic extracellular matrix-integrin interface and postsynaptic environments. Dev Dyn. 2009 Mar;238(3):554–71.

228. Anglister L, Eichler J, Szabo M, Haesaert B, Salpeter MM. 125I-labeled fasciculin 2: A new tool for quantitation of acetylcholinesterase densities at synaptic sites by EM-autoradiography. J Neurosci Methods. 1998;81(1–2):63–71.

229. Borsook D. Neurological diseases and pain. Brain. 2012;135(2):320–44.

230. Engel AG, Ohno K, Shen XM, Sine SM. Congenital myasthenic syndromes: Multiple molecular targets at the neuromuscular junction. Ann N Y Acad Sci. 2003;998:138–60.

231. Wendell LC, Levine JM. Myasthenic Crisis. The Neurohospitalist. 2011 Jan;1(1):16–22.

232. Juel VC. Myasthenia gravis: Management of myasthenic crisis and perioperative care. Semin Neurol. 2004;24(1):75–81.

233. Awad SS, Lightowlers RN, Young C, Chrzanowska-Lightowlers ZM, Lomo T, Slater CR. Sodium channel mRNAs at the neuromuscular junction: distinct patterns of accumulation and effects of muscle activity. J Neurosci. 2001;21(21):8456–63.

234. Albuquerque EX, Barnard EA, Porter CW, Warnick JE. The density of acetylcholine receptors and their sensitivity in the postsynaptic membrane of muscle endplates. Proc Natl Acad Sci U S A. 1974;71(7):2818–22.

235. Marangi PA, Forsayeth JR, Mittaud P, Erb-Vögtli S, Blake DJ, Moransard M, et al. Acetylcholine receptors are required for agrin-induced clustering of postsynaptic proteins. EMBO J. 2001;20(24):7060–73.

236. Choi HY, Liu Y, Tennert C, Sugiura Y, Karakatsani A, Kröger S, et al. APP interacts with LRP4 and agrin to coordinate the development of the neuromuscular junction in mice.

Elife. 2013;2:e00220.

237. Samuel MA, Valdez G, Tapia JC, Lichtman JW, Sanes JR. Agrin and Synaptic Laminin Are Required to Maintain Adult Neuromuscular Junctions. PLoS One. 2012;7(10).

238. Stocksley MA, Awad SS, Young C, Lightowlers RN, Brenner HR, Slater CR. Accumulation of NaV1 mRNAs at differentiating postsynaptic sites in rat soleus muscles. Mol Cell Neurosci. 2005;28(4):694–702.

239. Avila OL, Drachman DB, Pestronk A. Neurotransmission regulates stability of acetylcholine receptors at the neuromuscular junction. J Neurosci. 1989;9(8):2902–6.

240. Stanley EF, Drachman DB. Denervation accelerates the degradation of junctional acetylcholine receptors. Exp Neurol. 1981;73(2):390–6.

241. Flucher BE, Daniels MP. Distribution of Na+ channels and ankyrin in neuromuscular junctions is complementary to that of acetylcholine receptors and the 43 kd protein. Neuron. 1989;3(2):163–75.

242. Gilly WF, Lucero MT, Horrigan FT. Control of the spatial distribution of sodium channels in giant fiber lobe neurons of the squid. Neuron. 1990;5(5):663–74.

243. Ruff RL. Na current density at and away from end plates on rat fast- and slow-twitch skeletal muscle fibers. Am J Physiol Cell Physiol. 1992;262(1):229–34.

244. Caldwell JD, Campbell DT, Beam KG. Na channel distribution in vertebrate skeletal muscle. J Gen Physiol. 1986;87(June):907–32.

245. Tömböl T, Pataki G, Németh a, Hamar J. Ultrastructural changes of the neuromuscular junction in reperfusion injury. Cells Tissues Organs. 2002 Jan;170(2–3):139–50.

246. Cogswell AM, Stevens RJ, Hood DA. Properties of skeletal muscle mitochondria isolated from subsarcolemmal and intermyofibrillar regions. Am J Physiol. 1993;264(2 Pt

1):C383-9.

247. Yi J, Ma C, Li Y, Weisleder N, Ríos E, Ma J, et al. Mitochondrial calcium uptake regulates rapid calcium transients in skeletal muscle during excitation-contraction (E-C) coupling. J Biol Chem. 2011;286(37):32436–43.

248. Arnold A-S, Gill J, Christe M, Ruiz R, McGuirk S, St-Pierre J, et al. Morphological and functional remodelling of the neuromuscular junction by skeletal muscle PGC-1α. Nat Commun. 2014;5:3569.

249. Seene T, Umnova M, Kaasik P. Morphological peculiarities of neuromuscular junctions among different fiber types : Effect of exercise. 27(3):139–46.

250. Pour MB. Long-term Low-Intensity Endurance Exercise along with Blood-Flow Restriction Improves Muscle Mass and Neuromuscular Junction Compartments in Old Rats. 2017;42(6):569–76.

251. Handschin C, Kobayashi YM, Chin S, Seale P, Campbell KP, Spiegelman BM. PGC-1α regulates the neuromuscular junction program and ameliorates Duchenne muscular dystrophy. Genes Dev. 2007;21(7):770–83.

252. Sandri M, Lin J, Handschin C, Yang W, Arany ZP, Lecker SH, et al. PGC-1alpha protects skeletal muscle from atrophy by suppressing FoxO3 action and atrophy-specific gene transcription. Proc Natl Acad Sci U S A. 2006 Oct 31;103(44):16260–5.

253. Madsen K, Ertbjerg P, Djurhuus MS, Pedersen PK. Calcium content and respiratory control index of skeletal muscle mitochondria during exercise and recovery. Am J Physiol Endocrinol Metab. 1996;271(6):E1044-1050.

254. Vecellio Reane D, Vallese F, Checchetto V, Acquasaliente L, Butera G, De Filippis V, et al. A MICU1 Splice Variant Confers High Sensitivity to the Mitochondrial Ca2+ Uptake

Machinery of Skeletal Muscle. Mol Cell. 2016;64(4):760–73.

255. Barclay CJ, Woledge RC, Curtin NA. Energy turnover for Ca2+ cycling in skeletal muscle. J Muscle Res Cell Motil. 2007;28(4–5):259–74.

256. Biochem CJ. Conformational Binding Change of Troponin T Induced by Calcium to Troponin Contraction of skeletal muscle is regulated by the troponin (Tn) -tropomyosin complex in the thin filament (1 , 2). Troponin is composed of three subunits . Troponin C (TnC) . 1985;98(1):261–3.

257. He Z-H, Bottinelli R, Pellegrino MA, Ferenczi MA, Reggiani C. ATP Consumption and Efficiency of Human Single Muscle Fibers with Different Myosin Isoform Composition. Biophys J. 2000;79(2):945–61.

258. Joubert F, Wilding JR, Fortin D, Domergue-Dupont V, Novotova M, Ventura-Clapier R, et al. Local energetic regulation of sarcoplasmic and myosin ATPase is differently impaired in rats with heart failure. J Physiol. 2008;586(Pt 21):5181–92.

259. Nicholls DG. Calcium transport and porton electrochemical potential gradient in mitochondria from guinea-pig cerebral cortex and rat heart. Biochem J. 1978;170(3):511–22.

260. Duchen MR. Mitochondria and calcium: from cell signalling to cell death. J Physiol. 2000;529(1):57–68.

261. Zhou J, Yi J, Fu R, Liu E, Siddique T, Rios E, et al. Hyperactive intracellular calcium signaling associated with localized mitochondrial defects in skeletal muscle of an animal model of amyotrophic lateral sclerosis. J Biol Chem. 2010;285(1):705–12.

262. Duchen MR, Leyssens A, Crompton M. Transient mitochondrial depolarizations reflect focal sarcoplasmic reticular calcium release in single rat cardiomyocytes. J Cell Biol.

1998;142(4):975–88.

263. Glancy B, Willis WT, Chess DJ, Balaban RS. Effect of calcium on the oxidative phosphorylation cascade in skeletal muscle mitochondria. Biochemistry. 2013;52(16):2793–809.

264. Logan C V., Szabadkai G, Sharpe JA, Parry DA, Torelli S, Childs AM, et al. Loss-of-function mutations in MICU1 cause a brain and muscle disorder linked to primary alterations in mitochondrial calcium signaling. Nat Genet. 2014;46(2):188–93.

265. Turchanyi B, Hama J, Tombol T, Siklos L. Capsaicin delays regeneration of the neuromuscular junction of rat extensor digitorum longus muscle after ischemia. Muscle and Nerve. 2006;33(4):556–67.

266. Lyons PR, Slater CR. Structure and function of the neuromuscular junction in young adult mdx mice. J Neurocytol. 1991 Dec;20(12):969–81.

267. Kuznetsov A V, Winkler K, Wiedemann FR, vonBossanyi P, Dietzmann K, Kunz WS. Impaired mitochondrial oxidative phosphorylation in skeletal muscle of the dystrophin-deficient mdx mouse. Mol Cell Biochem. 1998;183(1–2):87–96.

268. Chakkalakal J V., Michel SA, Chin ER, Michel RN, Jasmin BJ. Targeted inhibition of Ca2+/calmodulin signaling exacerbates the dystrophic phenotype in mdx mouse muscle. Hum Mol Genet. 2006;15(9):1423–35.

269. Disatnik M-H, Dhawan J, Yu Y, Beal MF, Whirl MM, Franco AA, et al. Evidence of oxidative stress in mdx mouse muscle: Studies of the pre-necrotic state. J Neurol Sci. 1998;161(1):77–84.

270. Chen YW, Zhao P, Borup R, Hoffman EP. Expression profiling in the muscular dystrophies: Identification of novel aspects of molecular pathophysiology. J Cell Biol.

2000;151(6):1321–36.

271. Muller FL, Song W, Jang YC, Liu Y, Sabia M, Richardson A, et al. Denervation-induced skeletal muscle atrophy is associated with increased mitochondrial ROS production. Am J Physiol Regul Integr Comp Physiol. 2007;293(3):R1159–68.

272. Rudolf R, Khan MM, Labeit S, Deschenes MR. Degeneration of neuromuscular junction in age and dystrophy. Front Aging Neurosci. 2014;6(MAY):1–11.

273. Ibebunjo C, Chick JM, Kendall T, Eash JK, Li C, Zhang Y, et al. Genomic and Proteomic Profiling Reveals Reduced Mitochondrial Function and Disruption of the Neuromuscular Junction Driving Rat Sarcopenia. Mol Cell Biol. 2013;33(2):194–212.

274. Masiero E, Agatea L, Mammucari C, Blaauw B, Loro E, Komatsu M, et al. Autophagy Is Required to Maintain Muscle Mass. Cell Metab. 2009;10(6):507–15.

275. Call JA, Wilson RJ, Laker RC, Zhang M, Kundu M, Yan Z. Ulk1-mediated autophagy plays an essential role in mitochondrial remodeling and functional regeneration of skeletal muscle. Am J Physiol - Cell Physiol. 2017;4477:ajpcell.00348.2016.

276. Nichenko AS, Southern WM, Atuan M, Luan J, Peissig KB, Foltz SJ, et al. Mitochondrial maintenance via autophagy contributes to functional skeletal muscle regeneration and remodeling. Am J Physiol Cell Physiol. 2016;ajpcell.00066.2016.

277. Laker RC, Drake JC, Wilson RJ, Lira VA, Lewellen BM, Ryall KA, et al. Ampk phosphorylation of Ulk1 is required for targeting of mitochondria to lysosomes in exercise-induced mitophagy. Nat Commun. 2017;8(1):548.

278. Lira VA, Okutsu M, Zhang M, Greene NP, Laker RC, Breen DS, et al. Autophagy is required for exercise training-induced skeletal muscle adaptation and improvement of physical performance. FASEB J. 2013;27(10):4184–93.

279. Carnio S, LoVerso F, Baraibar M, Longa E, Khan M, Maffei M, et al. Autophagy Impairment in Muscle Induces Neuromuscular Junction Degeneration and Precocious Aging. Cell Rep. 2014;8(5):1509–21.

280. Gorman CM, Moffat LF, Howard BH. Recombinant genomes which express chloramphenicol acetyltransferase in mammalian cells. Mol Cell Biol. 1982;2(9):1044–51.

281. Alexopoulou AN, Couchman JR, Whiteford JR. The CMV early enhancer/chicken β actin (CAG) promoter can be used to drive transgene expression during the differentiation of murine embryonic stem cells into vascular progenitors. BMC Cell Biol. 2008;9(1):2.

282. Wilson RJ, Drake JC, Cui D, Zhang M, Perry HM, Kashatus JA, et al. Conditional MitoTimer reporter mice for assessment of mitochondrial structure, oxidative stress, and mitophagy. Mitochondrion. 2017 Dec;

283. Bonheur J a, Albadawi H, Patton GM, Watkins MT. A noninvasive murine model of hind limb ischemia-reperfusion injury. J Surg Res. 2004 Jan;116(1):55–63.

284. Laker RC, Xu P, Ryall K a, Sujkowski A, Kenwood BM, Chain KH, et al. A novel MitoTimer reporter gene for mitochondrial content, structure, stress, and damage in vivo. J Biol Chem. 2014 Apr 25;289(17):12005–15.

285. Valdez G, Tapia JC, Kang H, Clemenson GD, Gage FH, Lichtman JW, et al. Attenuation of age-related changes in mouse neuromuscular synapses by caloric restriction and exercise. Proc Natl Acad Sci U S A. 2010;107(33):14863–8.

286. Pratt SJP, Shah SB, Ward CW, Kerr JP, Stains JP, Lovering RM. Recovery of altered neuromuscular junction morphology and muscle function in mdx mice after injury. Cell Mol Life Sci. 2014;72(1):153–64.

287. Mufti SA, Carlson BM, Maxwell LC, Faulkner JA. The free autografting of entire limb

muscles in the cat: Morphology. Anat Rec. 1977;188(4):417–29.

288. Jaffrey SR, Snyder SH. The biotin switch method for the detection of S-nitrosylated proteins. Sci STKE. 2001 Jun 12;2001(86):pl1.

289. Pratt SJ, Shah SB, Ward CW, Inacio MP, Stains JP, Lovering RM. Effects of in vivo injury on the neuromuscular junction in healthy and dystrophic muscles. J Physiol. 2013;591:559–70.

290. Kurimoto S, Jung J, Tapadia M, Lengfeld J, Agalliu D, Waterman M, et al. Activation of the Wnt/β-catenin signaling cascade after traumatic nerve injury. Neuroscience. 2015;294:101–8.

291. Carmo-Araújo EM, Dal-Pai-Silva M, Dal-Pai V, Cecchini R, Anjos Ferreira AL. Ischaemia and reperfusion effects on skeletal muscle tissue: morphological and histochemical studies. Int J Exp Pathol. 2007 Jun;88(3):147–54.

292. Dennis DA, Kittelson AJ, Yang CC, Miner TM, Kim RH, Stevens-Lapsley JE. Does Tourniquet Use in TKA Affect Recovery of Lower Extremity Strength and Function? A Randomized Trial. Clin Orthop Relat Res. 2016;474(1):69–77.

293. Eastlack RK, Groppo ER, Hargens AR, Pedowitz RA. Ischemic-preconditioning does not prevent neuromuscular dysfunction after ischemia - Reperfusion injury. J Orthop Res. 2004;22(4):918–23.

294. Teng D, Hornberger TA. Optimal Temperature for Hypothermia Intervention in Mouse Model of Skeletal Muscle Ischemia Reperfusion Injury. Cell Mol Bioeng. 2011 Dec 19;4(4):717–23.

295. Lysakowski A, Figueras H, Price SD, Peng Y. Dense-Cored Vesicles , Smooth Endoplasmic Reticulum , and Mitochondria Are Closely Associated With Non-

Specialized Parts of Plasma Membrane of Nerve Terminals : Implications for Exocytosis and Calcium Buffering by Intraterminal Organelles. 1999;390(September 1998):378–90.

296. Wong M, Martin LJ. Skeletal muscle-restricted expression of human SOD1 causes motor neuron degeneration in transgenic mice. Hum Mol Genet. 2010;19(11):2284–302.

297. Alnaes E, Rahamimoff R. On the role of mitochondria in transmitter release from motor nerve terminals. J Physiol. 1975;248(2):285–306.

298. Hollenbeck PJ. Mitochondria and neurotransmission: Evacuating the synapse. Neuron. 2005;47(3):331–3.

299. O'Hanlon GM, Humphreys PD, Goldman RS, Halstead SK, Bullens RWM, Plomp JJ, et al. Calpain inhibitors protect against axonal degeneration in a model of anti-ganglioside antibody-mediated motor nerve terminal injury. Brain. 2003;126(11):2497–509.

300. Loschen G, Azzi A, Richter C, Plohi L. Superoxide Radicals As Precursors of Mitochondrial Hydrogen Peroxide. 1974;42(1):68–72.

301. Handy DE, Loscalzo J. Redox Regulation of Mitochondrial Function. Antioxid Redox Signal. 2012;16(11):1323–67.

302. Chen Q, Camara AKS, Stowe DF, Hoppel CL, Lesnefsky EJ. Modulation of electron transport protects cardiac mitochondria and decreases myocardial injury during ischemia and reperfusion. AJP Cell Physiol. 2006;292(1):C137–47.

303. Dröse S, Brandt U, Wittig I. Mitochondrial respiratory chain complexes as sources and targets of thiol-based redox-regulation. Biochim Biophys Acta. 2014 Feb 19;

304. Näpänkangas JP, Liimatta E V, Joensuu P, Bergmann U, Ylitalo K, Hassinen IE. Superoxide production during ischemia-reperfusion in the perfused rat heart: a comparison of two methods of measurement. J Mol Cell Cardiol. 2012 Dec;53(6):906–15.

305. Sun J, Murphy E. Protein S-nitrosylation and cardioprotection. Circ Res. 2010 Feb 5;106(2):285–96.

306. Chen YY, Chu HM, Pan KT, Teng CH, Wang DL, Wang AHJ, et al. Cysteine S-nitrosylation protects protein-tyrosine phosphatase 1B against oxidation-induced permanent inactivation. J Biol Chem. 2008;283(50):35265–72.

307. Chang AHK, Sancheti H, Garcia J, Kaplowitz N, Cadenas E, Han D. Respiratory substrates regulate S-nitrosylation of mitochondrial proteins through a thiol-dependent pathway. Chem Res Toxicol. 2014;27(5):794–804.

308. Sun J, Morgan M, Shen R-F, Steenbergen C, Murphy E. Preconditioning results in S-nitrosylation of proteins involved in regulation of mitochondrial energetics and calcium transport. Circ Res. 2007 Nov 26;101(11):1155–63.

309. Sasaki N, Sato T, Ohler a, O'Rourke B, Marbán E. Activation of mitochondrial ATP-dependent potassium channels by nitric oxide. Circulation. 2000;101(4):439–45.

310. Chouchani ET, Methner C, Nadtochiy SM, Logan A, Pell VR, Ding S, et al. Cardioprotection by S-nitrosation of a cysteine switch on mitochondrial complex I. Nat Med. 2013 Jun;19(6):753–9.

311. Ingram TE, Fraser AG, Bleasdale R a, Ellins E a, Margulescu AD, Halcox JP, et al. Low-dose sodium nitrite attenuates myocardial ischemia and vascular ischemia-reperfusion injury in human models. J Am Coll Cardiol. 2013 Jun 25;61(25):2534–41.

312. Standards of practice for safe use of pneumatic tourniquet [Internet]. Association of Surgical Technologies. 2007. Available from: http://www.ast.org/uploadedFiles/Main_Site/Content/About_Us/Standards Pneumatic Tourniquets.pdf

313. Walters TJ, Ph D, Wenke JC, Baer DA. Research on Tourniquet Related Injury for Combat Casualty Care. 2004;(August):16–8.

314. Apple FS, Rhodes M. Enzymatic estimation of skeletal muscle damage by analysis of changes in serum creatine kinase. J Appl Physiol. 1988;65(6):2598–600.

315. Brancaccio P, Maffulli N, Limongelli FM. Creatine kinase monitoring in sport medicine. 2007;209–30.

316. Karalaki M, Fili S, Philippou A, Koutsilieris M. Muscle regeneration: cellular and molecular events. In Vivo. 2009;23(5):779–96.

317. Hirsch NP. Neuromuscular junction in health and disease. Br J Anaesth. 2007;99(1):132–8.

318. Schoen M, Rotter R, Gierer P, Gradl G, Strauss U, Jonas L, et al. Ischemic preconditioning prevents skeletal muscle tissue injury, but not nerve lesion upon tourniquet-induced ischemia. J Trauma. 2007;63(4):788–97.

319. Gillon A, Sheard P. Elderly mouse skeletal muscle fibres have a diminished capacity to upregulate NCAM production in response to denervation. Biogerontology. 2015;16(6):811–23.

320. Mech LD. Common Pathway for the Red Chromophore Formation in Fluorescent Proteins and Chromoproteins. Can Field-Naturalist. 2014;128(2):189–90.

321. Aktaş E, Atay Ç, Deveci MA, Arikan M, Toğral G, Yildirim A. Impact of oxidative stress on early postoperative knee function and muscle injury biochemical markers: Is it possible to create an ischemic preconditioning effect in sequential ischemic surgical procedures? Acta Orthop Traumatol Turc. 2015;49(4):387–93.

322. Brini M, Marsault R, Bastianutto C, Alvarez J, Pozzan T, Rizzuto R. Transfected aequorin

in the measurement of cytosolic Ca2+ concentration ([Ca2+](c)). A critical evaluation. Vol. 270, Journal of Biological Chemistry. 1995. p. 9896–903.

323. Chang DTW, Reynolds IJ. Differences in mitochondrial movement and morphology in young and mature primary cortical neurons in culture. Neuroscience. 2006;141(2):727–36.

324. Li N, Brun T, Cnop M, Cunha DA, Eizirik DL, Maechler P. Transient oxidative stress damages mitochondrial machinery inducing persistent β-cell dysfunction. J Biol Chem. 2009;284(35):23602–12.

325. Piantadosi CA. Regulation of Mitochondrial Processes by Protein S-Nitrosylation. Biochim Biophys Acta. 2012;1820(6):712–21.

326. Forquer I, Covian R, Bowman MK, Trumpower BL, Kramer DM. Similar transition states mediate the Q-cycle and superoxide production by the cytochrome bc1 complex. J Biol Chem. 2006;281(50):38459–65.

327. Kohr MJ, Sun J, Aponte A, Wang G, Gucek M, Murphy E, et al. Simultaneous measurement of protein oxidation and S-nitrosylation during preconditioning and ischemia/reperfusion injury with resin-assisted capture. Circ Res. 2011;108(4):418–26.

328. Kumar A, Kaundal RK, Iyer S, Sharma SS. Effects of resveratrol on nerve functions, oxidative stress and DNA fragmentation in experimental diabetic neuropathy. Life Sci. 2007;80(13):1236–44.

329. Crow JP, Calingasan NY, Chen J, Hill JL, Beal MF. Manganese porphyrin given at symptom onset markedly extends survival of ALS mice. Ann Neurol. 2005;58(2):258–65.

330. Dorion D, Zhong A, Chiu C, Forrest CR, Boyd B, Pang CY. Role of xanthine oxidase in reperfusion injury of ischemic skeletal muscles in the pig and human. J Appl Physiol. 1993;75(1):246–55.

331. Stupka N, Tiidus PM. Effects of ovariectomy and estrogen on ischemia-reperfusion injury in hindlimbs of female rats. J Appl Physiol. 2001;91(4):1828–35.

332. Gillani S, Cao J, Suzuki T, Hak DJ. The effect of ischemia reperfusion injury on skeletal muscle. Injury. 2012 Jun;43(6):670–5.

333. Fink E, Fortin D, Serrurier B, Ventura-Clapier R, Bigard AX. Recovery of contractile and metabolic phenotypes in regenerating slow muscle after notexin-induced or crush injury. J Muscle Res Cell Motil. 2003;24(7):421–9.

334. Pintér S, Mendler L, Dux L. Neural impacts on the regeneration of skeletal muscles. Acta Biochim Pol. 2003;50(4):1229–37.

335. Kraft GH. Fibrillation potential amplitude and muscle atrophy following peripheral nerve injury. Muscle Nerve. 1990;13(9):814–21.

336. Leterme D, Tyc F. Re-innervation and recovery of rat soleus muscle and motor unit function after nerve crush. Exp Physiol. 2004;89(4):353–61.

337. Khalil AA, Aziz FA, Hall JC. Reperfusion Injury. Plast Reconstr Surg. 2006;117(3):1024–33.

338. Beekley AC, Sebesta JA, Blackbourne LH, Herbert GS, Kauvar DS, Baer DG, et al. Prehospital Tourniquet Use in Operation Iraqi Freedom: Effect on Hemorrhage Control and Outcomes. J Trauma Inj Infect Crit Care. 2008;64(Supplement):S28–37.

339. Pedowitz RA. Tourniquet-induced neuromuscular injury. Acta Orthop Scand. 1991;62(sup245):1–33.

340. Kam PCA, Kavanaugh R, Yoong FFY. The arterial tourniquet: Pathophysiological consequences and anaesthetic implications. Anaesthesia. 2001;56(6):534–45.

341. Zager RA, Sacks BM, Burkhart KM, Williams AC. Plasma membrane phospholipid

integrity and orientation during hypoxic and toxic proximal tubular attack. Kidney Int. 1999;56(1):104–17.

342. Coban YK, Ciralik H, Kurutas EB. Ischemic preconditioning reduces the severity of ischemia-reperfusion injury of peripheral nerve in rats. J Brachial Plex Peripher Nerve Inj. 2006;1:2.

343. Mattson MP. Hormesis defined. Ageing Res Rev. 2008;7(1):1–7.

344. Radak Z, Chung HY, Goto S. Systemic adaptation to oxidative challenge induced by regular exercise. Free Radic Biol Med. 2008;44(2):153–9.

345. Ji LL, Kang C, Zhang Y. Exercise-induced hormesis and skeletal muscle health. Free Radic Biol Med. 2016;98:113–22.

346. Arsenault BJ, Larose E. Appreciating the local and systemic effects of exercise training on vascular health. Atherosclerosis. 2013;231(1):15–7.

347. Delbin MA, Antunes E, Zanesco A. Role of exercise training on pulmonary ischemia/reperfusion and inflammatory response. Rev Bras Cir Cardiovasc. 2009;24(4):552–61.

348. Borges JP, Lessa MA. Mechanisms Involved in Exercise-Induced Cardioprotection: A Systematic Review. Arq Bras Cardiol. 2015;71–81.

349. Borges JP, Rodrigues A, Lessa MA. Aerobic exercise training induces superior cardioprotection following myocardial ischemia reperfusion injury than a single aerobic exercise session in rats. 2017;23:1–5.

350. Demirel H a, Powers SK, Zergeroglu MA, Shanely RA, Hamilton K, Coombes J, et al. Short-term exercise improves myocardial tolerance to in vivo ischemia-reperfusion in the rat. J Appl Physiol. 1991;91(5 Pt 2):2205–12.

351. Symbiosis SG, Shibamoto T, Kuda Y, Tanida M, Wang M, Kurata Y. Exercise Attenuates Ischemia-reperfusion Injury of Nonalcoholic Fatty Liver in OLETF Rat. 2015;

352. Tam BT, Siu PM. Autophagic cellular responses to physical exercise in skeletal muscle. Sport Med. 2014;44(5):625–40.

353. Sanchez a M, Bernardi H, Py G, Candau R. Autophagy is essential to support skeletal muscle plasticity in response to endurance exercise. Am J Physiol Regul Integr Comp Physiol. 2014;956–69.

354. Yan Z, Okutsu M, Akhtar YN, Lira VA. Regulation of exercise-induced fiber type transformation, mitochondrial biogenesis, and angiogenesis in skeletal muscle. J Appl Physiol. 2011;110(1):264–74.

355. Webb R, Hughes M, Thomas A, Morris K. The Ability of Exercise-Associated Oxidative Stress to Trigger Redox-Sensitive Signalling Responses. Antioxidants. 2017;6(3):63.

356. Ji LL. Exercise-induced Modulation of Antioxidant Defense. New York Acad Sci. 2002;82–92.

357. Laker RC, Drake JC, Wilson RJ, Lira VA, Lewellen BM, Ryall KA, et al. Ampk phosphorylation of Ulk1 is required for targeting of mitochondria to lysosomes in exercise-induced mitophagy. Nat Commun. 2017 Dec 15;8(1):548.

358. Sanchez AMJ, Candau R, Raibon A, Bernardi H. Autophagy, a Highly Regulated Intracellular System Essential to Skeletal Muscle Homeostasis — Role in Disease, Exercise and Altitude Exposure. Muscle Cell Tissue. 2015;171–99.

359. Ferraro E, Giammarioli AM, Chiandotto S, Spoletini I, Rosano G. Exercise-Induced Skeletal Muscle Remodeling and Metabolic Adaptation: Redox Signaling and Role of Autophagy. Antioxid Redox Signal. 2014;21(1):154–76.

360. Lawler JM, Rodriguez DA, Hord JM, Lawler JM, Hall H. Mitochondria in the Middle : Exercise Preconditioning Protection of Striated Muscle. (979):1–72.

361. Rattray B, Thompson M, Ruell P, Caillaud C. Specific training improves skeletal muscle mitochondrial calcium homeostasis after eccentric exercise. Eur J Appl Physiol. 2013;113(2):427–36.

362. Zampieri S, Mammucari C, Romanello V, Barberi L, Pietrangelo L, Fusella A, et al. Physical exercise in aging human skeletal muscle increases mitochondrial calcium uniporter expression levels and affects mitochondria dynamics. Physiol Rep. 2016;4(24):e13005.

363. Drake JC, Wilson RJ, Yan Z. Molecular mechanisms for mitochondrial adaptation to exercise training in skeletal muscle. FASEB J. 2016;30(1):13–22.

364. Tai T-W, Lin C-J, Jou I-M, Chang C-W, Lai K-A, Yang C-Y. Tourniquet use in total knee arthroplasty: a meta-analysis. Knee Surgery, Sport Traumatol Arthrosc. 2011;19(7):1121–30.

365. Ledin H, Aspenberg P, Good L. Tourniquet use in total knee replacement does not improve fixation, but appears to reduce final range of motion. Acta Orthop. 2012;83(5):499–503.

366. Kalliainen LK, Jejurikar SS, Liang LW, Urbanchek MG, Kuzon WM. A specific force deficit exists in skeletal muscle after partial denervation. Muscle and Nerve. 2002;25(1):31–8.

367. Chipman PH, Schachner M, Rafuse VF. Presynaptic NCAM is required for motor neurons to functionally expand their peripheral field of innervation in partially denervated muscles. J Neurosci. 2014;34(32):10497–510.

368. Gomez-Cabrera MC, Domenech E, Viña J. Moderate exercise is an antioxidant: Upregulation of antioxidant genes by training. Free Radic Biol Med. 2008;44(2):126–31.

369. Terskikh a. "Fluorescent Timer": Protein That Changes Color with Time. Science (80-). 2000 Nov;290(5496):1585–8.

370. Perry HM, Huang L, Wilson RJ, Bajwa A, Sesaki H, Yan Z, et al. Dynamin-Related Protein 1 Deficiency Promotes Recovery from AKI. J Am Soc Nephrol. 2017;ASN.2017060659.

371. Prasannarong M, Santos FR, Hooshmand P, Hooshmand P, Giovannini FJ, Henriksen EJ. The lipid peroxidation end-product and oxidant 4-hydroxynonenal induces insulin resistance in rat slow-twitch skeletal muscle. Arch Physiol Biochem. 2014;120(1):22–8.

372. Pizzimenti S, Toaldo C, Pettazzoni P, Dianzani MU, Barrera G. The "Two-Faced" effects of reactive oxygen species and the lipid peroxidation product 4-Hydroxynonenal in the hallmarks of cancer. Cancers (Basel). 2010;2(2):338–63.

373. Inserte J, Hernando V, Garcia-Dorado D. Contribution of calpains to myocardial ischaemia/reperfusion injury. Cardiovasc Res. 2012;96(1):23–31.

374. Neuhof C, Neuhof H. Calpain system and its involvement in myocardial ischemia and reperfusion injury. World J Cardiol. 2014;6(7):638–52.

375. Khorchid A, Ikura M. How calpain is activated by calcium. Nat Struct Biol. 2002;9(4):239–41.

376. Yang B, Jain S, Ashra SY, Furness PN, Nicholson ML. Apoptosis and caspase-3 in long-term renal ischemia/reperfusion injury in rats and divergent effects of immunosuppressants. Transplantation. 2006;81(10):1442–50.

377. Mashima T, Naito M, Tsuruo T. Caspase-mediated cleavage of cytoskeletal actin plays a

positive role in the process of morphological apoptosis. Oncogene. 1999;18(15):2423–30.

378. Lam TT, Abler AS, Tso MO. Apoptosis and caspases after ischemia-reperfusion injury in rat retina. Invest Ophthalmol Vis Sci. 1999;40(5):967–75.

379. Biochem J, Suzuki KY, Tsuji S, Ishiura S, Kubota S. Autolysis Chicken of Calcium-Activated Skeletal Neutral Protease of Calcium-activated neutral protease (CANP), which exists widely in various tissues , requires Ca2 + ions of mm order for activity . Previously we reported that its sensitivity to Ca2 + i. 1981;90(6):1787–93.

380. Baki a, Tompa P, Alexa A, Molnár O, Friedrich P. Autolysis parallels activation of mu-calpain. Biochem J. 1996;318 (Pt 3(February 2016):897–901.

381. Brown SB, Bailey K, Savill J. Actin is cleaved during constitutive apoptosis. Biochem J. 1997;323 (Pt 1:233–7.

382. Rossiter JP, Anderson LL, Yang F, Cole GM. Caspase-cleaved actin (fractin) immunolabelling of Hirano bodies. Neuropathol Appl Neurobiol. 2000;26(4):342–6.

383. Desouza M, Gunning PW, Stehn JR. The actin cytoskeleton as a sensor and mediator of apoptosis. Bioarchitecture. 2012;2(3):75–87.

384. Quindry JC, Hamilton KL. Exercise and Cardiac Preconditioning Against Ischemia Reperfusion. Curr Cardiol Rev. 2013;9(3):220–9.

385. Booth FW, Thomason DB. Molecular and cellular adaptation of muscle in response to exercise: perspectives of various models. Physiol Rev. 1991;71(2):541–85.

386. Egan B, Zierath JR. Exercise metabolism and the molecular regulation of skeletal muscle adaptation. Cell Metab. 2013;17(2):162–84.

387. Niess AM, Simon P. Response and adaptation of skeletal muscle to exercise--the role of reactive oxygen species. Front Biosci. 2007;12(April 2016):4826–38.

388. Gilchrist JSC, Cook T, Abrenica B, Rashidkhani B, Pierce GN. Extensive autolytic fragmentation of membranous versus cytosolic calpain following myocardial ischemia-reperfusion. Can J Physiol Pharmacol. 2010;88(5):584–94.

389. Zhang Z, Biesiadecki BJ, Jin J-P. Selective deletion of the NH 2 -terminal variable region of cardiac troponin T in ischemia-reperfusion by myofibril-associated μ- calpain cleavage. 2007;45(38):11681–94.

390. Callum K, Bradbury a. ABC of arterial and venous disease: Acute limb ischaemia. BMJ. 2000;320(7237):764–7.

391. Lee C, Porter KM, Hodgetts TJ. Tourniquet use in the civilian prehospital setting. Emerg Med J. 2007;24(8):584–7.

392. Saw KM, Hee HI. Tourniquet-induced common peroneal nerve injury in a pediatric patient after knee arthroscopy - raising the red flag. Clin Case Reports. 2017;5(9):1438–40.

393. Burton GW. Metabolic acidosis during profound hypothermia. 1964;19(3).

394. Zhang JX, Wolf MB. Effect of cold on ischemia--reperfusion-induced microvascular permeability increase in cat skeletal muscle. Cryobiology. 1994 Feb;31(1):94–100.

395. Arató E, Kürthy M, Sínay L, Kasza G, Menyhei G, Hardi P, et al. Effect of vitamin E on reperfusion injuries during reconstructive vascular operations on lower limbs. Clin Hemorheol Microcirc. 2010;44(2):125–36.

396. Cheng Y-J, Wang Y-P, Chien C-T, Chen C-F. Small-dose propofol sedation attenuates the formation of reactive oxygen species in tourniquet-induced ischemia-reperfusion injury under spinal anesthesia. Anesth Analg. 2002 Jun;94(6):1617–20, table of contents.

397. Mohler LR, Pedowitz RA, Ohara WM, Oyama BK, Lopez MA, Gershuni DH. Effects of

an antioxidant in a rabbit model of tourniquet- induced skeletal muscle ischemia-reperfusion injury. J Surg Res. 1996;60(1):23–8.

398. Fowler TJ, Danta G, Gilliatt RW. Recovery of nerve conduction after a pneumatic tourniquet: observations on the hind-limb of the baboon. J Neurol Neurosurg Psychiatry. 1972;35(5):638–47.

399. Martin FR, Paletta FX. Tourniquet paralysis: a primary vascular phenomenon. South Med J. 1966 Aug;59(8):951–3.

400. Kolb WH. The Effects of Prehabilitative Exercise on Functional Recovery Following Total Knee Arthroplasty.

401. Bleier L, Dröse S. Superoxide generation by complex III: From mechanistic rationales to functional consequences. Biochim Biophys Acta - Bioenerg. 2013;1827(11–12):1320–31.

402. Guillaud F, Dröse S, Kowald A, Brandt U, Klipp E. Superoxide production by cytochrome bc1 complex: A mathematical model. Biochim Biophys Acta - Bioenerg. 2014;1837(10):1643–52.

403. Korge P, Calmettes G, John SA, Weiss JN. Reactive oxygen species production induced by pore opening in cardiac mitochondria: The role of complex III. J Biol Chem. 2017;292(24):9882–95.

404. Votyakova T V, Reynolds IJ. DeltaPsi(m)-Dependent and -independent production of reactive oxygen species by rat brain mitochondria. J Neurochem. 2001 Oct;79(2):266–77.

405. Selivanov VA, Votyakova T V., Pivtoraiko VN, Zeak J, Sukhomlin T, Trucco M, et al. Reactive oxygen species production by forward and reverse electron fluxes in the mitochondrial respiratory chain. PLoS Comput Biol. 2011;7(3).

406. Mohanty JG, Jaffe JS, Schulman ES, Raible DG. A highly sensitive fluorescent micro-

assay of H2O2 release from activated human leukocytes using a dihydroxyphenoxazine derivative. J Immunol Methods. 1997;202(2):133–41.

407. Zhou M, Diwu Z, Panchuk-Voloshina N, Haugland RP. A stable nonfluorescent derivative of resorufin for the fluorometric determination of trace hydrogen peroxide: Applications in detecting the activity of phagocyte NADPH oxidase and other oxidases. Anal Biochem. 1997;253(2):162–8.

408. Lee S, Tak E, Lee J, Rashid M, Murphy MP, Ha J, et al. Mitochondrial H2O2 generated from electron transport chain complex I stimulates muscle differentiation. Cell Res. 2011;21(5):817–34.

409. Kudin AP, Bimpong-Buta NYB, Vielhaber S, Elger CE, Kunz WS. Characterization of Superoxide-producing Sites in Isolated Brain Mitochondria. J Biol Chem. 2004;279(6):4127–35.

410. Lee Y, Min K, Talbert EE, Kavazis AN, Smuder AJ, Willis WT, et al. Exercise protects cardiac mitochondria against ischemia-reperfusion injury. Med Sci Sports Exerc. 2012;44(3):397–405.

411. Zhang KR, Liu HT, Zhang HF, Zhang QJ, Li QX, Yu QJ, et al. Long-term aerobic exercise protects the heart against ischemia/reperfusion injury via PI3 kinase-dependent and Akt-mediated mechanism. Apoptosis. 2007;12(9):1579–88.

412. Call JA, Donet J, Martin KS, Sharma AK, Chen X, Zhang J, et al. Muscle-derived extracellular superoxide dismutase inhibits endothelial activation and protects against multiple organ dysfunction syndrome in mice. Free Radic Biol Med. 2017;113(October):212–23.

413. Cox GR, Clark SA, Cox AJ, Halson SL, Hargreaves M, Hawley JA, et al. Daily training

with high carbohydrate availability increases exogenous carbohydrate oxidation during endurance cycling. J Appl Physiol. 2010;109(1):126–34.

414. Knuiman P, Hopman MTE, Mensink M. Glycogen availability and skeletal muscle adaptations with endurance and resistance exercise. Nutr Metab. 2015;12(1):1–11.

415. Ørtenblad N, Westerblad H, Nielsen J. Muscle glycogen stores and fatigue. J Physiol. 2013;591(18):4405–13.